Polymer 54 (2013) 4729–4761

Contents lists available at SciVerse ScienceDirect

Polymer

journal homepage: www.elsevier.com/locate/polymer

Feature article

Energy-efficient polymeric gas separation membranes for a sustainable future: A review

David F. Sanders [a], Zachary P. Smith [a], Ruilan Guo [b], Lloyd M. Robeson [c], James E. McGrath [d], Donald R. Paul [a], Benny D. Freeman [a,*]

[a] University of Texas at Austin, Center for Energy and Environmental Resources, Department of Chemical Engineering, and Texas Materials Institute, 10100 Burnet Road, Building 133, Austin, TX 78758, USA
[b] University of Notre Dame, Department of Chemical and Biomolecular Engineering, Notre Dame, IN 46556, USA
[c] Lehigh University, Department of Materials Science and Engineering, Bethlehem, PA 18015, USA
[d] Virginia Polytechnic Institute and State University, Macromolecules and Interfaces Institute and Department of Chemistry, Blacksburg, VA 24061, USA

ARTICLE INFO

Article history:
Received 4 February 2013
Received in revised form
19 May 2013
Accepted 20 May 2013
Available online 4 July 2013

Keywords:
Membranes
Materials
Separations

ABSTRACT

Over the past three decades, polymeric gas separation membranes have become widely used for a variety of industrial gas separations applications. This review presents the fundamental scientific principles underpinning the operation of polymers for gas separations, including the solution-diffusion model and various structure/property relations, describes membrane fabrication technology, describes polymers believed to be used commercially for gas separations, and discusses some challenges associated with membrane materials development. A description of new classes of polymers being considered for gas separations, largely to overcome existing challenges or access applications that are not yet practiced commercially, is also provided. Some classes of polymers discussed in this review that have been the focus of much recent work include thermally rearranged (TR) polymers, polymers of intrinsic microporosity (PIMs), room-temperature ionic liquids (RTILs), perfluoropolymers, and high-performance polyimides.

1. Introduction – history, equations, and terminology

1.1. History

The first recorded description of semi-permeable membranes was in 1748 when Jean Antoine (Abbé) Nollet reported that a pig bladder (*i.e.*, a natural membrane) was more permeable to water than to ethanol [1–3]. Later, in 1831, a related observation regarding gas transport through balloons prepared from natural rubber, which is largely *cis*-poly(isoprene), was made by John Kearsley Mitchell [4]. After filling a series of these balloons with hydrogen and letting them rise to the ceiling of his lecture room, the balloons descended from the ceiling over time. Mitchell hypothesized that the hydrogen was somehow passing through the walls of these rubber balloons [4]. Further experiments showed that various gases passed through the same material at different rates, a critically important concept that foreshadowed the commercial development of polymeric gas separation membranes in the late 1970s [5].

Adolph Fick's laws of diffusion, derived by analogy with Fourier's law of heat conduction and Ohm's law of electrical conduction, provided the fundamental mathematical framework for mass transfer across nonporous membranes [6], and Sir Thomas Graham published a seminal paper in 1866 setting forth the basic principles underpinning the solution-diffusion model, which is understood to govern gas transport in all nonporous polymeric gas separation membranes [7]. In this model, gas is transported through a nonporous polymer film or membrane by dissolving into the face of the membrane exposed to high gas pressure, diffusing through the polymer, and desorbing from the face of the membrane exposed to low pressure [8]. The middle step, diffusion through the polymer, is the rate-limiting step for gas permeation in all polymer membranes today. The rate-limiting step in diffusion is the local scale segmental dynamics of the polymer chains that lead to the opening and closing of transient gaps (*i.e.*, free volume elements) in the polymer; the gas molecules execute Brownian motion (*i.e.*, diffusion) through these free volume elements. Thus, the local segmental motions of polymer chains and the packing of polymers are two critically

* Corresponding author. Tel.: +1 512 232 2803; fax: +1 512 232 2807.
E-mail address: freeman@che.utexas.edu (B.D. Freeman).

0032-3861
http://dx.doi.org/10.1016/j.polymer.2013.05.075

variables important in gating the diffusion of small gas molecules through polymers.

The gas separation membrane market has grown significantly since its beginnings in the 1970s (approximately), and continued growth is expected in the coming years as technology improves and applications expand [9]. Previously, several review articles and monographs have chronicled overall progress in the field as well as specific progress in applications and materials science [5,9–17]. This review focuses on the role of polymer science in current and future materials for gas separation applications. To provide context for the materials science discussion, current applications of polymeric gas separation membranes are discussed as well as potential future applications that may become feasible with improved membrane materials.

1.2. Equations and terminology

The equations and terminology discussed below illustrate basic concepts used to describe gas transport in polymers and evaluate membrane material performance. Detailed derivations and discussion of these equations are available elsewhere [5,8,11–13]. Membrane performance is often characterized by gas throughput and separation efficiency and these properties are most commonly expressed by permeability and selectivity coefficients.

1.2.1. Permeability coefficient

For a pure gas permeating through a polymer film or membrane, gas permeability, P_A, is defined as the trans-membrane pressure difference, p_2-p_1, and thickness normalized steady-state gas flux, N_A [18]:

$$P_A = \frac{N_A l}{(p_2 - p_1)} \tag{1}$$

where l is the membrane thickness, p_2 is the upstream pressure, and p_1 is the downstream pressure. Unlike flux, which depends upon l and Δp, P_A is typically viewed, to a first approximation, as being a material property that is much less dependent than flux on membrane thickness and Δp. For gas mixtures permeating through polymers, Δp is taken to be the partial pressure difference of the component of interest, and for nonideal gases, Δp can be replaced by the fugacity difference across a membrane or film [19].

Typically permeability coefficients are expressed in Barrer, where [13]:

$$1 \text{ Barrer} = \frac{10^{-10} \text{ cm}^3(\text{STP}) \text{ cm}}{\text{cm}^2 \text{ s cmHg}} \tag{2}$$

Each polymer has a different permeability coefficient for each gas, and the faster permeation of some gases relative to others provides the basis for the use of polymers to separation gas mixtures. The range over which permeability can vary in different polymers is enormous. For example, oxygen permeability in poly(acrylonitrile) (PAN), a high barrier polymer, is 2.8×10^{-4} Barrer [20]. At the other end of the scale, a polymer based upon an indane-containing poly(diphenylacetylene) derivative has an oxygen permeability of 18,700 Barrer, which is believed to be the highest oxygen permeability among nonporous polymers [21]. Thus, oxygen permeability values span nearly 8 orders of magnitude in these two examples, and there are polymers, such as dry poly(vinyl alcohol), that are more than an order of magnitude less permeable than PAN [22]. This enormous range of gas permeabilities in polymers illustrates the extraordinary sensitivity of gas permeability to polymer material structure.

Using the solution-diffusion model, the gas permeability coefficient can be written as the product of a gas solubility coefficient, S_A, and a concentration-averaged, effective diffusion coefficient, D_A [18]:

$$P_A = D_A S_A \tag{3}$$

The diffusion coefficient is commonly expressed in cm^2/sec, and solubility is often expressed in cm^3(STP)/(cm^3 polymer atm) or cm^3(STP)/(cm^3 polymer cmHg).

Penetrant size has a significant effect on diffusion coefficients, with larger gases generally having lower diffusion coefficients [18]. In polymers of interest for gas separations, gas diffusion coefficients range from approximately 10^{-4} cm^2/s for helium diffusion in poly(1-trimethylsilyl-1-propyne), PTMSP, which is among the most permeable polymers known, to approximately 3×10^{-9} cm^2/s for CH_4 in polycarbonate [18,23]. Diffusion coefficients are also sensitive to polymer chain flexibility and the free volume in the polymer, which depends on the amount of packing defects, gaps between polymer chains and other structural features that give rise to openings within a polymer large enough to permit penetrant diffusion.

The solubility coefficient in Eq. (3) is defined as the ratio of the concentration of gas in a polymer, C, to the pressure of gas, p, contiguous to the polymer [13]:

$$S_A = \frac{C}{p} \tag{4}$$

Solubility depends mainly on gas molecule condensability (as characterized, for example, by gas critical temperature, Lennard-Jones potential well depth, normal boiling point, enthalpy of vaporization, *etc.*) and, to a lesser extent, on gas–polymer interactions [18]. Polymer morphological features, such as crystallinity and liquid crystallinity, also influence gas solubility in polymers [24–27].

1.2.2. Selectivity

A common parameter characterizing the ability of a polymer to separate two gases (*e.g.*, A and B) is the ideal selectivity, $\alpha_{A/B}$: [28]

$$\alpha_{A/B} = \frac{P_A}{P_B} \tag{5}$$

By combining Eqs. (3) and (5), permeability selectivity can be written as a product of solubility and diffusivity selectivity:

$$\alpha_{A/B} = \frac{D_A}{D_B}\frac{S_A}{S_B} \tag{6}$$

Like permeability, the ideal selectivity is often treated as a material property of a polymer.

Another measure of the ability of a membrane to separate a particular gas mixture is the separation factor, α^*, where x_i is the concentration of gas i in the feed and y_i is the concentration of gas i in the permeate [28]:

$$\alpha^*_{A/B} = \frac{y_A/y_B}{x_A/x_B} \tag{7}$$

This value is less commonly reported in the membrane materials literature because it depends more sensitively on operating conditions (*e.g.*, upstream and downstream pressure and feed gas composition) than $\alpha_{A/B}$. Thus, the separation factor is not a material property of the polymer being used as the membrane. However, when the upstream pressure is much greater than the downstream pressure, the separation factor becomes equal to the ideal selectivity. This relationship can be shown by recognizing that the mole

fraction of component A produced in the permeate, y_A, is related to the flux of A and B as follows:

$$y_A = \frac{N_A}{N_A + N_B} \tag{8}$$

An analogous relation may be written for component B. Substituting Eq. (8) into Eq. (7) and using the definition of permeability in Eq. (1) to solve for flux, the following expression is obtained:

$$\alpha^*_{A/B} = \alpha_{A/B}\frac{p_2 - p_1\left(\frac{y_A}{x_A}\right)}{p_2 - p_1\left(\frac{y_B}{x_B}\right)} \tag{9}$$

Therefore, when the upstream pressure, p_2, is much greater than the downstream pressure, the downstream pressure p_1 (e.g., if $p_1 = 0$ (i.e. vacuum)), p_1, $\alpha^*_{A/B} = \alpha_{A/B}$.

1.2.3. Fractional free volume

Free volume is among the most important structural variables influencing gas transport properties in polymers. The Cohen–Turnbull model predicts that diffusion coefficients increase strongly as free volume increases [29]. This relationship is shown in Eq. (10) where A is a constant related to a geometric factor, molecular diameter, and gas kinetic velocity, v^* is a parameter related to the size of the gas molecule, γ is an overlap factor introduced to prevent double counting of free volume elements, and FFV is the fractional free volume of the polymer [18,29–31].

$$D = A\exp\left(-\frac{\gamma v^*}{\mathrm{FFV}}\right) \tag{10}$$

In gas separation polymers, free volume is the void space between polymer chain segments that is available to assist in molecular transport [14]. Free volume can be generated by inefficiencies in polymer chain packing in the solid state and by molecular motion of polymer chain segments, which effectively open gaps in the polymer matrix on a transient basis that allow penetrant molecules to diffuse through the polymer [32].

Fractional free volume is calculated as the difference between the experimental specific volume (*i.e.*, reciprocal of polymer density) and the theoretical volume occupied by the polymer chains [33,34]:

$$\mathrm{FFV} = \frac{V - V_0}{V} \tag{11}$$

where V is the measured experimental specific volume of the polymer in cm^3/g, and V_0 is the theoretical occupied volume of the polymer chains in cm^3/g. V_0 is typically estimated using group contribution theory as described by Bondi, where V_W is the van der Waal's volume of groups comprising the polymer chain Refs. [33–35].

$$V_0 = 1.3\sum V_W \tag{12}$$

Fig. 1A presents an example of a relationship between fractional free volume and diffusion coefficients in a systematic series of polysulfones of varying chemical structure. Often, there is a good correlation between FFV and diffusion coefficients. Due to uncertainties associated with estimating occupied volume increments with various families of polymers, correlations of FFV with gas diffusion coefficients are often strongest when restricted to polymers with similar backbone structures [36]. Because gas solubility typically depends weakly on free volume, gas permeability coefficients often correlate well with FFV, and many studies report strong correlations of permeability with FFV as seen in Fig. 1b [37].

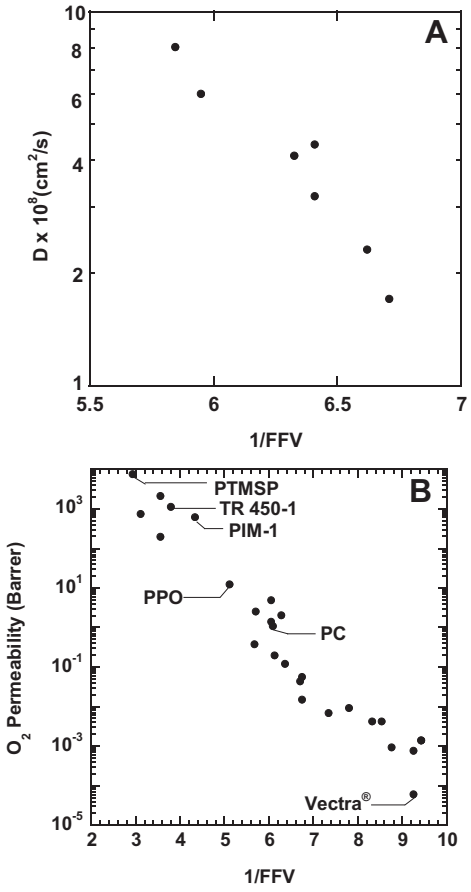

Fig. 1. (A) Oxygen diffusion coefficient in polysulfones of varying fractional free volume [30]. (B) Oxygen permeability for many families of polymers including poly(1-trimethylsilyl-1-propyne) (PTMSP), 6F-containing thermally rearranged polymer (TR 450-1), polymer of intrinsic microporosity (PIM-1), polycarbonate (PC), poly(2,6-dimethyl-1,4-phenylene oxide) (PPO), Vectra® (a commercial polyester liquid crystalline polymer), and various polymers from Refs. [38–40].

2. Membrane fabrication and competing technologies for gas separation processes

2.1. Membrane fabrication processes

Today, virtually all gas separation membranes are made by processes based on the concept of phase inversion because it is the only commercially viable way known for making thin (*i.e.*, of the order of 100 nm or less), defect-free membranes at large enough surface areas to be useful for practical applications. The phase inversion process, invented by Loeb and Sourirajan to make cellulose acetate desalination membranes [41], can be used to produce asymmetric membranes with very thin, dense films on a porous substrate and provided a practical route to prepare high flux membranes. This process remains the primary method by which commercial gas separation membranes are prepared and has allowed membranes to be prepared in sufficiently large area to process, for example, from 50 to 700 million standard cubic feet of natural gas per day in some locations [42]. To prepare membranes via phase inversion, a water-insoluble polymer is dissolved in a water miscible, high boiling solvent or mixture of solvents; the resulting solution is often referred to as a polymer dope. This dope

is then cast using a doctor blade onto a porous backing material, for flat sheet, spiral wound membranes, or extruded through a hollow fiber spinneret to prepare hollow fibers [43]. After passing through a short air gap to allow solvent evaporation from the surface of the nascent membrane to begin formation of a thin, dense layer on the surface, the cast or extruded polymer dope is immersed in a non-solvent (usually water) bath. In this bath, solvent exchange and polymer coagulation produce a porous substrate with a thin, dense skin on top of it, in the case of spiral wound membranes, or on the outside of hollow fibers. Often, the polymer dope concentration would be in the range of 30–35 wt%, and small amounts of a water-soluble polymer (*e.g.*, poly(vinyl pyrrolidone) or poly(ethylene oxide) oligomers) could be added to optimize the porous structure [14,15,44,45]. To reduce macrovoid formation, water, alcohols or other additives are included in the original polymer dope, so that the dope is very close to the phase separation boundary before being cast or extruded [15]. For example, polysulfone hollow fibers can be spun from a dope containing 37% total solids (*i.e.*, polymer) dissolved in a mixture of 43 wt% propionic acid and 57 wt% *N*-methyl-2-pyrrolidone or 13 wt% formamide and 87 wt% formylpiperidine [44,45].

An example of a ternary phase diagram for polymer, solvent(s), and a coagulating non-solvent (typically water) is shown in Fig. 2. The path followed by the polymer during phase inversion is labeled "Coagulation path" in this figure. Two-phase separation processes can occur, as noted in the literature [46–48]. Spinodal decomposition will occur if the membrane formation path goes through the critical point or rapidly into the unstable region. Nucleation and growth can occur in the metastable region as well as the unstable region [43]. The initial morphologies resulting from these processes are different [43], and spinodal decomposition yields a more desired intertwined structure. As the phase separation process continues, the initial features of spinodal decomposition can become less recognizable due to structure coalescence. The thermodynamic interpretations of nucleation and growth versus spinodal decomposition and information directly related to membrane formation are available elsewhere [14,15,43,48,49].

Many commercial gas separation systems are based on hollow fibers produced by this phase inversion process [9,45]. During spinning, the bore of the hollow fiber often has a bore fluid to provide a compensating pressure to maintain the hollow interior, coagulate the spin dope, and stabilize the forming fiber; gases such as N_2 and liquids such as H_2O or aqueous based liquids have been reported as bore fluids [44,45,52–54]. After the phase inversion process, the resultant membrane is typically stored in water to further remove solvent prior to drying and subsequent post-treatment to caulk any defects in the membrane surface [55,56]. While the common method used to prepare hollow fibers produces a dense film on the outer surface, a variation has been noted whereby a coagulating medium is added to the bore of the hollow fiber extrudate allowing dense film formation on the inner wall [14]. However, this method has the drawback that the effective surface area of membrane per unit length of fiber is reduced, since the bore diameter of the hollow fiber is necessarily less than the outer diameter. An example of an asymmetric hollow fiber and its dense skin are illustrated in Fig. 3 for a hollow fiber prepared via the conventional non-solvent phase inversion procedure.

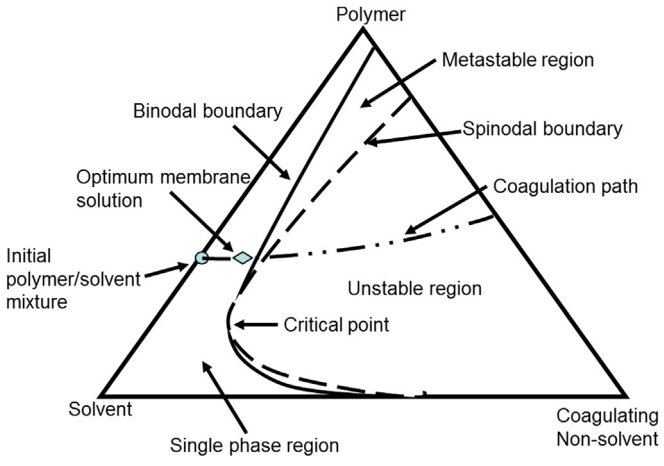

Fig. 2. Qualitative illustration of a phase diagram for a polymer/solvent/non-solvent system. The path followed during formation of a phase inversion membrane is illustrated by the line labeled "Coagulation path" [43,50,51].

A major concern for membranes prepared via phase inversion is the elimination of pinholes in the dense layer. It is difficult to produce pinhole-free membranes, so repair techniques usually are employed to seal any defects to achieve effective dense layer thicknesses of 100 nm or less. Henis and Tripodi [55,56] reported that pinhole defects in asymmetric membranes could be repaired by coating a slightly defective phase inversion membrane with a thin layer of a highly permeable (but relatively non-selective) polymer such as silicone rubber (*i.e.*, poly(dimethylsiloxane)). This so-called "caulking" step largely eliminates non-selective pore flow through defects with little change in the inherent flux of the dense layer.

Typically, flat sheet membranes would be used to prepare spiral wound membrane modules, and hollow fibers would be assembled into a hollow fiber module [9]. These two configurations of membranes are shown schematically in Fig. 4. The objective of putting membranes into such configurations is to maximize the amount of membrane surface area that can be accommodated in a given volume. Higher surface to volume ratio assemblies of membranes reduce the cost of pressure vessels, *etc*. required to use such membranes.

A typical hollow fiber bundle contains on the order of 10^5 hollow fibers which are tightly packed (packing fractions on the order of 50% are common) with both ends embedded in a thermosetting polymer epoxy [57]. A hollow fiber bundle would then be housed in a polymeric or metal pressure vessel, depending on the pressure that the system was expected to encounter during operation. A high pressure feed gas can be introduced into the bore side or the shell side of a hollow fiber module, depending on the application. Generally, to maximize the available driving force for mass transfer, hollow fiber modules are designed to operate as close to countercurrent flow as possible. However, due to flow maldistribution in the fiber bundles or other factors, gas flow through the shell is typically not in perfect countercurrent flow [58–63].

For applications such as air dehydration, where the objective is to remove a highly permeable species (*e.g.*, water) present at relatively low mole fractions in the feed, a sweep gas on the permeate side of the membrane is utilized to facilitate transport of water across the membrane, thereby increasing the driving force for permeation of water from the feed into the permeate stream [57,58]. In the air dehydration case, the permeate sweep is often generated by flowing a small amount of dry retentate product gas through the permeate side of the membrane or allowing some of the feed gas to leak through defects in the fibers (brought about by not caulking the fibers or portions of the fibers) into the permeate [57,64]. Such approaches are routinely used in gas separation modules for dehydration of air [64,65]. More recently, process designs to remove CO_2 from flue gas for carbon capture applications rely on sweeping the permeate stream with air to reduce the partial pressure of CO_2 in the permeate stream, thereby increasing the driving force for CO_2 transport across the membrane [66].

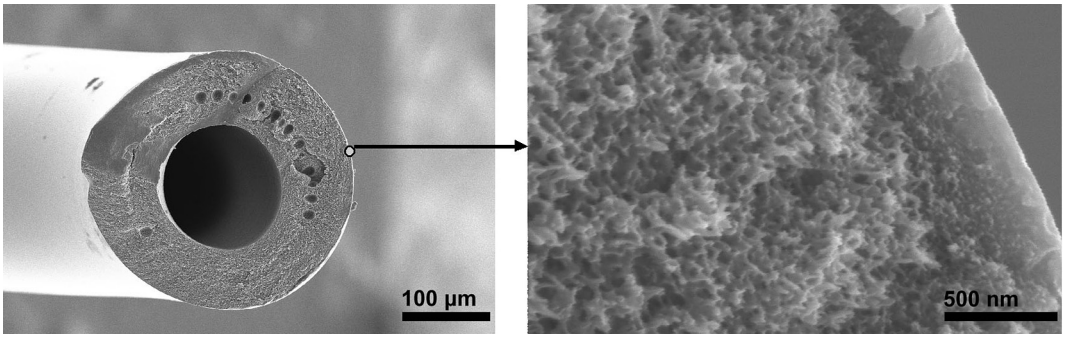

Fig. 3. Typical hollow fiber morphology, shown for polysulfone, produced by the phase inversion process. Reprinted from Ref. [48] with permission from Elsevier.

The spiral wound membrane module configuration involves alternating layers of flat sheet asymmetric membranes with porous spacers between the membrane sheets [14]. The permeate and feed streams travel through alternate layers in a spiral wound module. The hollow fiber module is much more common than spiral wound systems for gas separation due to cost of production [9], higher membrane surface area to module volume and generally easier fabrication methods [67]. With water purification, and specifically reverse osmosis applications, the preferred configuration is spiral wound due to the large pressure drop of liquids in small bore hollow fibers and to help reduce the feed pretreatment needed to prevent fouling of hollow fibers [14]. Because gas viscosity is orders of magnitude lower than liquid viscosity, pressure drop in hollow fibers for gas separation is much less than it would be if liquid were flowing through the bore of the fibers as could be the case in, for example, desalination of water [14]. Specific process designs and details of modular construction are reported elsewhere [9,67–70].

2.2. Competing technologies/membrane competiveness

Presently, gas separation using polymeric membranes competes with several other technologies, and often gas separation membranes are not the dominant technology for a given gas separation application. For example, cryogenic distillation, pressure (and vacuum) swing adsorption, and chemical absorption processes dominate commercial gas separation processes [71].

2.2.1. Cryogenic distillation

Cryogenic distillation is no different than conventional distillation except that the temperatures are considerably lower [72]. Plate and tray (or packed column) distillation columns are employed at cryogenic temperatures. As in conventional distillation, temperature differences from the bottom to the top of the column allow for separation. In the case of air separation, large quantities of air are compressed, purified, cooled and then liquefied before being separated in distillation columns [72,73]. Water, CO_2 and trace hydrocarbons are removed prior to distillation using molecular sieves. Nitrogen is taken from the top of the column, due to its lower boiling point relative to oxygen, and oxygen and argon are taken from the bottom of the column [74]. Argon can thus be collected from this operation and further purified to high purity argon. Several distillation stages are required to produce high purity oxygen, nitrogen and argon. The other noble gases (neon, xenon, krypton) can also be collected from this process and further purified [75]. Cryogenic distillation can also be employed for separation of deuterium and tritium from hydrogen [76]. In addition, cryogenic separation (not specifically involving distillation) can be used to separate hydrogen from much more readily condensable hydrocarbons [77]. For obvious reasons, cryogenic distillation is the method of choice for the large liquid oxygen and liquid nitrogen markets as well as applications requiring high purity [72–74].

2.2.2. Pressure swing adsorption (PSA)

Pressure swing adsorption is another common gas separation process widely practiced commercially [78]. This technique

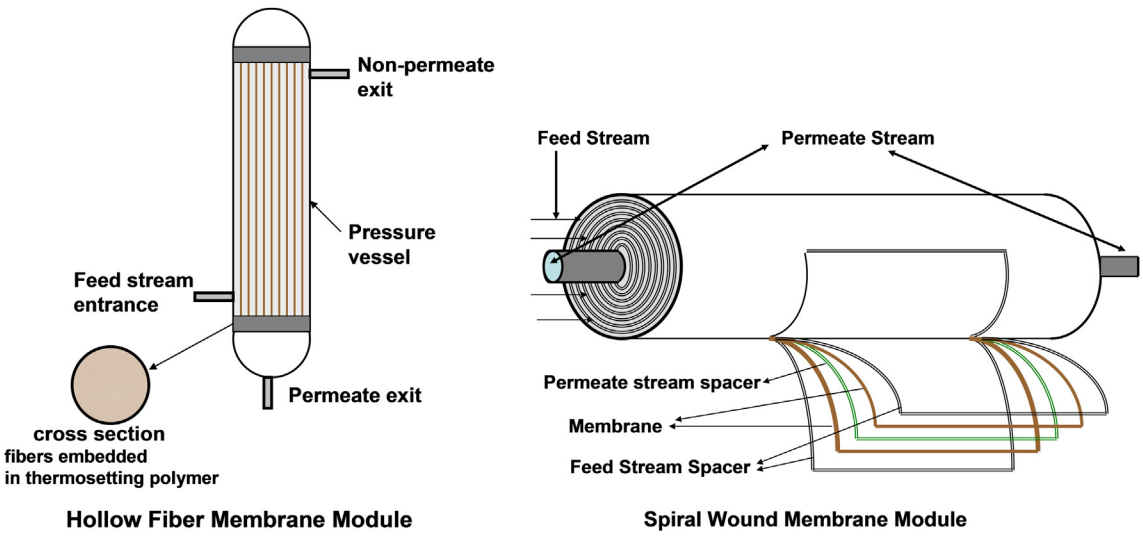

Fig. 4. Modular constructions employed for gas separation processes. Reprinted from Ref. [48] with permission of Elsevier.

involves pressurizing a gas mixture in the presence of specific adsorbents such as zeolites, silica, alumina and activated carbon [79]. PSA can operate at ambient conditions thus the energy costs associated with heating or cooling are minimized. These adsorbents are porous structures with extremely high internal surface areas and can adsorb one gas preferentially to the other [79]. Molecular sieves (such as carbon molecular sieves and certain zeolites) can prevent a larger diameter gas from entering the pores and can thus provide separation based on gas molecule size [80,81]. Once pressurization is conducted (and time elapsed to reach a condition close to equilibrium), the system is depressurized, allowing the lower sorbing gas to leave the adsorption bed first. This depressurization step leaves the chamber enriched in the gas with the higher sorption value on the adsorbent [82]. Usually, this process involves at least two beds because one is being pressurized (*i.e.*, is being used to adsorb gases) and the other is being depressurized (*i.e.*, regenerated) to allow continuous operation [83]. If operated near ambient pressure for one cycle of the process and vacuum for the other cycle, the process is referred to as vacuum swing adsorption (VSA) [82].

The removal of CO_2 from the steam reforming reaction of hydrocarbons to produce hydrogen often employs PSA [84]. Hydrogen can be separated from both CO_2 and CO produced in this process, and PSA is the primary process used for hydrogen purification [84]. Refineries use PSA for hydrotreating and hydrocracking processes as well as the removal of H_2S from hydrogen [85]. PSA is also used to separate carbon dioxide from methane for natural gas purification [86]. Nitrogen generation also uses PSA to produce high purity nitrogen in the range of 99.5% or higher where membrane systems would require multistage operations and cryogenic processes may be too expensive [82,87,88]. Separation of *n*-paraffins from isoparaffins has also been reported [89]. Oxygen generation for medical oxygen is another common use for pressure swing adsorption since volumes required are low and small units employing conventional electrical power sources are desired [73,90]. Pressure swing adsorption processes generally offer favorable economics in the mid volume range versus cryogenic distillation (high volume) and membrane separation (low volume) [87,88,91].

2.2.3. Chemical absorption processes

Presently, the primary process to remove CO_2 from natural gas and power plant flue gas involves a monoethanolamine chemical absorbent-based process [92,93]. When an amine is reacted with carbon dioxide, a nitrogen substituted carbamic acid is formed [94]. This is a rather unstable product which will decompose to the original amine and carbon dioxide at modest temperatures ($>100\ ^\circ C$) [95]. Thus amines can be used to capture CO_2 at ambient temperatures and the amines can be regenerated and CO_2 collected as a gas at higher temperatures [95]. This approach provides a facile method to separate CO_2 from gas mixtures and collect CO_2 at high purity [93]. This process is widely used and has been proposed for the collection of CO_2 for sequestration from power plant flue gas [96]. While monoethanolamine is one of the preferred amines used in this process, other similar amines such as diethanolamine, methyl diethanolamine and triethanolamine, which can also remove H_2S from natural gas streams, have been employed [95].

As noted later, membrane separation processes have favorably competed with conventional processes for a number of reasons. First, membrane processes are generally more energy efficient, offer simplicity of operation and are favorable for smaller scale operations where gas purity is not critical [9,10]. Drawbacks of membrane gas separation include limited ability to achieve high purity separation, lack of feasibility in large-scale operation and sometimes higher capital cost [9,14]. In spite of what might be considered a "fragile" system based on ~100 nm dense film thicknesses, membranes have shown durability and reliability during long-term use even under continuous use with high pressure drop (approaching 1000 psi (69 bar) in specific cases) across the hollow fiber or flat membrane [14]. Cases exist where membrane processes can be combined with more conventional gas separation processes described above to optimize specific separations [97]. A detailed comparison of membrane technology versus conventional gas separation processes has been reported by Prasad et al. [98].

The separation of air to produce ~98% N_2 for inert atmosphere blanketing applications for food preservation and combustible fuel storage is an area where membrane gas separation enjoys the advantage of smaller scale economics, lower weight and space as well as lower energy requirements relative to the more conventional gas separation technologies described above [87,99]. Compact units for delivering dry nitrogen for laboratory use favor membrane technology where cylinder usage may not suffice or could be inconvenient [98]. Other examples of commercial membrane applications are discussed later.

3. Challenges in membrane science and limits of technology

3.1. Permeability/selectivity tradeoff (the upper bound)

The polymer used to make a membrane is crucial to separation performance. Thus, structure/property studies related to membrane separation have been a significant area of research since the early 1980s [5,11,12,100,101]. Several key factors in membrane transport performance include flux, permeability, and selectivity.

The flux is governed by the choice of the polymer (permeability) and its effective thickness. The selectivity is also determined by the choice of polymer and the ability to achieve "pinhole-free" membranes. As thickness is a process fabrication parameter, the permeability and selectivity of the polymer are key material properties for polymer studies.

A considerable number of structure–property studies have identified polymer structural components that yield high permeability, and many of these studies have defined structural characteristics desirable for gas separation [100,101]. Specifically, polymers offering the best combinations of α_{ij} and P_i are generally glassy and have rigid structures that exhibit poor chain packing [101]. In essence, these polymers offer the size distribution of free volume elements required for approaching molecular sieving characteristics.

Since the advent of commercial membrane gas separation systems, structure-property data on polymeric membranes has significantly increased in the literature. It became apparent that a balance (tradeoff relationship) existed between selectivity and permeability [102–105]. A concept emerged in the literature called the "upper bound" where log–log plots of selectivity versus permeability of the more permeable gas demonstrated that virtually all the data points were below a well-defined line [100,106]. An example of the upper bound relationship for CO_2/CH_4 is shown in Fig. 5. This relationship was found to be valid for gas pairs chosen from the common gases of He, H_2, O_2, N_2, CO_2, and CH_4. The "upper bound" line has the following form [100,101]:

$$P_i = k\alpha_{ij}^n \tag{13}$$

where P_i is the permeability of the more permeable gas, n is the slope of the upper bound line, and k is a constant for a specific gas pair termed the front factor. The value of the upper bound slope was shown to correlate with kinetic diameters determined from zeolite data, which gave a better fit than other gas diameter data in

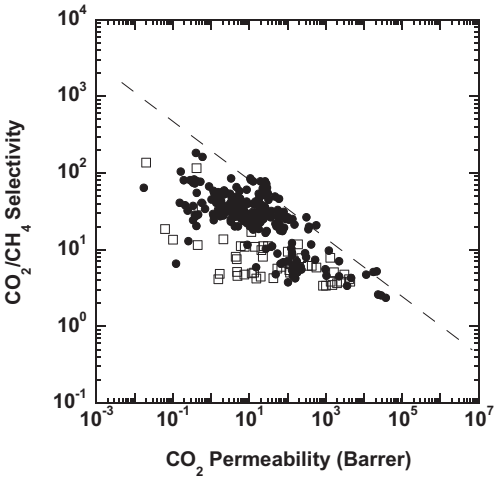

Fig. 5. Experimental pure gas data for CO_2/CH_4 separation demonstrating an empirical upper bound for glassy (●) and rubbery (□) polymers from 1991. Adapted from Ref. [100]; copyright Elsevier.

the literature [100,107]. An empirical analysis demonstrated a linear relationship between $1/n$ and the difference in the gas diameters (d_j–d_i) [100].

The upper bound analysis is based on homogeneous membranes utilizing data from studies where the permeability and selectivity data were determined on the same films using the same measurement methods. Data from different studies or different film preparation methods would not be accurate enough to provide reliable data for the analysis. Surface modified films, laminates of different films, phase separated polymer blends, polymers containing particulates (such as zeolites) and phase separated block copolymers would not be relevant for this analysis as specific combinations could be fabricated whereby the upper bound can be surpassed based on heterogeneous membrane models [108]. Specifically, a film laminate of a low permeability polymer with a high permeability polymer (both comprising values on or near the upper bound relationship) can yield laminate film values well above the upper bound based on the series resistance model.

The upper bound relationship is an empirical correlation based on experimental data, but a theoretical analysis by Freeman [109] yielded good agreement with the observed empirical results. This theory allowed for the prediction of both the upper bound slope and the front factor. Freeman identified the upper bound slope predicted from activation energy theory as:

$$\lambda_{A/B} = -\frac{1}{n} = \left(\frac{d_B}{d_A}\right)^2 - 1 = \left(\frac{d_B + d_A}{d_A^2}\right)(d_B - d_A) \tag{14}$$

The value of $(d_B + d_A)/d_A^2$ has modest variation compared to d_B–d_A and, therefore, gave reasonable agreement between theory and experimental observations. The value of the front factor, k, required a more complex analysis, yielding the following relationship:

$$\beta_{A/B} = k^{-1/n} = \frac{S_A}{S_B} S_A^{\lambda_{A/B}} \exp\left\{-\lambda_{A/B}\left[b - f\left(\frac{1-a}{RT}\right)\right]\right\} \tag{15}$$

where S_A and S_B represent the gas solubilities. The linear free energy relationship between the activation energy of diffusion, E_{di} and D_{0i} [109–111]:

$$\ln D_{0_A} = a\frac{E_{d_A}}{RT} - b \tag{16}$$

was employed to determine values of a and b, where a is 0.64 and b has values of 9.2 and 11.5 for rubbery and glassy polymers, respectively [35]. The parameter, f, was determined from the following expression relating activation energy of diffusion with the diameter of the penetrant molecule [109,112]:

$$E_{d_A} = cd_A^2 - f \tag{17}$$

Values of c and f are adjustable and relate to a specific polymer. Freeman observed the best match between the empirical upper bound lines and the theory was attained with $f = 12{,}600$ cal/mole [109]. The solubility constant for gases may be correlated with the gas critical temperature, T_c, boiling point, T_b, or Lennard-Jones temperature (ε/k) by the following equations [35]:

$$\begin{aligned} \ln S_A &= m + 0.025T_b \\ \ln S_A &= x + 0.016T_c \\ \ln S_A &= y + 0.023(\varepsilon_A/k) \end{aligned} \tag{18}$$

where m, x and y have unique values for each polymer. These relationships appear to work well for a wide variety of polymers (specifically aliphatic and aromatic polymers), except for the polymer class of perfluorinated polymers where the slope values are different [101]. For this analysis, Freeman chose the Lennard-Jones solubility relationship with $y = -9.84$ cm^3(STP)/(cm^3 polymer cmHg) [109]. The comparison of the empirical upper bound results with the predicted results are shown in Fig. 6 for comparison of the front factor k.

The upper bound observation for gas separation has been also proposed for other transport processes including fuel cell membranes and water desalination using similar log–log plots [114–117]. For fuel cell membranes, an empirical upper bound was observed with experimental data plotted as proton conductivity versus water sorption for proton exchange membranes. For water desalination, experimental water/salt selectivity versus water permeability was plotted and compared with theoretical considerations.

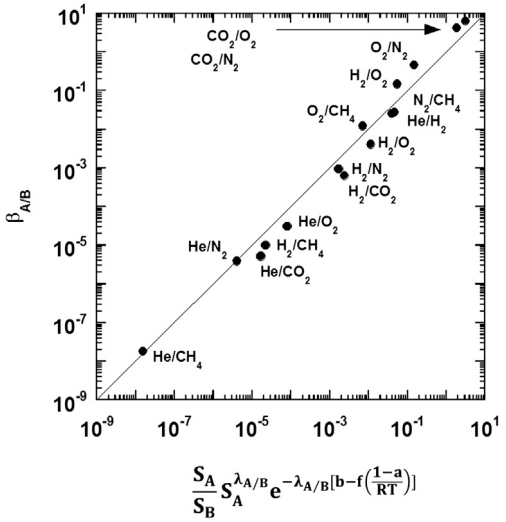

Fig. 6. Comparison of the front factor k from the experimental data with the prediction values. The parameter f was set to 12,600 cal/mol. The units of $\beta_{A/B}$ are (cc(STP)-cm/cm^2-sec-cmHg)$^{-1/n}$ ($\beta_{A/B} = k^{-1/n}$) (note i = A and j = B relative to the discussion from Ref. [109]; Adapted from Ref. [113]; Copyright Elsevier).

As more data on polymer gas separation characteristics beyond what was utilized in the 1991 analysis became available, a revised compilation was published [101]. As would be expected, some shifts in the upper bound resulted. However, most of these shifts were minor and involved changes in the front factor while the upper bound slope values remained virtually unchanged. Significant shifts in the front factor are primarily due to recent data on perfluorinated polymers that did not exist in 1991. The solubility relationship for perfluorinated polymers for gases is different than that for aliphatic and aromatic polymers as discussed above [118]. The gas pairs where significant shifts were noted for perfluorinated polymers primarily involved helium as the fast gas. Without the inclusion of the perfluorinated polymer data, the upper bound relationships noted in 1991 showed minor changes for all gas pairs of interest. The results of the recent data on O_2/N_2 separation compared with the initial 1991 publication are illustrated in Fig. 7 showing a minor shift in the empirical upper bound resulting from intensive optimization of structure–property relationships. An illustration of the deviation of perfluorinated polymer data, involving He as the fast gas, from data obtained with other polymeric structures is given in Fig. 8. This figure illustrates that perfluorinated polymers exhibit a unique upper bound relationship relative to their aliphatic and aromatic counterparts.

The permeability database from the recent upper bound paper [101] was also used to correlate gas permeability data in a different format. The data show that as the permeability of one gas (from the list of common gases) increases, the permeability for other gases also increases [113]. This result is a consequence of the diffusion coefficient of the gases being related to the free volume of the polymer. The solubility ratio of the gases is also predicted to be in a tight range for the myriad of polymers available [100]. The database covers over ten orders of magnitude in permeability values that form a linear log–log relationship for all gas pairs (chosen from He, H_2, O_2, N_2, CO_2 and CH_4). In this correlation, log P_i is plotted against log P_j yielding a linear relationship for all gas pairs over the experimental permeability range. The value of i and j are chosen such that $n > 1$ in the relationship:

$$P_j = k_c P_i^n \tag{19}$$

A representation of the above analysis is shown in Fig. 9 for the gas pair CO_2/N_2. Alentiev and Yampolskii reported similar correlations [119].

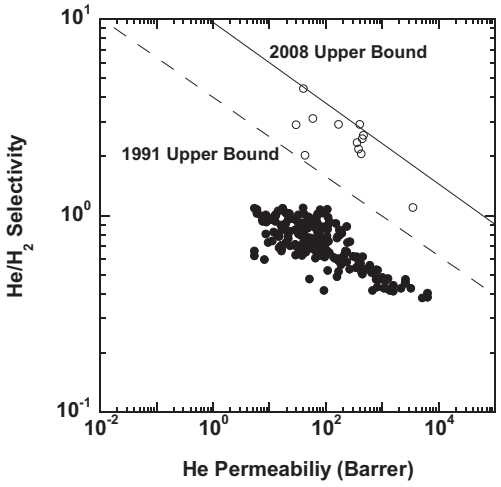

Fig. 8. The upper bound correlation for He/H_2 membrane separation. Adapted from Ref. [101]; copyright Elsevier. Unfilled circles represent perfluoropolymers and filled circles represent other polymers.

The value of k_c in Eq. (19) is correlated with the Freeman theory developed for the upper bound relationship and gives an excellent fit of the experimental data with theoretical predictions. This analysis provides strong additional verification of the validity of the theory and provides a means for determination of kinetic diameters for the common gases of interest that represent an improvement over the values employed previously based on the zeolite based data of Breck [107]. These updated gas diameter values are recorded in Table 1 along with the kinetic diameter values from Breck for comparison.

The upper bound relationship is based on data in the temperature range of 25–35 °C. In a recent publication [120], it was noted that the upper bound shifts with temperature and the Freeman theory was utilized to predict the shift for a number of gas pairs of interest.

Group contribution methods have been applied to ascertain the specific structural features of aromatic polymers that lead to optimizing permeability and separation. Two approaches from separate groups were published by Park and Paul [121] and by Robeson et al. in a similar time frame [122,123]. While both approaches superficially appeared to be quite different, close observation show they

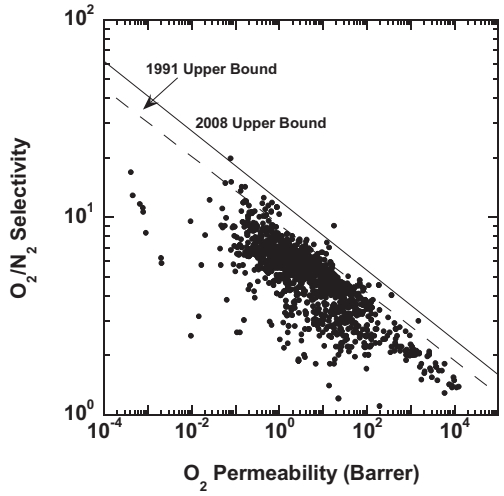

Fig. 7. The upper bound correlation for O_2/N_2 separation. Adapted from Ref. [101]; copyright Elsevier.

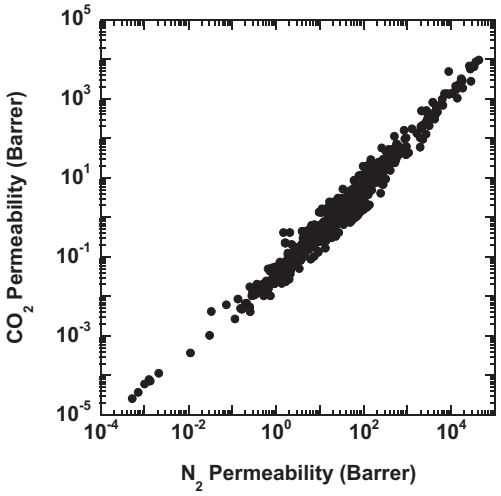

Fig. 9. Permeability correlation for CO_2/N_2. Reprinted with permission from Ref. [113]; copyright Elsevier.

Table 1
Breck kinetic diameter and correlation diameters for common gases.

Gas	Breck kinetic diameter, Å [107]	Correlation diameter, Å [113]
He	2.6	2.644
H_2	2.89	2.875
CO_2	3.3	3.325
O_2	3.46	3.347
N_2	3.64	3.568
CH_4	3.8	3.817

were actually quite similar and allowed for predicting both permeability and selectivity of aromatic polymers with good accuracy. The resulting group contribution predictions allowed for a quantitative determination of the effect of many structural variables including linking groups, *iso* versus *para* substitution, aromatic group substitutions, alkyl versus halide substitution and symmetry around the main chain. A much larger (and unpublished) analysis was employed in the industrial laboratory approach [122,123] to circumvent the synthesis of large numbers of polymers for experimental analysis.

3.2. Physical aging

While the permeability/selectivity tradeoff is a widely recognized challenge, there are other significant material challenges, such as physical aging, that affect a polymer's industrial viability. Many polymers used in gas separations are glassy materials [15,124]. Glassy polymers are nonequilibrium materials having excess free volume due to kinetic constraints on polymer segmental motion that prevent such materials from coming completely to equilibrium properties (*e.g.*, specific volume) once they are below their glass transition temperature. However, even in the kinetically constrained glassy state, polymers undergo at least local scale segmental motions, and these motions act to gradually increase the density of the polymer (and, therefore, reduce its free volume) toward the thermodynamic equilibrium value [125]. Physical aging slows over time for two reasons: (1) as the excess free volume gradually decreases the driving force for physical aging is diminished, and (2) as free volume is reduced, polymer chain mobility decreases, which decreases segmental motions available to assist in reorganizing the polymer chains. Physical aging reduces gas permeability and alters other physical properties of polymers (*e.g.*, specific volume, enthalpy, entropy, *etc.*) [126–133]. The observed decrease in permeability, usually accompanied by an increase in selectivity, is seen as a reduction in membrane flux over time. Recently, it has become widely recognized that physical aging also depends on the thickness of the polymer under study, particularly when the thickness becomes of the order of less than 1 micron. Gas separation membranes are often believed to be on the order of approximately 0.1 μm thick, making the effects of thickness on aging a relevant field of study [127].

Eq. (20) presents the most common framework used to describe physical aging [125,127]

$$\frac{dV}{dt} = \frac{-(V - V_\infty)}{\tau} \tag{20}$$

where the rate of change in the specific volume, V, of a polymer with time depends on the departure of the polymer's specific volume from its equilibrium value, V_∞, and the characteristic timescale for relaxation of the specific volume toward equilibrium, τ. The characteristic relaxation time is related to the mobility of the polymer chains, and it is typically taken to be a function of the specific volume of the polymer and temperature [127]. Additionally, the dependence of physical aging on sample thickness is typically accounted for by allowing τ to vary with thickness, suggesting that molecular mobility of polymer chains near free interfaces may be greater, at least initially following the beginning of an aging experiment, than that of polymer chains in bulk polymer [127]. The fractional free volume is directly related to a polymer's specific volume, as discussed in Section 1. Therefore, as a polymer ages and fractional free volume decreases, gas permeability also decreases, albeit at slower and slower rates as time goes on, due to the self-retarding nature of physical aging. Because the losses in permeability and densification due to physical aging come from relaxation of the polymer matrix, they are thermally reversible, so losses in permeability (*i.e.*, increases in density) can be restored by heating the polymer above its T_g [134].

Because of the relationship between free volume and physical aging, the aging of high free volume polymers has been a point of interest in the literature. In particular, the aging of PTMSP, one of the most permeable polymers known, has been widely studied [135–140]. Many of these studies have documented a rapid loss in gas permeability as a function of time, but the permeability of PTMSP films is also affected by contaminants, such as vacuum pump oil, that can lead to discrepancies in these measurements. In a study accounting for this contamination, PTMSP films with thicknesses of approximately 100 μm still showed significant physical aging [137]. Permeabilities of CH_4, O_2, and N_2 decreased by more than 20% over roughly 200 days. These films were first preconditioned in methanol, increasing the initial free volume, which increases the driving force for physical aging [137]. In contrast, Pfromm and Dorkenoo found no loss in permeability in an 85 μm PTSMP film that was not pretreated with methanol; however, thin films with thicknesses of 1 and 3 μm showed 76% and 38% losses in N_2 permeability, respectively [140]. These results show the complexity of physical aging and the importance of membrane preparation conditions in physical aging studies.

However, physical aging is not restricted to only high free volume glassy polymers; it occurs in any glassy material. For example, thin films of glassy polyimides, such as 6FDA-DAM, underwent an order of magnitude decrease in permeability over 1000 h [131]. The rate of physical aging is often characterized by a parameter, r, which is defined as follows [137]:

$$r = -\left(\frac{d \ln V}{d \ln t}\right)_{P,T} \tag{21}$$

In Eq. (21), the higher the value of r, the more rapid the physical aging in a material. Interestingly, a rough correlation between the rate of physical aging and the fractional free volume has been observed for a number of polymers; a basic form of this correlation is presented in Fig. 10, although the relationship is likely more complicated. That is, higher free volume glassy polymers tend to age more rapidly than lower free volume polymers, all other factors (*e.g.*, thickness) being equal.

The dependence of physical aging on thickness on physical aging has become a growing area of study. Physical aging rates increase substantially, as tracked both by gas transport and optical properties, as films approach sub-micron thicknesses [127–129,132,134,141–152]. For example, in polysulfone, significant deviation from the aging behavior in bulk films is seen once films become thinner than roughly 10 μm, while thicker films age at rates similar to bulk films [144].

The physical aging of ultrathin films has also been examined. The ultrathin regime encompasses polymer films thinner than 400 nm [127]. Fig. 11 presents the impact of film thickness on oxygen permeability of Matrimid®, pictured later in Fig. 25, a commonly studied gas separation polymer. The differences in oxygen permeability as a function of thickness at short aging times

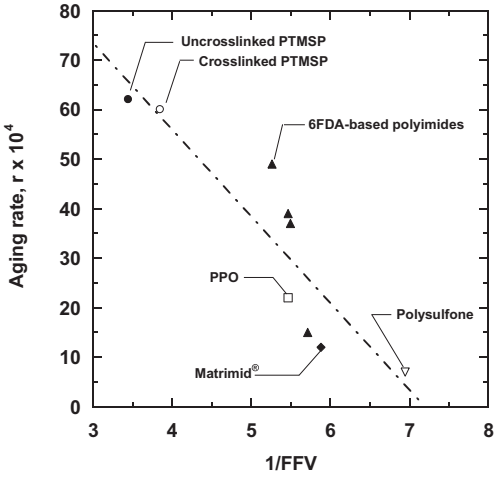

Fig. 10. Effect of fractional free volume on the physical aging rate of selected polymers including cross-linked and uncross-linked poly(1-trimethylsilyl-1-propyne) (PTMSP), and poly(2,6-dimethyl-1,4-phenylene oxide) (PPO). Aging rate is defined in Eq. (21). All films were approximately 400 nm thick. Adapted from Kelman et al. [137]; copyright Elsevier.

is attributed to rapid physical aging in the first hour after quenching the samples from above to below T_g to start the aging experiment, but before the samples could be prepared for permeability testing [127]. Even within the ultrathin regime, thinner samples generally have higher rates of physical aging, as judged by the slope of the permeability versus log aging time results in Fig. 11. Increased physical aging at such thicknesses is practically relevant, because commercial membranes have effective thicknesses on the order of 100 nm. At this thickness or thinner, physical aging can lead to a rapid loss in transport properties that would not be expected based on bulk properties.

The thickness dependence of physical aging has interesting implications for gas separation membranes. Historically, the effective thickness of the dense layer of asymmetric gas separation membranes is estimated by measuring gas flux and back-calculating the thickness based on bulk permeability values. However, because the calculated thickness of these dense layers is in the ultrathin regime, the bulk permeability may not be an accurate indicator of the permeability through the thin, dense skin of the membrane. If so, then the true thickness of the separating layer of commercial gas separation polymers may, in fact, be substantially thinner than the often-quoted figure of approximately 100 nm.

3.3. Plasticization

As the concentration of gas inside a polymer increases, the polymer can swell, which increases free volume and chain motion that, in turn, increases gas diffusion coefficients and decreases diffusion selectivity. This phenomenon is known as plasticization. Plasticization often results in higher gas flux but lower mixed gas selectivities, particularly at high pressures [30,153,154]. One common signature of plasticization is an increase in permeability of a gas as the upstream partial pressure of that gas increases. However, strictly speaking, increases in permeability can be due to either increases in solubility, increases in diffusivity, or both, and plasticization is typically associated with increases in permeability driven by increases in gas diffusion coefficients as upstream pressure and, therefore, the concentration of gas dissolved in the polymer, increases [155]. Another common symptom of plasticization is an increase in permeability of all components in a mixture and a loss in selectivity as upstream total pressure (or partial pressure of one or more components) increases [156].

CO_2 is a common gas used in plasticization studies [50,141,142,157–164]. Among gases of importance in gas separation applications, CO_2 is often among the more soluble gases, and plasticization by CO_2 is widely known and studied in relation CO_2 removal from natural gas (*i.e.*, methane) [165]. Many polymers sorb enough CO_2 at accessible pressures to strongly plasticize, so it is a convenient penetrant for such studies.

For glassy polymers that plasticize, gas permeability generally decreases with increasing feed (*i.e.*, upstream) pressure until plasticization occurs and gas permeability begins to increase with increasing pressure [159,164,166]. For CO_2 in glassy polymers, typical plasticization pressures are 10–35 bar for polymers relevant to gas separations, and it has been suggested that the CO_2 concentrations in such polymers are similar, ranging from 30 to 45 cm^3(STP)/cm^3 polymer, at the plasticization pressure [159]. Polymers that sorb less CO_2 are often thought to be less prone to plasticization than those sorbing more CO_2 at a given pressure,

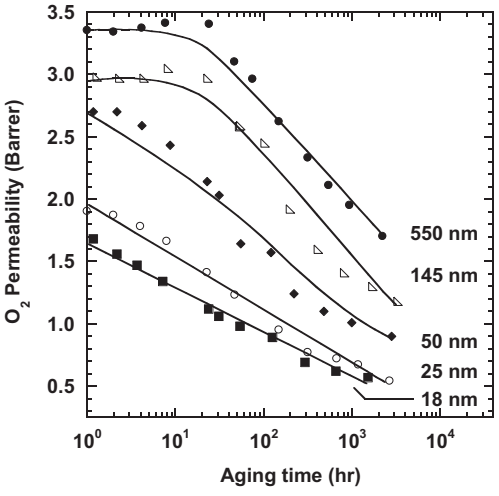

Fig. 11. The effect of film thickness on Matrimid® with PDMS coating O_2 permeability in ultrathin films. Permeability measured at 35 °C and 2 bar. Adapted from Rowe et al. [127]; copyright Elsevier.

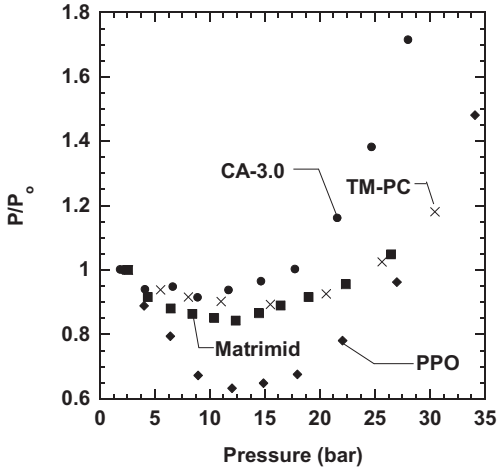

Fig. 12. Relative permeability (where P_0 is permeability at a feed pressure of roughly 1 bar) as a function of feed pressure for selected glassy polymer films. Cellulose triacetate (CA-3.0) at 24 °C (●), Matrimid® at 22 °C (■), tetramethyl bisphenol A polycarbonate (TM-PC) at 25 °C (×), and poly(2,6-dimethyl-1,4-phenylene oxide) (PPO) at 25 °C (◆) [159].

though this guideline should not be viewed as a universal rule. Fig. 12 presents the relative change in permeability with feed pressure for four polymers commonly studied in the gas separation literature. The relative increase in permeability and plasticization pressure varies from polymer to polymer, highlighting the continuing need to explore plasticization in greater depth as new materials are developed.

In addition to a rapid increase in permeability with increasing feed pressure, polymers undergoing plasticization may also display a slow increase in permeability over timescales far exceeding those required to achieve steady state. This behavior in Matrimid® polyimide is shown in Fig. 13. Despite an expected time lag of seconds or minutes, depending on film thickness, CO_2 permeability continues to increase with time even after 2 h [141]. The effect of film thickness on these increases in permeability will also be discussed later [141]. This upward drift in permeability and related properties has also been noted in other polymers. For example, CO_2 sorption in polyethersulfone at high pressures can continue to increase for more than six days without reaching equilibrium [167]. Cellulose acetate, which is widely known to plasticize in the presence of CO_2, has shown approximately a 40% increase in CO_2 permeability with time at constant feed pressure [168].

This change in permeability with time suggests that, when exposed to CO_2, the properties of these glassy, nonequilibrium materials are changing due to CO_2 swelling-induced structural relaxation and solid-state reorganization in the polymer [158,168]. As polymers swell due to increased penetrant concentration, diffusion coefficients can increase due to increasing free volume, increasing chain mobility, or both [159,167]. These increases in diffusivity are often described as plasticization. In addition to changing diffusion coefficients, increased penetrant concentration at higher pressure can also influence permeability, solubility, selectivity, and mechanical properties.

Glassy polymers undergoing plasticization may also show hysteresis in permeation properties, with transport properties at a given pressure being different depending on whether permeability was measured during pressurization or depressurization, but this phenomenon alone does not definitively identify plasticization. This effect has been observed in many different polymers, but the degree of hysteresis often varies from polymer to polymer [165,168–171]. Fig. 14 presents an example of CO_2 permeability hysteresis in cellulose acetate. In this case, CO_2 permeability was first measured as a function of increasing feed gas pressure; then, the permeability was measured as the sample was held at the highest gas pressure considered; finally, gas permeability was measured as feed pressure was decreased [168]. Gas permeabilities measured as feed pressure was decreased are substantially higher than those measured while feed pressure was being increased. When the sample was continuously exposed to the highest feed pressure considered (*i.e.*, 30.4 bar), permeability gradually drifted upwards, reflecting a slow swelling of the polymer by the gas. This hysteresis is the result of conditioning this glassy polymer by the CO_2, where exposure to CO_2 presumably causes the polymer to dilate, increasing the free volume of the material; because the polymer is a nonequilibrium glass, changes in the free volume of the polymer due to such process history effects can be relatively long-lived [32]. This phenomenon of permeation hysteresis is, like physical aging, another manifestation of the nonequilibrium nature of glassy polymers used in most gas separation applications today.

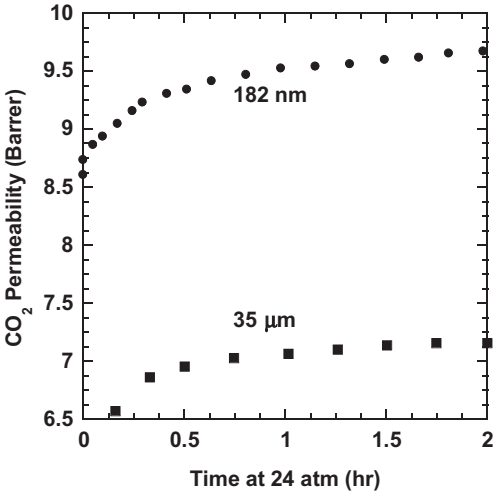

Fig. 13. CO_2 Permeability through Matrimid® films as a function of time after the feed pressure was set to 24.3 bar. Films were previously held at 8.1 bar and 16.2 bar. 182 nm (●) and 35 µm (■) thick films were considered at 35 °C [141].

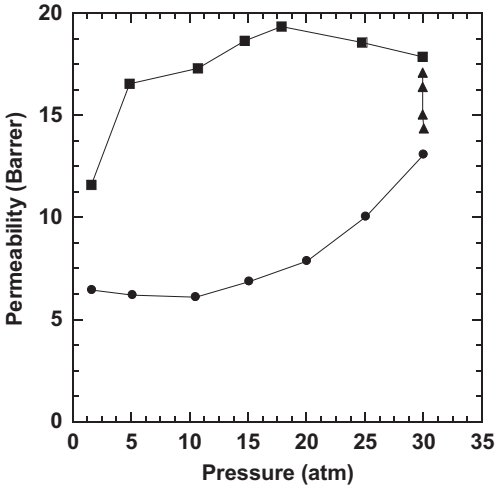

Fig. 14. CO_2 permeability as a function of feed pressure for cellulose acetate at 35 °C. (●) indicates permeability measurements made as feed pressure was increased, (▲) indicates measurements made while feed pressure was held constant at 30.4 bar, and (■) indicates permeability measurements made as feed pressure was decreased. Adapted from Ref. [168]; copyright Elsevier.

Increasing CO_2 permeability and plasticization of the polymer membrane can cause selectivity to decrease under mixed gas conditions in separations such as natural gas purification, which is typically represented as a CO_2/CH_4 separation [154,156]. This decrease in selectivity is due to the CH_4 permeability increasing more with increasing pressure than that of CO_2, and it is typically thought to be a result of the free volume increases caused by CO_2-induced plasticization, similar to the way CO_2 plasticization has been shown to effect CO_2/ethane and CO_2/CH_4 selectivity in various polymers [172]. A more rapid increase in CH_4 than CO_2 permeability as free volume increases is predicted by the Cohen-Turnbull theory Cohen-Turnbull theory as seen in Eq. (1) [29]. This decreasing selectivity has been observed in cellulose acetate, Matrimid®, and many other materials [168,173].

While this section has focused on plasticization caused by CO_2, plasticization can be caused by any component or even impurities in a feed stream [160,174]. Penetrants that exhibit higher sorption in polymers are more likely to cause plasticization and conditioning effects. One practical example is the plasticization of membranes used for natural gas purification by higher hydrocarbon contaminants in the feed [175].

Recently, the plasticization behavior of films with thicknesses of about 200 nm was characterized. These results were compared to those obtained using films with thicknesses ranging from 20 to 50 μm, and the thin films showed a much larger increase in permeability at the same CO_2 concentration [141,142]. These changes in permeability also occurred over a much shorter timescale in thin films. While much is still unknown about this behavior, the discrepancies between thick and thin film behavior have been attributed to the difference in relaxation time distribution between thick and thin films [141,142]. Plasticization and physical aging occur in both thin and thick films; however, as demonstrated in Fig. 15, these effects are much more prominent in thin films [141,142]. In roughly the first 5 h, the transport properties of the thin film are dominated by plasticization and permeability increases. However, at longer times, the transport properties are dictated by physical aging, and a decrease in permeability is observed. Because the timescale for plasticization is longer and the effects of physical aging less dramatic in thick films, the same behavior is not seen in the thick film. An understanding of plasticization in thin films and how it differs from widely studied thick films with thicknesses of 20–50 μm is interesting from a fundamental standpoint, but it also has practical ramifications because commercial gas separation membranes have effective thicknesses in the hundreds of nanometer range [9].

4. Current commercial membrane gas separation

Separations consume 4500 trillion Btu of energy per year in the United States, which is approximately 22% of all in-plant energy use [71]. Much of this energy consumption is associated with distillation. Over 40,000 distillation columns are used for over 200 different separations in the United States, which accounts for 49% of industrial separation energy consumption [71]. Other separation processes include absorption, crystallization, and membrane separations. Of these processes, membranes are attractive because they do not involve sorbents and do not require a thermal driving force to separate mixtures.

Industrially, membranes are currently used for acid gas removal, nitrogen enrichment, ammonia purge gas recovery, refinery gas purification, oxo-chemical synthesis, and dehydration. Representative gas pairs needing separation in these applications are shown in Table 2.

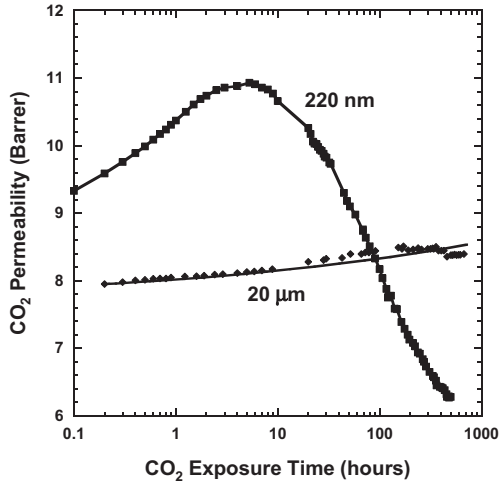

Fig. 15. Simultaneous physical aging and plasticization in 200 nm and 20 μm Matrimid® films, which were aged 200 h at 35 °C and then exposed to CO_2 at 32.4 bar [141].

Table 2
Primary current industrial gas separations for polymer membranes.

Gas pair	Application
CO_2/CH_4	Acid gas treatment
N_2/O_2	Nitrogen enrichment
H_2/N_2	Ammonia purge gas recovery
H_2/CH_4	Refinery gas purification
H_2/CO	Syngas ratio adjustment
H_2O/Air	Dehydration

4.1. Hydrogen recovery

Hydrogen is often highly permeable in polymers and typically is much more permeable than other gases, such as nitrogen, methane, and carbon monoxide, leading to high selectivity for hydrogen in gas mixtures for many polymers. As a result, hydrogen separation from mixtures with other gases was an initial target for membrane separations [71]. Currently, hydrogen separation membranes are used for recovering ammonia purge gas, oxo-chemical synthesis, and refinery off-gas purification [9,14,176,177].

Hydrogen recovery from ammonia purge gas was the first large-scale commercial gas separation membrane application [14]. Ammonia is synthesized via the Haber process by reacting nitrogen and hydrogen over a catalyst at high pressures (*e.g.*, >101 bar) and high temperatures (*e.g.*, >400 °C) [178]. Nitrogen is typically obtained by cryogenic distillation of air. Small quantities of argon, which is a trace component in air, remain in the nitrogen feedstock even after liquefaction. Hydrogen is produced by steam reforming of hydrocarbons (often methane), so even after purification, hydrogen will contain low levels of residual methane [178]. Because reactor yield is less than 30%, a recycle loop is needed to achieve adequate conversion of reagents, and argon and methane that would otherwise build up in the reactor are purged from the recycle loop, resulting in a loss of hydrogen gas from the process [178]. Today, gas separation membranes are used on the reactor purge stream to mine hydrogen from the purge gas, recycling it to the process.

Monsanto was the first company in this market, offering a polysulfone hollow fiber system marketed as Prism® membranes around 1979 [11]. Today, membranes used for ammonia purge gas recovery represent proven technology. Prism® membranes can achieve 95% recovery of H_2, and certain systems have been in operation since 1979 [179].

Other hydrogen separations involve adjusting molar ratios of syngas (H_2/CO) and hydrogen recovery in refinery hydrotreaters (H_2/CH_4). Syngas is a mixture of H_2 and CO produced from steam reforming of natural gas, oxidation of heavy oils, or gasification of coal or coke [180]. Depending on the method used to produce syngas, H_2:CO ratios will vary between 1 and 5 [181], and this ratio must be adjusted for specific synthesis applications. Because H_2 can easily be separated from CO with gas separation membranes, this application was an early target for membrane-based separations. Prism® membranes introduced by Monsanto were first installed in 1977 for syngas ratio adjustment [179], and other companies now offer a range of gas separation membranes for these applications [176].

Refinery off gas purification is another hydrogen-based commercial membrane application. Petroleum crude feedstocks contain many different molecular weight products that must be separated before use. The heavier fraction of these products is often cracked, *i.e.*, broken into smaller components, through a catalytic process known as hydrocracking. This process relies on injecting hydrogen into the cracker to improve several aspects of the reaction chemistry. For example, hydrogen often reacts with polycyclic

aromatic compounds that are generally inert to other cracking processes. Furthermore, hydrogen helps eliminate unsaturated hydrocarbons and reduces the formation of tar and coke [182]. Increasing the purity of hydrogen used in a hydrocracker can increase the life of the cracker catalyst and increase the production of higher paraffinic compounds [182]. It is highly desirable to recycle H_2 from the hydrocracker products to the hydrocracker feed. Polymer membranes are used in the recycle loop to achieve this separation. Being a high-throughput process, membranes with H_2/CH_4 selectivities of approximately 20–25 and very high permeabilities are suitable for this application [182]. Such selectivities are readily obtained with many glassy polymers, and membrane systems have also been deployed using polymers having H_2/CH_4 selectivities above 100, though the higher selectivity is often accompanied by lower permeability [183]. Like with many other hydrogen separations, Prism® membranes are often used for refinery off gas purification [14].

4.2. Air separation

Today, air separation is accomplished by several industrial processes, including cryogenic distillation, pressure swing adsorption (PSA), and membranes [82,98,184]. By far, the largest market penetration for membrane-based air separation is for nitrogen enrichment applications [9,14,98]. However, for users who require N_2 flowrates between approximately 5000 scfd (5.9 m^3/h) to 1 MMscfd (1180 m^3/h), membranes are often the most economical option, especially if required N_2 purity is between about 95 and 99% [14]. The competing technologies (*i.e.*, cryogenic distillation and PSA), are used to process higher gas flowrates and, for cryogenic distillation, to achieve higher purity N_2 [87]. Over the past 25 years, developments of higher performance polymers have helped advance the range of N_2 purity and flowrate that can be economically accessed with membrane systems [9,14,87,98,185].

Several N_2 enrichment applications for membranes include refrigeration, inerting [184], and other niche markets [186]. Many other high-volume, high-purity N_2 applications exist, such as enhanced oil recovery, metallurgical processes, and gas feeds for the electronics industry, but these applications are not typically pursued as membrane-specific separation processes because of the large gas volumes or high gas purity that is required for these N_2 streams [98].

Designing a membrane system requires a balance and optimization of many parameters such as compressor costs, purity requirements, gas flowrates, and gas rejection specifications that are highly process-specific [9,14,73,98]. Membranes with selectivities as low as 2 can be used to produce 99% pure N_2; however, at these conditions, N_2 recovery is very low, and compressor costs are, accordingly, high for such N_2 enrichment applications [14]. Therefore, much of the early work in this field focused on improving membrane selectivity.

Some of the earliest air separation membranes were produced by Generon and Permea in the mid-1980s [9]. The Generon membranes were made of poly(4-methyl-1-pentene) (TPX), and had selectivities of approximately 4, which limited their use [9]. Research into new membrane materials and design quickly improved air separation performance, and by the early 1990s, several new hollow fiber membranes were brought to market, including tetrahalogenated bisphenol based polycarbonates by Generon [54], polyimides by Praxair [9], and polyimide and polyaramide membranes by Medal [9]. During this time, the push for nitrogen enrichment applications brought about significant advances in the design and fabrication of many asymmetric membrane systems. Eikner et al. summarize 44 patents describing these advances [187].

Commercial membranes have also been developed for applications in air dehydration [97,188,189]. These membranes lower the dew point of air by selectively permeating water over nitrogen, oxygen, argon, and other components in air [97]. The first type of air dehydration membrane was marketed in 1987 by Permea Inc. and was used to replace desiccants in refrigeration dehydrators [190]. These membranes were also used to produce dry air for military applications such as fire control, electronics, and communication systems [190]. Today, Air Products sells dehydration membranes under the trade name CACTUS® for high pressure dehydration applications up to 1200 psig (83.7 bar). In the US, China and the European Union, compressing air requires approximately 10% of all electricity used by industry [191], and membrane dehydrators are widely used today to dry compressed air due, in part, to the simplicity and reliability of such systems relative to the competing technology, which is based on condensation or solid desiccants [14].

An additional air separation membrane application is On-Board Inert Gas Generation Systems (OBIGGS), which involves generation of nitrogen-enriched air for fuel tank blanketing to reduce the potential for explosion of flammable fuel/air mixtures in the head space of fuel tanks [99,192–197]. Although military aircraft fuel tanks, in many cases, were inerted using air separation membranes for many years [192,198], following the explosion and crash of TWA Flight 800 in 1996, which was blamed on a fire in the fuel tank, the US Federal Aviation Administration (FAA) began exploring the possible use of such systems on commercial aircraft [199]. These systems have been installed on many commercial aircraft to date to reduce the potential for sparks from rotating components and wires installed in fuel tank systems causing fires [200].

4.3. Natural gas purification

Natural gas is a complex mixture of methane, carbon dioxide, ethane, higher hydrocarbons, hydrogen sulfide, inert gases, and trace components of many other compounds, such as BTEX aromatics (benzene, toluene, ethylbenzene, and xylenes) [10]. The actual composition of natural gas varies depending on the well, and delivery of gas to the U.S. national pipeline grid requires that all natural gas be treated, at least to some degree. This treatment is designed to prevent pipeline corrosion as well as adjust the heating value and dew point of the fuel to a standard level. U.S. pipeline specifications require that natural gas contains less than 2% CO_2, 4 ppm H_2S, and 7 lb/MMscf water [201]. Moreover, it must have a heating value of 950–1050 Btu/scf and a dew point of −20 °C or less [14].

Removal of CO_2 and H_2S (*i.e.*, acid gases) from natural gas is a growing area for membrane technology. In 2008, it was estimated that the worldwide market for natural gas separation equipment was approximately $5 billion/yr, and membrane technology accounted for approximately 5% of this market [10]. Furthermore, the membrane market is estimated to grow to $220 million/yr by 2020 [9]. Membrane separation competes most directly with amine absorption, which has existed since the 1930s and is commonly used for acid gas separations [202]. The capital costs, energy consumption, plant footprint, and maintenance costs of amine absorption have encouraged the development of membrane systems and membrane/absorption hybrid systems for natural gas purification [203]. The first membranes for natural gas purification were developed in the early to mid-1980s. W.R. Grace (now part of UOP) and Separex (now part of UOP) developed spiral-wound membranes, and Cynara (now part of Cameron) developed hollow-fiber membranes based on cellulose acetate [10]. These cellulose acetate membranes are still widely used today, but polyimides and other materials have gained some traction in this field over the past

15–20 years [10]. These membranes can be configured a variety of ways, but the number of membrane modules, compressors, and the configuration of these system often depends on the desired flow-rate [10,14,185].

5. Selected commercially relevant polymers

Over the last 30 years, polymer membranes have developed into a feasible industrial process for gas separations. During this time, several polymers have been established as common gas separation membranes. This section will highlight commercially relevant polysulfones (PSF), polycarbonates – particularly tetrabromo bisphenol A polycarbonate (TB-BisA-PC), cellulose acetates (CA-DS, where DS is the degree of acetylation of the cellulose), poly(-phenylene oxides) – particularly poly(2,6-dimethyl-1,4-phenylene oxide) (PPO), aramids, and polyimides (PI). In particular, the polysulfone section will focus on Bisphenol A based polysulfones and other modifications of these polymers. The polyimides section will focus on Matrimid® and BPDA-ODA, pictured later in Figs. 25 and 26 respectively, while a later section will highlight new developments in polyimides. For comparison, Table 3 and Table 4 present pure gas permeabilities, pure gas selectivities, and free volume measured on dense films for these selected polymers.

5.1. Polysulfones

Polysulfones are characterized by diphenylene sulfone repeat units (–Ar–SO_2–Ar'–), and they are regarded as among the most chemically and thermally durable thermoplastic polymers available [210]. Repeating phenylene rings create backbone rigidity, steric hindrance to rotation within the molecule and an electronic attraction of resonating electron systems between adjacent molecules. These properties contribute to a high degree of molecular immobility, resulting in high rigidity (high T_g), high strength, good creep resistance, dimensional stability, and high heat deflection temperature [211]. The basic repeat units of several commercially available polysulfones (Vitrex® PES, Udel® PSF and Radel®R) are illustrated in Fig. 16. A broad range of polysulfones can be prepared via nucleophilic aromatic (S_NAr) polycondensation of an aromatic dihydroxy compound with a bis-(halophenyl) sulfone. Detailed description of the synthesis of polysulfones can be found elsewhere [210].

Polysulfones are an important commercial membrane material for gas separations due to their excellent mechanical properties, a wide operating temperature range, fairly good chemical resistance, and easy fabrication of membranes in a wide variety of configurations and modules [210]. The first large-scale membrane separation process, developed by Monsanto Co. in the late 1970s, utilized asymmetric hollow fiber membranes of bisphenol A polysulfone coated with a thin layer of silicone rubber [212]. The gas transport properties of commercial PSF and PSF variants, particularly the influence of various bridging moieties between the phenyl rings and the groups substituted on the phenyl rings on gas permeation properties, have been extensively studied [88,206,213–219]. Symmetric bulky substitutions (*e.g.*, methyl groups) on the phenyl rings significantly increase gas permeability, while asymmetric substitution of these same groups decreases gas permeability [220]. For example, replacing the isopropylidene bridging moiety with bulkier groups, like hexafluoro isopropylidene (–$C(CF_3)_2$–), makes the polymers much more permeable, mainly due to the enhanced free volume [213]. However, these large increases in CO_2 permeability can also affect the susceptibility of gas transport properties to plasticization by gases such as CO_2. A combination of hexafluoro isopropylidene groups and symmetric substitution led to the appearance of plasticization effects when CO_2 pressure exceeded approximately 15.2 bar [219].

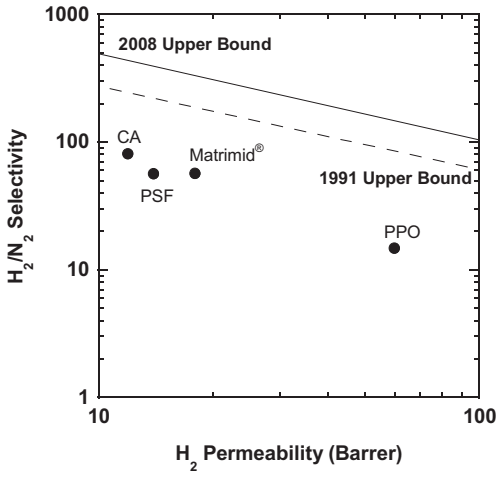

Fig. 17. H_2/N_2 upper bound plot for representative common commercially relevant polymers in Table 3 [100,101].

Polysulfone remains widely used for hydrogen and air separations [9]. Figs. 17 and 18 present the gas separation performance of representative commercial polymers listed in Table 3. Polysulfone has a higher H_2 permeability than cellulose acetate and a lower H_2 permeability than Matrimid®. However, CA, Matrimid®, and PSF are all similar distances from the upper bound in Fig. 17, showing that they tradeoff permeability for selectivity as expected. As seen in

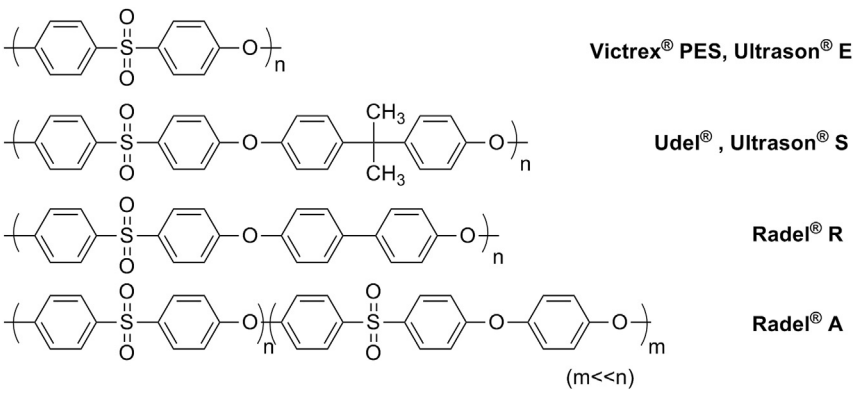

Fig. 16. Chemical structures of several polysulfones.

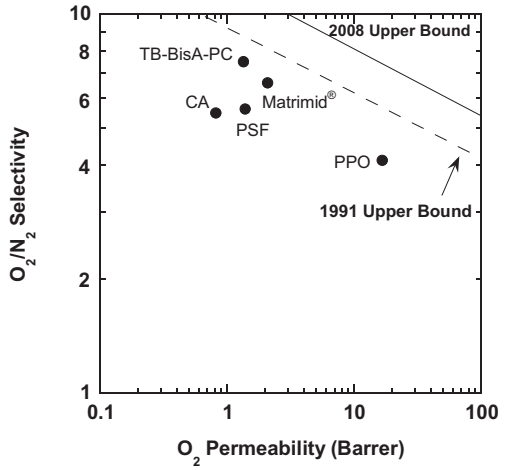

Fig. 18. O_2/N_2 upper bound plot for representative common commercially relevant polymers in Table 3 [100,101].

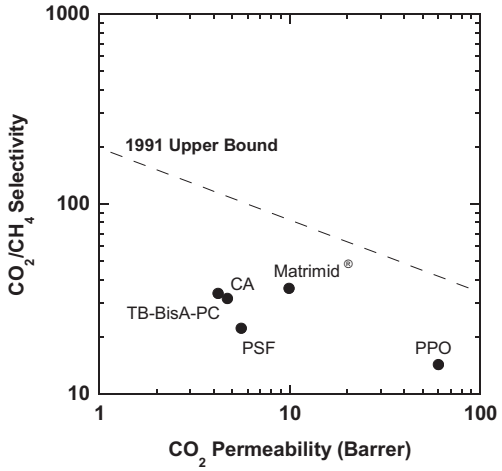

Fig. 20. CO_2/CH_4 upper bound plot for representative common commercial polymers. The data are from the same sources as those in Table 3 [100,101].

Fig. 18 for O_2/N_2 separations, PSF falls below Matrimid® and the tetrabromo bisphenol A-polycarbonate in overall performance as judged by distance from the upper bound line. These polymers will be discussed in more detail in the following sections.

5.2. Cellulose acetates

Cellulose acetate (CA) and its derivatives were among the first generation of commercial membranes used for natural gas separation [9,221–223]. In addition to desirable transport properties, the development of the asymmetric membrane concept by Loeb and Sourirajan, which greatly reduced the surface area necessary to achieve high gas productivity, led to the commercialization of cellulose acetate membranes, initially for use in desalination applications [224]. CA continues to be used in gas separations for removal of acid gases (CO_2 and H_2S) from natural gas as well as the separation of CO_2 from mixtures with hydrocarbons in enhanced oil recovery operations [185].

CA polymers are produced by acetylation of cellulose with a source of acetate esters, typically acetic anhydride or acetic acid, and a catalyst such as sulfuric acid [225]. In general, the family of CA polymers includes a spectrum of semi-crystalline materials of varying degrees of acetylation of the hydroxyl groups on cellulose and will be referred to as CA-DS, where DS refers to the degree of acetylation, or degree of substitution (DS). The degree of substitution refers to the number of −OH groups on each glucose unit that have been esterified by acetyl groups (*i.e.*, $0 \leq DS \leq 3$) [225]. Fig. 19 shows the chemical structure of a cellulose repeat unit with all three hydroxyl groups esterified, commonly referred to as cellulose triacetate (CTA). Cellulose acetates with specific degrees of substitution are commonly produced by converting CA to CTA and hydrolyzing acetates until the desired degree of substitution is reached. CA polymers of varying DS are soluble in organic solvents because acetylation greatly reduces hydrogen bonding and membranes may then be manufactured using the phase inversion process [49].

Although cellulose acetate has been used for nearly 30 years commercially, pure gas permeability and selectivity values position this polymer well below Robeson's upper bound [100,101]. As seen in Table 3, cellulose acetate with a DS of 2.45 has a pure gas CO_2 permeability of 4.8 Barrer, which is less than half that of Matrimid®. This permeability value is a function of the degree of acetylation in these polymers, and varying the degree of acetylation from 1.75 to 2.85 increases CO_2 permeability from 1.84 to 6.56 Barrer [168]. This increase is due to the replacement of polar hydroxyl groups with bulky acetate groups, which decreases polymer density and creates a higher free volume structure [168]. However, as seen in Fig. 20, with a fairly high DS of 2.85, the CO_2/CH_4 selectivity is 33, significantly below 175, which is the selectivity value of the 2008 upper bound at a permeability of 6.56 Barrer.

CA membranes are relatively inexpensive in part because cellulose (the raw material) is an abundant and renewable resource [226]. The technology to produce membrane modules from cellulose acetate is also relatively well developed [227]. There are, however, several inherent limitations of CA membranes, which restrict its use in membrane gas separations. One limitation of cellulose acetate is that it plasticizes in the presence of CO_2. Plasticization can cause the CO_2/CH_4 selectivity of cellulose acetate to decrease in mixed gas environments. For example, the CO_2/CH_4 selectivity decreased from 35 to 31 as CO_2 partial pressure increased from roughly 4.1 bar to 12.7 bar in a 30% CO_2 mixture [156]. This decrease in selectivity would reduce methane recovery in natural gas separations, but it is also accompanied by an increase

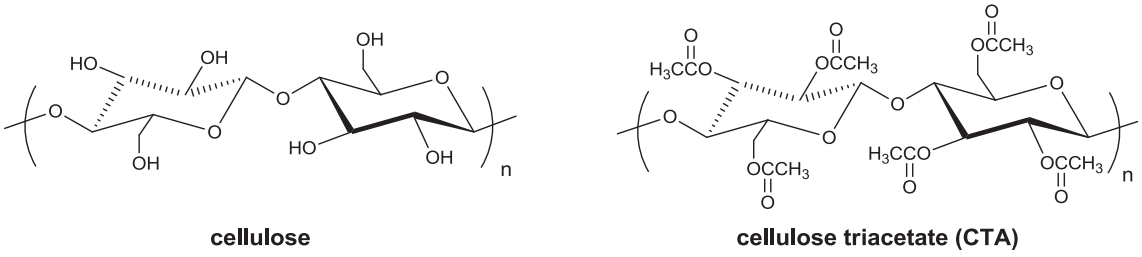

Fig. 19. Chemical structures of cellulose and cellulose triacetate (CTA).

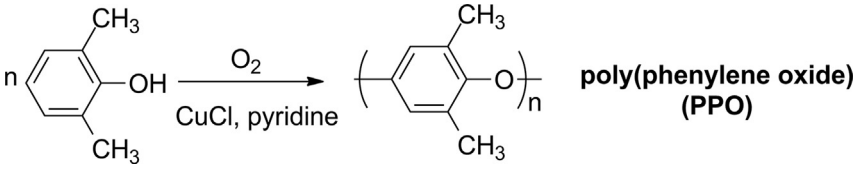

Fig. 21. Synthesis of PPO via oxidative coupling polymerization.

in CO_2 permeability, which would reduce the membrane area required for removing CO_2 from a given amount of natural gas. These changes, which vary with feed gas concentration, mean that the separation performance of cellulose acetate depends on feed composition and feed pressure [228].

5.3. PPO

Poly(2,6-dimethyl-1,4-phenylene oxide) (PPO) is a high-performance engineering thermoplastic with good mechanical properties and thermo-oxidative stability because of a low barrier to rotation and resonance stabilization of the aromatic ether bond (–Ar–O–Ar'–) [229,230]. PPO was the first member of the family of poly(-phenylene oxides) to be commercialized. The material was discovered by Hay [231] over 50 years ago and was commercialized by General Electric [232] (now SABIC Plastics) and AKZO [233]. PPO can be synthesized from substituted phenols via oxidative coupling polymerization which involves the room-temperature oxidative C–O coupling of 2,6-dimethylphenol in the presence of stoichiometric amounts of oxygen. This process is catalyzed by CuCl and an amine ligand, such as pyridine, as shown in Fig. 21. Care must be taken during the oxidative coupling of 2,6-dimethylphenol to avoid undesired C–C coupling that gives rise to small dimeric molecules rather than high molecular weight polymers [210]. The C–O/C–C coupling selectivity and the molecular weight of polymers in oxidative coupling are both strongly dependent on the chemical structure of the phenol monomer, *i.e.*, the substituents and the position of substitution [210]. Other synthetic methods, such as aromatic nucleophilic substitution (S_NAr), electrophilic aromatic substitution using Friedel–Crafts catalysts, Ullman polycondensation, *etc.*, have also been developed to synthesize high molecular weight PPOs [210]. Compared with those methods, catalytic oxidative polymerization is considered a much cleaner process because the reaction can be conducted at moderate temperatures, halogen-free monomers can be utilized, and the only by-product is water.

PPO was the first commercialized aromatic polyether and is still being used in many industrial applications like gas separations [234]. As shown in previous upper bound plots, PPO displays relatively high permeabilities to light gases with moderate overall selectivities, which stems from its chemical and conformational structure of the aromatic ether bond. The kinked ether linkage and the absence of polar groups suppress efficient chain packing and densification, resulting in a relatively large fractional free volume in PPO, as seen in Table 3. The high free volume and the ease of rotation of the phenyl rings about the ether linkages contribute to high diffusivity and permeability, while the moderate gas selectivity comes in part from the absence of polar moieties on the polymer backbone [235]. Therefore, most research on PPO has focused on chemical modification of PPOs with various functional groups to improve the selectivity [217,236–243]. For example, Monsanto developed a cross-linked PPO membrane by brominating PPO and then cross-linking it [241]. The brominated material is typically spun into hollow fibers which are coated with silicone rubber to repair defects [244]. The transport properties can be manipulated by altering the bromine content and degree of substitution [242,243]. PPO has also been modified in various other ways to enhance gas transport properties, and is often blended with impact polystyrene for commercial use [237–240]. In all cases, the membrane properties strongly depend on the extent of chemical modification and the location of substitution, *i.e.*, on the ring or on the methyl groups. Although the properties can be improved via chemical modification, there is still a need to develop an economic and efficient way to conduct such modifications in a controllable manner.

5.4. Aramids

Aromatic polyamides, or aramids, are generally produced from step polymerization or the polycondensation reaction of aromatic diamines with aromatic diacid chlorides. Examples of aramids include poly(*p*-phenylene terephthalamide) (*i.e.*, Kevlar®) and poly(*m*-phenylene isophthalamide) (*i.e.*, Nomex®) [245]. Fig. 22 shows the chemical structures of isomeric phenylenediamines and aromatic diacid chlorides in commercial *meta*- and *para*-aramids.

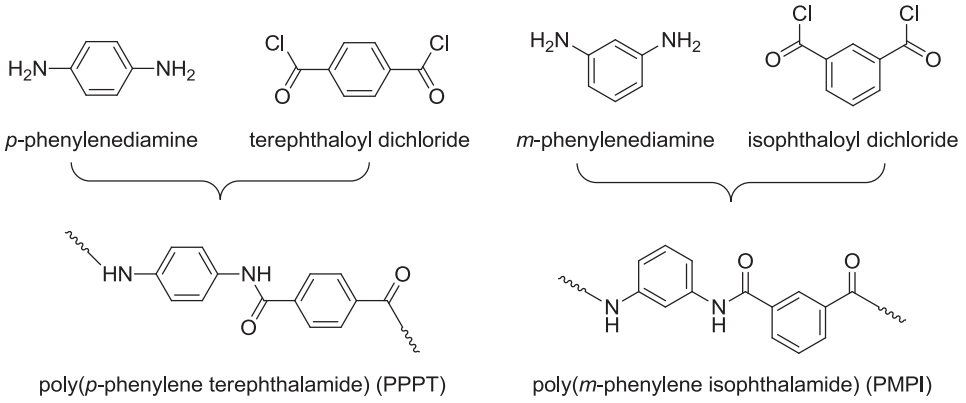

Fig. 22. Chemical structures of phenylenediamines and aromatic diacid chlorides in commercial meta (PMPI) and para-aramids (PPPT).

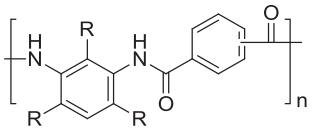

Fig. 23. General structure of aramids reported by Eikner et al. [245].

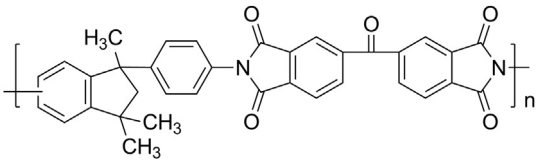

Fig. 25. Chemical structure of Matrimid® polyimide.

These polymers are commercially synthesized via low-temperature polycondensation, typically in a solution of diacid dichloride and phenylenediamine with a tertiary base present to scavenge the liberated hydrogen chloride [246]. The resulting polymer solutions from these polymerizations are often used directly to spin fibers [247,248]. The polycondensation reaction can also be conducted in a two-phase system, via so-called interfacial polymerization [249]. Interfacial polymerization usually produces polymers with a broad molecular weight distribution that are unsuitable for use as fibers [249]. However, cross-linked aramids synthesized via interfacial polymerization of trimesoyl chloride (TMC) with *m*-phenylene diamine (MPD) on a microporous polysulfone support have been commercially applied for many years as reverse osmosis (RO) membranes [250,251].

The wholly aromatic structures of the aramid polymers give them excellent thermal and mechanical properties, which make them useful in technologies such as gas separations [248]. Aramids have been traditionally considered to be very efficient barrier materials; traditional aramids, such as PPPT and PMDI, have extremely low gas permeabilities due to the high packing density (high cohesive energy) of the polymer chains [248]. Therefore, research efforts have been directed toward reducing the interchain hydrogen bonding, thus increasing the free volume via chemical modifications, to yield materials with better solubility (processibility) and improved gas permeability. Using this idea, aromatic polyamides with bulky substitutions on aromatic rings have been designed and synthesized to improve transport properties [252–256].

Publications from DuPont in 1990 and 2001 discuss fiber spinning and properties of high-performance aramids. Theses aramids have the general structure shown in Fig. 23 and, as of 1990, were used to purify a hydrogen feed stream at Conoco's Ponca City Refinery [183,245,257]. Such materials are now more widely used in a variety of hydrogen separation applications. These polymers have H_2 permeabilities ranging from 4 to 40 Barrer and selectivities ranging from 75 to 600 for H_2/CH_4 for a 50/50 mixture of H_2/CH_4 at 90 °C [183]. The transport properties are superior to those of the commercial polysulfone UDEL-3500, and aramids also had higher yield stress and modulus than those polysulfones [183]. Despite their limited number of solvents, aramids can be prepared into spin dopes using a combination of organic and inorganic additives such as polyvinyl pyrrolidone, polyvinylpyridine, LiCl, $MgCl_2$ and others [183].

5.5. Polycarbonates

Polycarbonates are polyesters of carbonic acid (especially derived from phosgene or diphenyl carbonate) that are tough engineering thermoplastics. A commonly used commercial polycarbonate is based on bisphenol A (4,4′-isopropylidene diphenol). Conventionally, polycarbonate was produced via an interfacial phase-transfer catalyzed aqueous caustic process where alkali salts of bisphenol A (or its tetra-substituted variants) in aqueous solution are phosgenated in the presence of an inert solvent (cf., Fig. 24) [258]. Phosgene-free solution or melt processes have been developed to produce polycarbonates via transesterification of diphenyl carbonate with bisphenol A. The melt transesterification process has found special commercial viability in recent years, largely due to its ability to eliminate the need for toxic phosgene [259].

A common modification to polycarbonates is the substitution of aromatic hydrogens with various functional groups as shown in Fig. 24. One of the bisphenol A polycarbonates of interest for gas separation applications is tetrabromo bisphenol A polycarbonate (TB-BisA-PC), where the four hydrogen atoms are symmetrically replaced by Br atoms in the benzene ring (X = Br in Fig. 24) [208]. This material is believed to be a key material in gas separation membranes marketed by Innovative Gas Systems, formerly Generon [186,260]. At the time it was reported, the O_2/N_2 selectivity of 7.5 made TB-BisA-PC one of the most selective polymers available for air separations, and this high selectivity was coupled with a relatively good O_2 permeability of 1.83 Barrer [208]. Among the tetra-substituted polycarbonates reported in the literature, TB-BisA-PC has the highest T_g and density, and, as expected, the lowest free volume, diffusion coefficient, and gas permeability coefficients [208,261]. These properties are a consequence of the introduction of stronger cohesive forces owing to polar halogens that may result in more dense packing and reduced rates of local segmental motion believed to be important in gas diffusion in polymers [208]. This enhanced chain packing contributes to increased O_2/N_2 selectivity in this polymer, making it more attractive for use as an air separation membrane.

Commercial TB-BisA-PC is most likely a polyestercarbonate copolymer, which contains both ester linkages and carbonate linkages in the backbone of the polymer [262]. These polymers are generally prepared via a hybrid process of reacting the tetrabromo bisphenol A with a dicarboxylic acid or dicarboxylic acid halide and phosgene [262].

5.6. Polyimides

In general, aromatic polyimides have high gas permeability and high intrinsic selectivity combined with desirable physical properties, which make them attractive membrane materials. As of 2002, polyimides were reportedly used by Air Liquide, Praxair, Parker-Hannifin, and Ube for various gas separation applications

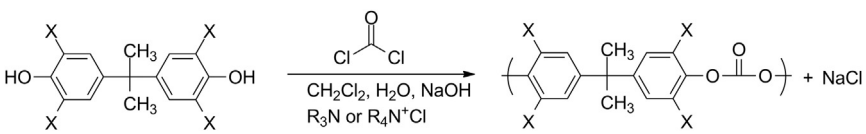

Fig. 24. Interfacial polymerization of polycarbonates. Where X = CH_3 is tetramethyl bisphenol A PC (TM-BisA-PC), X = Cl is tetrachlorobisphenol A PC (TC-BisA-PC), X = Br is tetrabromo bisphenol A PC (TB-BisA-PC).

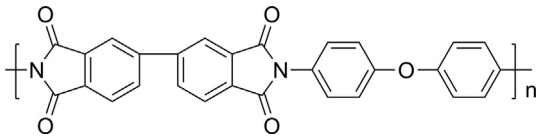

Fig. 26. Chemical structure of BPDA-ODA polyimide.

[9]. Aromatic polyimides are typically the polycondensation products of aromatic dianhydride and aromatic diamine monomers. In a classic method of polyimide synthesis, a tetracarboxylic acid dianhydride is added to a solution of diamine in a polar aprotic solvent at relatively low temperatures (15–75 °C). The resulting poly(amic acid) is cyclodehydrated to the corresponding polyimide by extended heating at elevated temperatures (*i.e.*, bulk solid-state thermal imidization or solution imidization), or by treatment with chemical dehydrating agents (*i.e.*, chemical imidization) [263].

Matrimid® is a commercial aromatic polyimide, consisting of 3,3′-4,4′-benzophenone tetracarboxylic dianhydride (BTDA) and diaminophenylindane (DAPI) [264–266]. DAPI (5(6)-amino-1-(4-aminophenyl)-1,3,3-trimethylindane) has an isomeric phenyl indane; therefore the polyimide formed is a mixture of 6-amino and 5-amino isomers, which are fully imidized during the manufacturing process [266]. The repeat unit structure of Matrimid® polyimide is shown in Fig. 25. The DAPI monomer has a bent phenyl indane ring structure, which is centered about the carbon bridging the indane structure and the phenyl ring. Four bulky groups (*i.e.*, three methyl groups and one phenyl group) stretch out of the plane, which stiffen the polymer backbone (its T_g is greater than 300 °C), and disrupt efficient chain packing. As a result of its isomeric composition and bulky nature, Matrimid® polyimide, along with 6F-containing polyimides, was one of the first aromatic polyimides truly soluble in common organic solvents [264,267].

Matrimid® was originally developed for use in the microelectronics industry [265], but it is also used in gas separation membranes [146,158,268,269]. In addition, its mechanical strength and high T_g suit it better for more rigorous working environments, especially at high temperatures [270]. Furthermore, the good solubility of Matrimid® in common organic solvents allows it to be solution processed, which is a requirement for fabrication into a gas separation membrane [270].

Matrimid® has the best combination of CO_2 permeability and CO_2/CH_4 selectivity among the commercially relevant polymers listed in Table 3, as judged by distance from the 1991 upper bound. With a pure gas CO_2 permeability of 10 Barrer and a CO_2/CH_4 selectivity of 36, Matrimid® has a higher pure gas permeability and selectivity than polysulfone, TB-BisA-polycarbonate or cellulose acetate [204]. However, like cellulose acetate, Matrimid® may plasticize when exposed to gas streams with condensable components such as CO_2 [158,159]. Plasticization results in increased CO_2 and CH_4 permeabilities and a significant loss in CO_2/CH_4 selectivities. Matrimid® CO_2/CH_4 selectivity decreases by approximately 45% in a 55/45 mol% CO_2/CH_4 mixture as the total feed pressure increases from 5 to 50 bar [158]. This decrease in separation efficiency highlights the importance of characterizing mixed gas separation performance (rather than relying solely on pure gas permeation properties to judge a material's performance) and the need for high-performance polymers that maintain their separation characteristics in the presence of plasticizing components.

Table 3
Permeability of common gases and fractional free volume of representative commercially used polymers.

Polymer	CO_2	H_2	O_2	N_2	CH_4	FFV
Matrimid®[a,g]	10	18	2.1	0.32	0.28	0.170
CA-2.45[b]	4.8	12	0.82	0.15	0.15	–
PSF[c,g]	5.6	14	1.4	0.25	0.25	0.144
PPO[d,g]	61	61	16.8	4.1	4.3	0.183
TB-BisA-PC[e,h]	4.2	–	1.4	0.18	0.13	0.092
Selected Aramid[f]	–	24.5	–	–	0.1	–

[a] O_2, N_2, CH_4 at 35 °C, 2 bar (all pressures in these notes refer to feed pressure) from Ref. [146]; CO_2 at 3.4 bar and 35 °C from Ref. [204]; H_2 at 4.1 bar and 35 °C from Ref. [205].
[b] Cellulose acetate (2.45 degree of acetylation), 1 bar and 35 °C from Ref. [168].
[c] Polysulfone, CO_2, CH_4 at 10 bar and 35 °C; O_2, N_2, H_2 at 1 bar and 35 °C from Ref. [206].
[d] Poly(2,6-dimethylphenylene oxide), data from Ref. [207].
[e] CO_2, CH_4 at 20 bar and 35 °C; O_2, N_2 at 1 bar and 35 °C from Ref. [208].
[f] Selected aramid at 90 °C from Ref. [183].
[g] FFV for Matrimid®, PSF, PPO bulk films from Ref. [209].
[h] FFV for TB-BisA-PC bulk film from Ref. [208].

Table 4
Common gas selectivities for commercially relevant polymers.

Polymer	H_2/CH_4	H_2/N_2	CO_2/CH_4	CO_2/N_2	CO_2/H_2	O_2/N_2	N_2/CH_4
Matrimid®	64	56	36	31	0.56	6.6	1.1
CA-2.45	80	80	32	32	0.4	5.5	1
PSF	56	56	22.4	22.4	0.4	5.6	1
PPO	14	15	14	15	1	4.1	0.95
TB-BisA-PC	–	–	32	23	–	7.8	1.4
Selected aramid	245	–	–	–	–	–	–

Research efforts have been directed to modify the morphology of Matrimid® membranes via either thermal treatment ("annealing") [158,271,272] or chemical cross-linking [157,273,274] to reduce or suppress plasticization, but these approaches often result in lower gas permeability. Although Matrimid® is significantly more expensive than many other commercial polymers, such as polysulfone, the economic production of membranes with Matrimid® separating layers is facilitated by advances in composite spinning technology, where a thin Matrimid® separating layer can be applied to a support material prepared from a more economical material [187].

Another polyimide relevant to gas separations is BPDA-ODA, or Upilex® (Type R), which was developed by UBE Industries by polymerizing biphenyl tetracarboxylic dianhydride (BPDA) and 4,4′-oxydianiline (ODA) (cf., Fig. 26) [275]. The commercialization of Upilex® is largely due to the successful development of BPDA, which can be readily produced by oxidative coupling of inexpensive phthalic acid esters with a palladium catalyst [276,277]. Instead of using the conventional two-step process of solid-state thermal imidization of poly(amic acid) intermediates, the industrial synthesis of BPDA-ODA is based on a one-step high temperature solution polymerization in a phenolic solvent [275]. Solution polymerization of diamine and dianhydride at high temperature is accompanied by imidization. High quality films and fibers can be produced from the polyimide-containing solution. However, it should be noted that the final treatment of solution-cast films at high temperature (300 °C) completes the closure of imide rings that are not fully imidized during solution polymerization, similar to the process of high temperature thermal imidization in solid-state. The polyimides produced by such a process have an almost completely imidized structure and provide superior properties than those prepared by solid-state imidization of poly(amic acid)s. For example, long-term oxidative and hydrolytic stabilities and retention of electrical properties are substantially better [278].

UBE has supplied gas separation systems since 1985 using polyimides similar to the Upilex® polyimides. Due to their high thermal resistance (T_g of ~285 °C), BPDA-ODA membranes can be operated at temperatures up to 100 °C [279]. The transport

properties, particularly the sorption and diffusion of CO_2 and water vapor, of BPDA-ODA membranes have been reported in the literature [280,281]. BPDA-ODA shows a relatively low T_g and free volume, and it has relatively low water sorption compared to other common polyimides [281]. Because of this low water solubility, permeability, solubility and diffusivity are independent of water activity. Plasticization also does not occur in the presence of CO_2 up to approximately 30.4 bar [280].

In 2010, Honeywell UOP patented a blend of polyethersulfone and polyimides for natural gas and air separations [282]. This blend is roughly 90% by weight polyimide, based on 3,3′-4,4′-diphenylsulfone tetracarboxylic dianhydride (DSDA) and 3,3′-5,5′-tetramethyl-4,4′-methylene dianiline (TMMDA), and 10% polyethersulfone. This blend has a pure gas CO_2 permeability of 18.5 Barrer and a CO_2/CH_4 selectivity of 24.8. These transport properties place the blend well below the 2008 upper bound and show that there is commercial interest in a polymer with higher permeability and slightly lower selectivity than Matrimid® and cellulose acetate.

6. Emerging membrane materials

In recent years, membrane science has developed new classes of materials and continued to improve existing families of gas separation membranes. The new classes of materials that will be highlighted in this review include thermally rearranged (TR) polymers, polymers of intrinsic microporosity (PIMs), polymerized room-temperature ionic liquids (poly(RTIL)s), and perfluoropolymers. This section will also continue to discuss polyimides, as modification of polyimides continues to be an active area of study for producing high-performance polymers. Mixed matrix membranes are beyond the scope of this review, but additional information can be found elsewhere [283,284].

6.1. Thermally rearranged (TR) polymers

Recently, Park et al. [38] reported a new family of polymeric membranes which were termed thermally rearranged (TR) polymers, for CO_2/CH_4 separations. These materials exhibit high CO_2 permeability, good CO_2/CH_4 permselectivity and excellent resistance to CO_2-induced plasticization. For example, the widely studied TR-1 polymer, based on a fluorinated diamine and dianhydride, exhibits a CO_2 permeability of roughly 2000 Barrer and a CO_2/CH_4 selectivity of roughly 40, with no evidence of plasticization up to 15.2 bar. These TR polymers, which have polybenzoxazole (PBO) structures, are believed to be formed via molecular thermal rearrangement of aromatic polyimides containing hydroxyl groups *ortho* to the imide ring. The general scheme of thermal rearrangement of an *ortho*-functional polyimide is shown in Fig. 27. Upon heating at high temperatures (generally > 400 °C) in an inert atmosphere (such as N_2 or Ar), aromatic poly(hydroxyimide)s thermally rearrange to PBOs with quantitative loss of carbon dioxide. In addition to the extraordinary membrane performance resulting from TR process, a noticeable advantage of the TR approach is that it circumvents the typical insolubility of PBOs by starting from a soluble precursor, which makes industrial processing such as hollow fiber spinning possible [51].

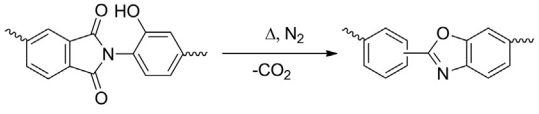

Fig. 27. General scheme of thermal rearrangement (TR) of poly(hydroxyimide)s. End groups are not shown.

The exceptional combinations of permeability and selectivity in TR polymers have been attributed to an increase in fractional free volume and a narrowing of the free volume distribution [38]. Positron annihilation lifetime spectroscopy and molecular modeling have been used to show that thermal rearrangement increases the average size of free volume elements and also makes the size distribution of these elements more uniform [38,285]. The conversion of the initial polyimide to the PBO structure and the resulting increase in free volume leads to both an increase in solubility and diffusivity [286–288]. However, diffusivity provides a much larger contribution than solubility to gas permeability increases. Thus, the rigid nature of the resulting PBO and large increase in fractional free volume after rearrangement are most likely critical to the large increases in permeability seen as a function of thermal rearrangement.

Following initial publications, additional studies have continued to explore the structure–property relationship of TR polymers [289–292]. However, most research efforts and some earlier fundamental studies on imide-to-benzoxazole conversion [293–295] require high temperature treatments (generally > 400 °C) to produce PBOs with good separation properties, and thermal degradation may overlap with the TR process after long treatment times and result in the poor mechanical properties of the TR membranes [286]. Therefore, high processing temperatures can reduce the mechanical properties of TR polymers. Reducing the TR temperature can be achieved by lowering the T_g of the precursors by using a flexible bisphenol A type dianhydride. Reductions in conversion temperature of up to 100 °C (from ~450 °C to ~350 °C) have been reported using this approach [296].

As next generation gas separation membranes, TR polymers have three major benefits: high combinations of permeability and selectivity, resistance to plasticization, and a high chemical resistance. As shown in Fig. 28, TR polymers often show transport properties well above the 2008 CO_2/CH_4 upper bound, making these polymers among the best materials known for natural gas processing [101]. The permeability, selectivity, and position relative to the upper bound can vary significantly depending on the nature of the polymer backbone, allowing the transport properties of these polymers to be tuned for specific applications [38].

Polyimides with *ortho*-functional groups other than hydroxyl groups (via either chemical imidization or chemical derivatization of poly(hydroxyimide)s) showed a much higher permeability after the

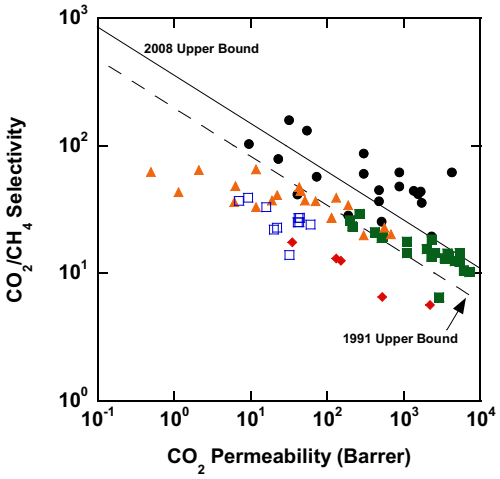

Fig. 28. CO_2/CH_4 separation properties of various emerging polymer materials reported in the literature. TR polymers (●) from Refs. [38,286]. PIMs (■) from Refs. [297–300]. Perfluoropolymers (♦) from Refs. [216,301–303]. Polyimides (▲) from Refs. [132,151,152,304–306]. Poly(RTIL)s (□) from Refs. [307–309].

TR process than TR polymers derived from its poly(hydroxyimide) analogs [286,287,310,311]. An increase in gas permeability as the size of the *ortho*-functional group increased was obtained with some loss in selectivity [296]. This *ortho*-position group is lost during thermal rearrangement, resulting in a large increase in permeability as thermal rearrangement temperature increases. Thus, the nature of the *ortho*-position group of the TR polymer precursor can be used to tailor permeability and selectivity in TR polymers.

TR polymers are promising candidates for high-performance membrane materials for gas separations. Their practical applications can be significantly advanced if the conversion temperature could be reduced to a more energy-efficient level and commercially available monomers could be used. Additional studies are also necessary to continue examining effects of precursor structure and understand the effects of physical aging on TR polymer thin films.

6.2. Polymers of intrinsic microporosity (PIMs)

Among the many efforts to develop organic or organic–inorganic hybrid materials that mimic the structure of zeolites, one recent example is a family of non-network polymers featuring "intrinsic microporosity" (PIMs) introduced by Budd et al. [297,312–315]. The "microporous" structure in PIMs is due to the highly rigid and contorted molecular structures, which prevent efficient packing of the macromolecules in the solid state. Two key features of PIMs are their kinked backbone (spiro-type structure) and highly restricted backbone rotational movements. The "microporosity" of PIMs is termed "intrinsic" as it arises solely from their molecular structures and does not derive from the thermal or processing history of the material. The synthesis of the most studied PIM-1 and PIM-7 materials and a molecular model of PIM-1 are shown in Fig. 29 [314].

The molecular scaffold used to synthesize PIMs is generally derived from an aromatic tetrol and an activated halogen-containing aromatic monomer, which are assembled via double nucleophilic aromatic substitution (S_NAr) reactions to form a dibenzodioxane. The efficiency of the double substitution reaction strongly depends on the reactivity of the aromatic halides. As shown, the spirocyclic feature of 5,5′,6,6′-tetrahydroxy-3,3,3′,3′-tetramethyl-1,1′-spirobisindane gives a kinked (contorted) conformation, and the formation of ladder-like dibenzodioxane structure results in rigid backbones, contributing to the "intrinsic microporosity". Other PIMs (PIM-2 to PIM-6) were also prepared in a similar manner using different aromatic tetrols and polyfluorine-containing aromatic compounds. Although the aromatic tetrol in PIM-1 and PIM-7 is commercially available, the activated aromatic halides, particularly the polyfluorine-containing aromatics, are limited in commercial availability and are relatively expensive. Despite the various chemical structures reported in the literature, PIM-1 and PIM-7 were the only two PIMs originally reported to form films sufficient for membrane tests. Moreover, low molecular weights (and low yields) have been issues in the synthesis of PIMs, which can make film formation difficult and contribute to poor mechanical properties. The first example of using PIMs as membrane materials was reported for PIM-1 in organo-selective pervaporation [313]. Membrane samples had a density in the range 1.06–1.09 g cm^{-3} and high specific surface areas (600–900 m^2 g^{-1}, by nitrogen BET). A promising combination of high flux and selectivity in pervaporative removal of phenols from aqueous solution was reported. Later, as shown in Figs. 28 and 30, gas separation properties were examined for PIM-1 and PIM-7; both of these materials showed transport properties above the 1991 Robeson upper bound and near the 2008 upper bound for both CO_2/CH_4 and O_2/N_2 separations [297]. PIMs with varying backbones and pendant groups have also been developed [17,300,316,317]. More recently, some PIM-based systems, *i.e.*, PIM-polyimides, have been prepared via derivatizing the aromatic tetrol into bis(carboxylic anhydride) as the building monomer [298,318,319]. These new PIM-polyimides showed relatively similar properties to original PIMs, and they offered additional structures that could be cast into freestanding films. When compared with TR polymers for CO_2/CH_4 separations, PIMs, including PIM-polyimides, also exhibit high permeabilities but often lower selectivities. On average, the PIMs form a tighter cluster than the TR polymers, showing less variation in permeability and selectivity across the range of chemical

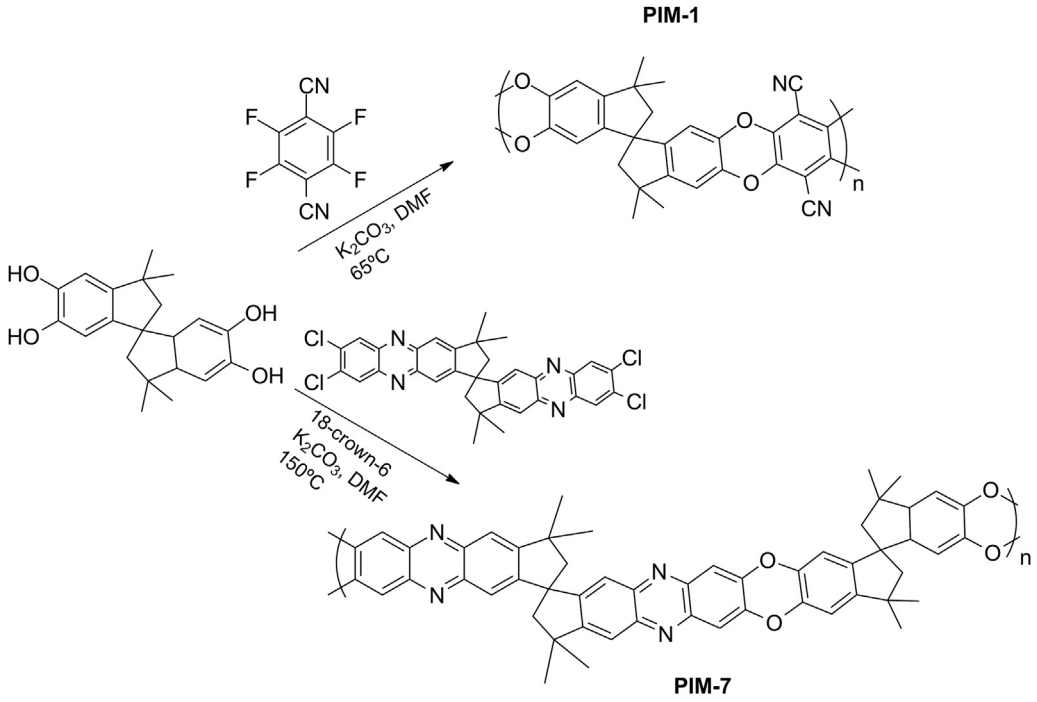

Fig. 29. Synthesis and chemical structures of PIM-1 and PIM-7 [314].

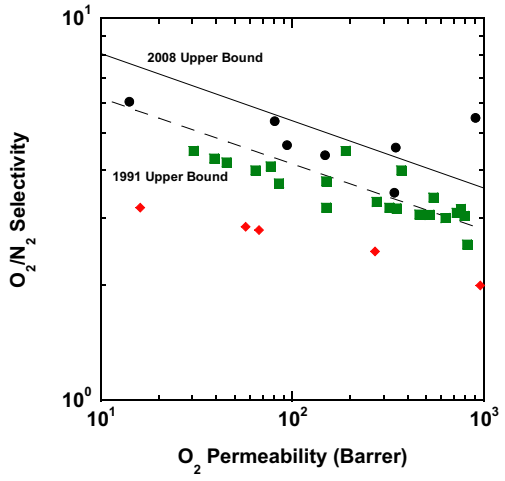

Fig. 30. O_2/N_2 separation performance for emerging materials plotted on the 1991 and 2008 Robeson upper bound. TR polymers (●) from Refs. [286,289]. PIMs (■) from Refs. [297–300,317]. Perfluoropolymers (♦)from Refs. [118,248,301,302].

structures examined than TR polymers. For O_2/N_2 separations, as shown in Fig. 30, PIMs also show generally lower selectivities at similar permeabilities when compared to TR polymers.

Despite the relatively low selectivities compared to TR polymers, PIMs show permeability/selectivity combinations that put them at the forefront of currently available membrane materials. In addition, these polymers do not need to be heat treated at the high temperatures necessary to form TR polymers. The removal of this heat treatment step means that PIMs can be solution cast directly into their final form.

The CO_2/CH_4 and CO_2/N_2 mixed gas selectivity in tetrazole-containing PIMs (TZPIMs) do not show a decrease in selectivity under mixed gas conditions [317]. For example, TZPIMS showed a CO_2/CH_4 selectivity of roughly 17.5 at 10 atm CO_2 partial pressure in pure gas measurements and in measurements made using a 50:50 CO_2/CH_4 mixed gas stream [317]. Additionally, the CO_2/N_2 mixed gas selectivity at 10 atm CO_2 partial pressure for a 50:50 mixture was 37.5, which was higher than the CO_2/CH_4 selectivity of 27.5 reported for pure gas measurements at the same CO_2 pressure. This increase in selectivity has been attributed to solubility effects [317]. Thus, these PIMs maintain their separation efficiency in a mixed gas environment.

However, additional work is still necessary to further investigate the effect of contaminants on mixed gas permeation properties. Additionally, little information is currently available on physical aging at thicknesses of 1 micron or less, molecular weights, and mechanical behavior of PIMs.

6.3. Perfluoropolymers

Perfluoropolymers possess many unique properties that have made them suitable for numerous commercial applications, including automotive, aerospace, electronics, chemical, and medical industries [320]. The strong C–F bonds (485 kJ/mol) and the protective sheath of fluorine atoms around the carbon backbone result in the extremely high chemical resistance and thermo-oxidative stability for these polymers [321,322]. Early generations of perfluoropolymers, such as polytetrafluoroethylene (PTFE), however, did not attract much interest for gas separation membranes, largely due to the low gas permeability and poor processability associated with the semicrystalline nature and lack of solubility in common solvents [320]. A major breakthrough in the use of perfluoropolymers for gas and vapor separation membranes was the development of a new family of amorphous glassy perfluoropolymers, *i.e.*, Teflon® AF, by DuPont in the late 1980s [323,324]. Teflon® AF polymers are copolymers based on tetrafluoroethylene and 2,2-bis(trifluoromethyl)-4,5-difluoro-1,3-dioxole, and the chemical structure of these completely fluorinated (*i.e.*, perfluoro-) copolymers is shown in Fig. 31. The bulky dioxole monomer disrupts chain packing in these materials so, unlike poly(tetrafluoroethylene), the commercial grades of Teflon® AF are wholly amorphous. Therefore, high gas permeability and much improved processability, related to their high solubility in perfluorinated solvents, are obtained for these polymers. Similarly, other amorphous perfluoropolymers were developed, such as Hyflon® AD (produced by Solvay), and Cytop™ (by the Asahi Glass Company) [325–328]. The gas transport properties of these materials have been extensively studied [118,321,329–335].

As seen in Figs. 28 and 30, for gas separations such as CO_2/CH_4 and O_2/N_2, perfluoropolymers show gas separation properties well below the 2008 upper bound. However, one potential use for this class of polymers is the separation of nitrogen from natural gas. This separation, simplified to N_2 and CH_4, would be helpful to improve the heating quality of natural gas. Unfortunately, the physical properties, such as size and condensability, are similar for these two gases making their separation difficult [18]. Fig. 32 shows the N_2/CH_4 separation performance of perfluoropolymers and other modern membrane materials. Perfluoropolymers, along with TR polymers, exhibit performance near the 2008 upper bound for this difficult separation [248,301,302]. This improved performance for N_2/CH_4 separations is attributed to fluorinated polymers having high light gas solubility relative to hydrocarbon solubility [118,336]. The low solubility of hydrocarbons in perfluoropolymers has been implicated in improved plasticization resistance for hydrocarbon-based separation (*e.g.*, olefin/paraffin separations) [118]. The reason for the low solubilities of hydrocarbons in perfluoropolymers is not well-understood, and the details are discussed at length by Merkel et al. [118].

6.4. Polyimides

Of the emerging polymers listed in this section, polyimides are among the most studied materials for gas separation polymers. Although aromatic polyimides are used as gas separation membrane materials today, the polyimide family encompasses a large number of structural variants, and many studies on polyimide gas separation membranes indicate that the separation properties can

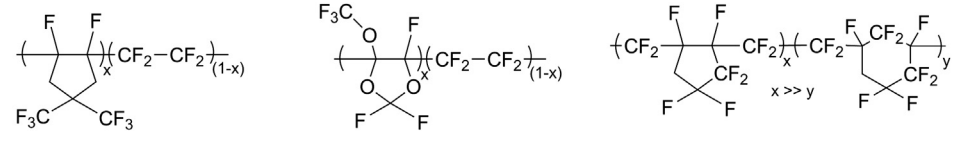

Fig. 31. Chemical structure of commercial amorphous perfluoropolymers.

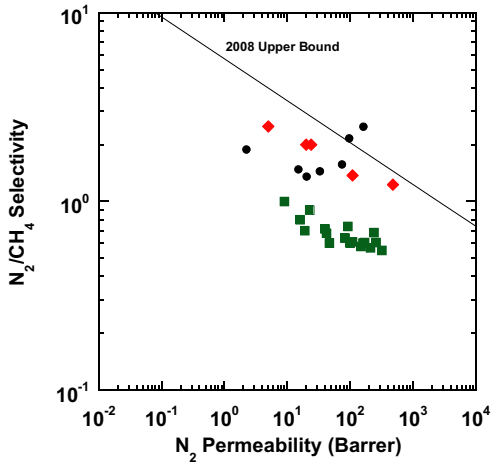

Fig. 32. N_2/CH_4 upper bound performance for various emerging membrane materials. TR polymers (●) from Refs. [286,289]. PIMs (■) from Refs. [297–300,317]. Perfluoropolymers (♦) from Refs. [118,248,301,302].

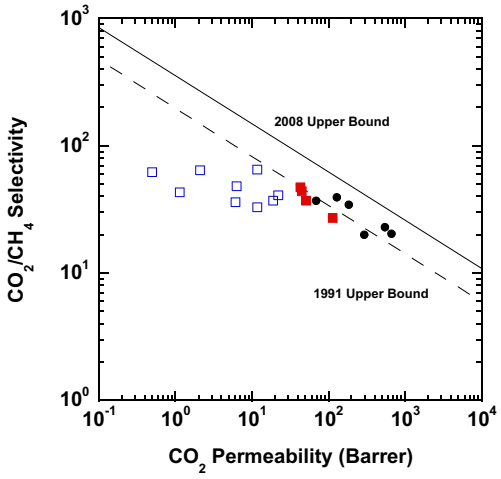

Fig. 34. Robeson upper bound plot for CO_2/CH_4 separations. First generation polyimides (□) from Ref. [104]. Current generation polyimides (●) from Refs. [151,304,306]. Treated polyimides (■) from Ref. [132].

be tailored by using different dianhydride and diamine monomers. Structure/property studies in the late 1980s showed that restricting both chain mobility and chain packing can simultaneously increase permeability and selectivity in polyimides [104,105]. In particular, polyimides with a hexafluoro substituted carbon (*e.g.*, $-C(CF_3)_2-$) in the polyimide backbone have been the object of much research, as they tend to be considerably more gas-selective, particularly toward CO_2 relative to CH_4, than other glassy polymers with comparable permeabilities. The hexafluoro group in the dianhydride moieties (*e.g.*, hexafluoro isopropylidene diphthalic anhydride (6FDA)) increases the stiffness of the polymer chain, and it frustrates chain packing due to the steric hindrance from the CF_3 groups, which serve as molecular spacers and chain stiffeners in the polymer [97,337]. The general structure of 6FDA-based polyimides is shown in Fig. 33. These initial 6FDA-based polymers are labeled as "First Generation Polyimides" in Fig. 34.

In addition to their relatively high cost, major drawbacks of 6FDA-based polyimides in gas separation are their tendency to plasticize and undergo physical aging [132,151,163]. There has been significant research to suppress plasticization and to retard the changes in the membrane performance caused by physical aging. In this regard, cross-linking may be an effective method for improving membrane stability, specifically referring to these two properties [163,338]. Various curing techniques have been reported to cross-link the polyimides, *i.e.*, thermal cure, UV irradiation, ion beam irradiation, or by reactions with added compounds [152,157,162,339–343]. Examples of such cross-linked polymers are labeled as "Treated polyimides" in Fig. 34, which highlights changes in polyimide transport properties as polyimide materials have advanced. In Fig. 34, "First Generation Polyimides" are those studied in the 1980s, specifically high-performance CF_3-containing materials, while the "Current Generation Polyimides" are modern polyimides. Both of these groups will be discussed more specifically in the following paragraphs.

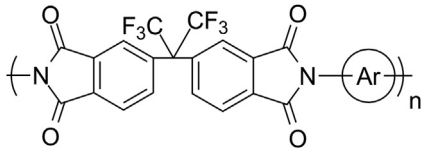

Fig. 33. General structure of 6FDA-based aromatic polyimides (Ar represents the aromatic moieties in the diamine).

Current generation polyimides populate much of the area near the 2008 Robeson CO_2/CH_4 upper bound. Of the 16 polymers highlighted as "close to the present upper bound" in Robeson's analysis, 7 are polyimides [101]. The majority of these polyimides contain 6FDA dianhydride and bulky diamines. For example, two of these polymers were made up of 6FDA and aromatic diamines containing three or four pendant methyl groups. These bulky diamines help disrupt chain packing and increase free volume. The 6FDA-durene polymer, with four methyl groups, has a CO_2 permeability of 678 Barrer and a CO_2/CH_4 selectivity of 20.2 [304]. The 6FDA-TMPD polymer, with three methyl groups, has a CO_2 permeability of 556 Barrer and a CO_2/CH_4 selectivity of 22.7 [306]. These polymers show relatively high selectivities at high CO_2 permeabilities, putting them near the upper bound for CO_2/CH_4 separations. Examples of these polymers are shown in Fig. 34 as "Current Generation Polyimides."

Recently, highly soluble polyimides with very high gas permeabilities have also been reported [151,298,304,306,318,344–346]. These polyimides tend to have common characteristics in their backbone structure featuring bulky side groups and/or non-coplanar spatial configuration, which make them highly soluble and permeable due to lack of efficient chain packing (*i.e.*, high free volume). However, the synthesis of such polyimides is much more complicated than that of typical polyimides because it generally involves multiple steps of synthesis and purification to obtain monomers at high enough purity to produce high molecular weight polyimides. A recent review of the design of polyimide-based membranes for CO_2 removal from natural gas can be found elsewhere [337].

6.5. Room temperature ionic liquids

Room-temperature ionic liquids (RTILs) are defined as organic/inorganic salts having a melting point lower than 100 °C and are typically non-volatile and inflammable liquids [347]. Because of their unique chemical and physical properties, RTILs have attracted attention for various applications [348]. The use of RTILs as solvents for CO_2 capture has been an active research area for these materials due to their low vapor pressure, which makes them environmentally friendly [349]. In addition to being used as absorbents in CO_2 capture, RTILs have been impregnated in porous materials to create supported ionic liquid membranes (SILMs). The ethylmethylimidazolium dicyanamide ([emim][dca]) shown in Fig. 35,

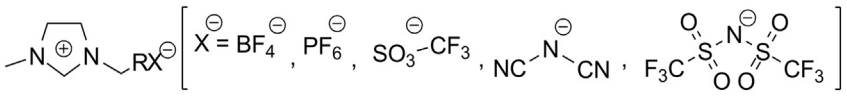

Fig. 35. Chemical structures of alkyl-imidazolium type ionic liquids. The cation is ethylmethylimidazolium ([emim]) and the anions, from left to right, are tetrafluoroborate ([BF_4]), hexafluorophosphate ([PF_6]), dicyanamide [dca], and bis(trifluoromethanesulfonyl)amide [CF_3SO_3] [350,351].

has a CO_2 permeability of roughly 600, a CO_2/N_2 selectivity of 20 and a CO_2/CH_4 selectivity of 11 [350]. The CO_2/N_2 permeabilities and selectivities were better than many common polymers as of 2004 [350–352]. The ionic liquids that have been examined most in SILMs have an organic cation and either an organic or an inorganic anion, in particular, the 1-*n*-alkyl-3-methylimidazolium cation with various anions [353]. The general structure of alkyl-imidazolium ionic liquids with some typical anions is presented in Fig. 35. The CO_2 solubility of ionic liquids depends on the nature of their cations, anions, and substituents [350,351,354].

An upper bound has been created for these SILMs, and future improvements are primarily expected in selectivity rather than permeability [353]; however, significant increases in selectivity without losses in permeability would be necessary for these polymers to perform near the upper bound. For example, when compared to the most recent 2008 upper bound, a polymer with a CO_2 permeability of 600 would need a CO_2/N_2 selectivity of roughly 43 to lie on the upper bound, meaning an SLIM with the CO_2 permeability of [emim][dca] would need double the selectivity to lie on the 2008 upper bound [101]. These materials are also often tested at low trans-membrane pressures, such as 0.2 bar, for [emim][dca] discussed earlier, due to the stability of the impregnated film at higher pressures, but it has been suggested that such these films could withstand pressure differences as high as 3 bar [350]. These stability concerns helped lead to the development of a polymerized form of these room-temperature ionic liquids.

Polymeric ionic liquids, or poly(ionic liquid)s (poly(RTIL)s), exhibited higher CO_2 sorption capacity than the corresponding monomeric ionic liquids [309,355–358]. The chemical structures of common types of poly(RTIL)s and their monomers are shown in Fig. 36.

These poly(RTIL)s are film forming, so they permit the preparation of polymer films containing high concentrations of ionic liquid groups. The most studied poly(RTIL)s for CO_2 absorption/separation are alkyl-imidazolium type polymers featuring alkyl-imidazolium salts tethered to a polystyrene or polyacrylate backbone. Poly(RTIL)s with a poly(ethylene oxide) backbone have also been synthesized via post-modification of a PEO-like polymer with small molecule RTILs [358]. Poly(RTIL)s with short side chains of EO units were produced via direct reaction of ethylene oxide and RTILs followed by tethering to a polystyrene backbone [359,360]. Generally, most of the imidazolium-type poly(RTIL)s with polystyrene or polyacrylate backbones have been synthesized from their corresponding vinyl RTIL monomers by conventional free radical polymerization in bulk or in solution. Such cationic poly(-RTIL)s bearing a large variety of counter anions (X^-), such as tetrafluoroborate (BF_4^-) and hexafluorophosphate (PF_6^-), have been reported. In addition to linear poly(RTIL)s, cross-linked poly(RTIL)s were also synthesized via free radical polymerization of multifunctional acrylic or styrenic RTIL monomers. A comprehensive review of the synthesis of various polymeric ionic liquids can be found elsewhere [348].

Additional formulations of poly(RTIL)s have been made by combining poly(RTIL)s and RTILs. These composites are formed by polymerizing RTILs in the presence of non-polymerizable RTILs [307,308,361]. These materials show no phase separation after permeation experiments performed at 2 bar, and the strong interaction between polymerized and “free” RTILs is anticipated to hold

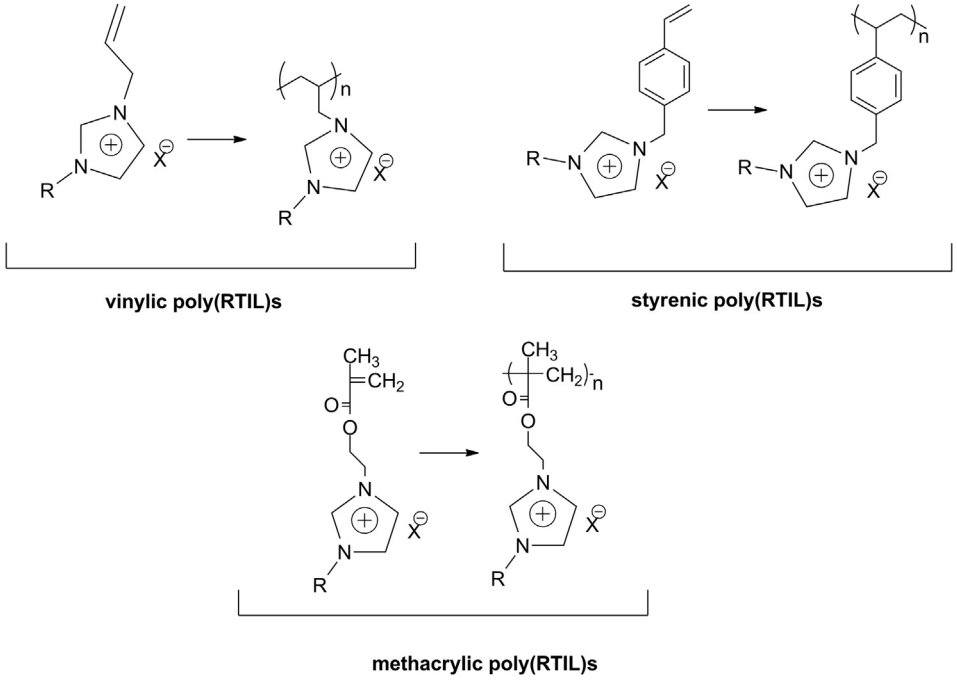

Fig. 36. Chemical structure of poly(RTIL)s with polystyrene or polymethacrylate backbone. Where R = H or alkyl substitution, X = anion (BF_4, PF_6, CF_3SO_3, etc.).

the “free” RTILs in place better than the typical capillary forces in SILMs [307]. Including these “free” RTILs into the polymer matrix increases the gas permeability due to increased diffusion through the unbound RTILs [307,308]. For example, one poly(RTIL) showed a factor of 4 increase in permeability and a 20% increase in CO_2/N_2 selectivity with the incorporation of 20% “free” RTIL [308]. However, Fig. 37 shows various poly(RTIL) and composites on the 2008 Robeson upper bound for CO_2/N_2 separation, which is widely studied using these materials [308], and many of these RTIL-based polymers show permeabilities much lower than TR polymers or PIMs with similar selectivities.

7. Emerging commercial membrane gas separations

As membrane technology matures and new materials are produced, the range of applications may expand. Several gas pairs of interest and their applications are shown in Table 5. Many of these applications require advances in membrane materials to tune transport properties and increase chemical resistance to aggressive feed conditions.

7.1. Olefin/paraffin separation

In 2009, over 22 million metric tons of ethylene, and over 13 million metric tons of propylene were produced in the US, making ethylene and propylene the two largest-volume organic chemical feedstocks [364]. The variety of synthetic chemicals derived from these olefins highlights their utility. Ethylene is used in the synthesis of polyethylene, ethylene oxide, ethylene chloride, and ethylbenzene, among others [365]. Propylene is used in the synthesis of polypropylene, acrylonitrile, oxo-alcohols, cumene, and propylene oxide [365].

Olefin/paraffin separation is accomplished through a distillation process that requires high capital cost and high energy consumption. A large ethylene unit can cost several billion dollars [366], and a large portion of the cost is devoted to the olefin/paraffin separation train [367]. Because olefin/paraffin components have very similar condensabilities, ethylene/ethane and propylene/propane splitters are large, standing between 200 and 300 feet high, containing over 100 trays, and operating with reflux ratios between 10 and 15 [184,368]. The total energy cost for these

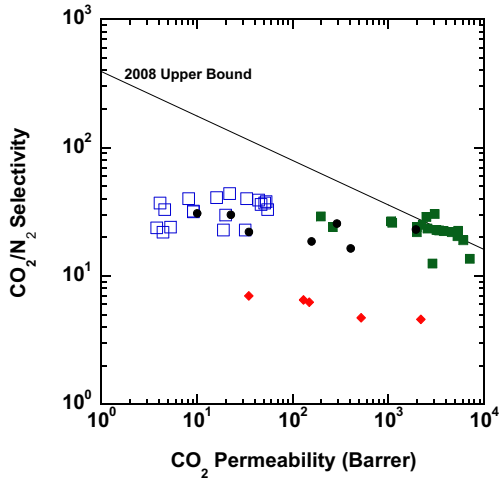

Fig. 37. CO_2/N_2 separation properties of various emerging polymer materials. TR polymers (●) from Refs. [286,289]. PIMs (■) from Refs. [297–300,317]. Perfluoropolymers (♦) from Refs. [118,248,301,302]. Poly(RTIL)s (□) from Refs. [101,308,309,359,361–363].

Table 5
Emerging commercial gas separations.

Gas pair	Application
CO_2/N_2	Carbon capture
C_3H_6/C_3H_8	Propylene/propane
C_2H_4/C_2H_6	Ethylene/ethane
$EtOH/H_2O$	Ethanol/water

operations is approximately 0.12 Quads (1 Quad = 1×10^{15} BTU = 1.06×10^{15} kJ) per year [367], which accounts for 6% of the total distillation energy consumption in the US, making olefin/paraffin separation the fourth most energy intensive separation process in the US, behind only petroleum, crude oil, and liquefied petroleum gas [71].

Worldwide, 99% of ethylene and over 50% of propylene are produced from steam cracking of paraffins [369]. Additionally, propylene is also derived from fluidized catalytic cracking, propane dehydrogenation, oxygenate conversion, and isomerization [365,370]. These processes produce an assortment of chemicals that require extensive treatment, making separations an important part of olefin production. The opportunity for capital and energy savings in olefin/paraffin separations has spurred research to explore the feasibility of polymer membranes for these separations [174,370–373]. Koros et al. have defined a polymer upper bound, fit by the Freeman model [109], for propylene/propane [372] analogous to those originally described by Robeson for other gas pairs [100,101]. Still, as Table 6 demonstrates, ethylene/ethane and propylene/propane separation is inherently difficult because of the small differences in size and condensability of these gas molecules. These Lennard-Jones diameters are from viscosity data, as there are not sufficient transport properties available in the literature to obtain a correlation diameter similar to those Robeson et al. derived for light gases [113]. Furthermore, the best performing polymers for these separations are glassy [372], and at high gas activities, or in the presence of mixtures, there is often a significant loss in selectivity due to plasticization [174].

The propylene/propane upper bound is shown in Fig. 38, and several upper bound materials are highlighted. Interestingly, while 6FDA-based polyimides define this upper bound, they are inherently susceptible to plasticization. Fig. 39 shows pure and mixed gas permeability of C_3H_6 and C_3H_8 for 6FDA-TrMPD at 323 K [174]. At these low gas activities, typical dual-mode behavior is observed for both gases [374]. The mixed-gas results in Fig. 39 demonstrate the effect of plasticization on glassy polymers for propylene and propane. At feed pressures near 2 bar, propane permeability begins to increase with increasing pressure, which is an indication of plasticization [18,375]. Additionally, due to competitive sorption, selectivity is lower in mixed-gas experiments compared to pure-gas experiments [174].

Finding high-performance polymeric materials that operate under realistic feed conditions will be essential for the development of membranes in olefin/paraffin separation. To date, the lack of acceptable materials has been a key reason that this separation has not been reduced to practice, and advances in materials science will be needed to realize the full possibility of polymer membranes for these separations. Two major applications for membranes in olefin/paraffin separations would be: (1) to recover propylene vent gas from a propylene reactor [9], and (2) to incorporate membranes into the separation train with membrane-distillation hybrid systems [184].

A long-range goal of using membranes in propylene/propane separation would be to replace the entire propylene/propane distillation column. However, compared to currently available

Table 6
Size and critical temperature of ethylene, ethane, propylene and propane.

Gas	Lennard-Jones diameter (Å)	Critical temperature (K)
Ethylene	4.16	282.5
Ethane	4.44	305.3
Propylene	4.68	365.2
Propane	5.12	369.9

polymers, materials with higher selectivity, adequate flux, and good stability would be required [9,14,372]. Two and three-stage membrane systems have been proposed to make chemical and polymer grade propylene, respectively [365]. The two-stage system could operate economically using membranes having propylene/propane selectivities of 35 and propylene permeabilities of 1 Barrer [365]. The three-stage system could operate with membranes having a selectivity of 15 and a propylene permeability of 2 Barrer, but far lower energy costs result from more selective membranes (*e.g.*, selectivity = 35, permeability = 1 Barrer) in the intermediate membrane module [365].

7.2. Ethanol/water

In recent years, significant research and government policy focused on developing renewable biofuels as an alternative to petroleum [377]. An important subset of biofuels is bioethanol, which is used as an additive to gasoline. While a liter of ethanol only contains 66% of the energy in a liter of gasoline, it has a higher octane rating. Additionally, mixing ethanol with gasoline improves exhaust gas emissions by reducing carbon monoxide, hydrocarbons, sulfur content, and carcinogens [378].

Bioethanol is produced from fermentation of a number of sugar-rich sources, including corn, sugarcane, wheat, sugar beets, *etc.* [378]. Furthermore, starch and cellulose, which can easily be converted to sugar, are also used to produce bioethanol [378]. Fermented products from these sources are generally dilute, containing only 5–12 wt.% ethanol [379]. Therefore, separation steps are required to reach the fuel-grade ethanol purity levels of greater than 99% [14].

Because of the relative volatilities of ethanol and water at low ethanol concentrations, distillation is an obvious choice for separating these compounds. However, ethanol/water mixtures form an azeotrope at approximately 95.7 wt.% ethanol [380], and an alternative process to distillation is needed to reach fuel-grade ethanol purity, which must contain less than 1% water [381]. Today, most large-scale ethanol/water mixtures are separated using two stages of distillation followed by molecular sieve adsorption to break the azeotrope [382]. The first step in this distillation process is a beer column, used to elevate the ethanol concentration from the fermentation broth to approximately 50%, followed by a rectification column, which raises the ethanol concentration near the azeotrope to approximately 93% [383]. This stream is then fed to a molecular sieve bed to increase ethanol purity to over 99% [384].

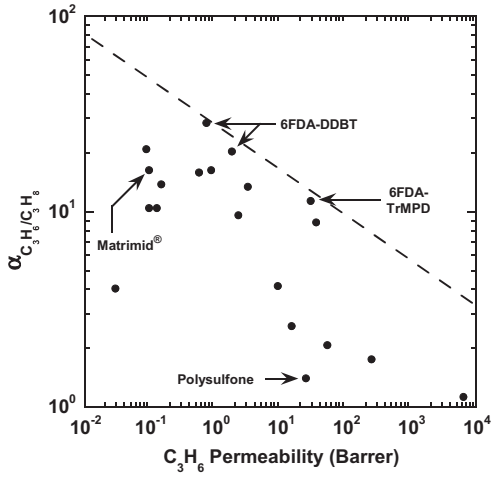

Fig. 38. Propylene/propane upper bound. The data were taken between 26 °C and 50 °C, and for feed pressures between 1 and 4.1 bar. Polysulfone and several fluorinated polyimides (Matrimid®, 6FDA-DDBT, and 6FDA-TrMPD) are highlighted [372]. The two 6FDA-DDBT points are reported from two independent studies [372,376]. Adapted from Refs. [372]; copyright Elsevier.

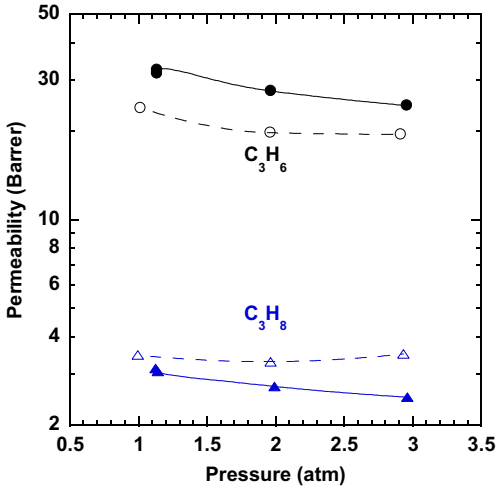

Fig. 39. 6FDA-TrMPD propylene and propane permeability. Filled symbols are pure gas results, and unfilled symbols are mixed gas results. Data was taken at 323 K, and mixed gas data is for a 50:50 mixture. Adapted from Ref. [174]; copyright Elsevier.

Alternative separation processes, including gas stripping, steam stripping, liquid–liquid extraction, adsorption, pervaporation, and vapor permeation have also been pursued for ethanol/water purification [382]. Of these alternatives, pervaporation and vapor permeation offer the best option for replacing molecular sieves in small-scale plants. For plants that treat less than 5000 L/h of feed, pervaporation is less expensive than using molecular sieves, but as feed rate increases, distillation/adsorption processes become more economical [14].

A basic schematic of pervaporation and vapor separation systems is shown in Fig. 40. In pervaporation a liquid feed must be vaporized and permeated through a membrane. Therefore, the separation factor associated with pervaporation is equal to the separation factor of evaporation times the separation factor of permeation [14]. The driving force for permeation comes from the permeate-side condenser, which, during condensation of the permeate, creates a vacuum at the downstream side of the membrane.

There are a number of challenges with using polymer membranes for ethanol/water separation. These challenges can be separated into two categories: membrane performance and process integration. More specifically, needs include: higher membrane selectivity, higher membrane flux, better membrane stability, better heat/energy integration, and better process design to increase pervaporation temperature [385].

Interestingly, membrane selectivity and flux are not a major concern, at least in terms of material design, for these separations. The most widespread ethanol–water pervaporation membrane used today is the PERVAP™ membrane produced by Sulzer [386]. These membranes are cross-linked polyvinyl alcohol [386], have ethanol/water selectivities of approximately 200 [14], and their

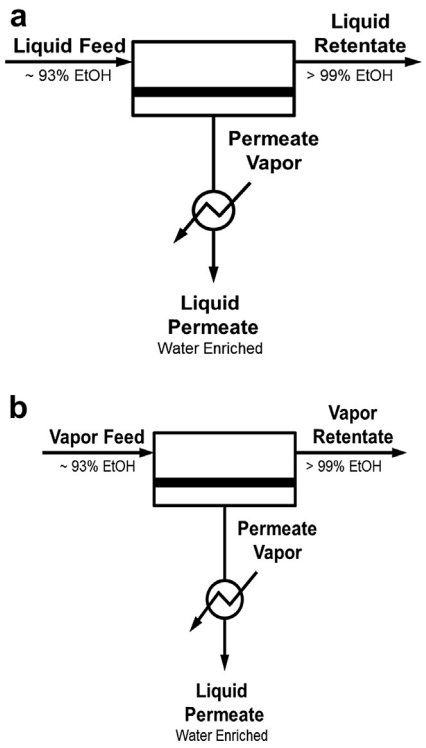

Fig. 40. Comparison of (a) pervaporation and (b) vapor permeation.

performance (*i.e.*, selectivity and flux) at various feed temperatures and compositions have been summarized by Chapman et al. [387]. Industrially, this high selectivity can only be achieved when the process is designed with a high feed/permeate pressure ratio. Therefore, the condensers in Fig. 40 are essential for creating permeate-side vacuum, thus preventing the pervaporation/vapor permeation system from operating in a pressure ratio limited regime. Still, most ethanol/water plants are relatively small, and membrane module costs for these small systems can be 15–40% of the total plant cost [14]. Therefore, increasing membrane flux can reduce the area of membrane needed to make a separation and can reduce system costs.

Membrane stability is also a critical requirement for separation performance. Hot ethanol/water solutions are aggressive feed streams, and for this reason, most pervaporation tests for polymeric films are run at low temperatures. Chapman et al. have reviewed the literature for pervaporation tests on poly(vinyl alcohol), chitosan, alginate, polysulfone, polyimides, polyamides, polyelectrolytes, and polyaniline, among other polymers [387]. With a few exceptions, most of these experiments were performed at temperatures at or below 60 °C. Many polymers have limited stability as the system temperature increases to higher temperatures. For example, cellulose esters, poly(vinyl alcohol), chitosan, and fluorinated ion-exchange membranes begin to show signs of degradation after exposure to 100 °C water for only 24 h [388,389]. Furthermore, polyimides are susceptible to hydrolysis [390], and condensation on polyimide films can lead to degradation under typical pervaporation conditions [389].

One approach for advancing market penetration of membranes in ethanol/water separation is to replace both the distillation column and molecular sieve adsorption unit from the separation process. This approach, which operates with a hybrid stripper column/vapor permeation unit, has been pursued by Membrane Technology and Research (MTR) [388,389,391]. Because heat/energy integration and process design have prevented widespread acceptance of membranes for ethanol/water separation [385], MTR has addressed these problems by using membrane materials that can operate under very aggressive vapor permeation conditions. In pervaporation, 3–5 membranes are typically used in series, and heat must be applied to each feed stream to vaporize the liquid permeate [14]. Alternatively, at slightly higher temperatures, vapor permeation can be run isothermally, greatly simplifying the heat integration process for membrane modules [14]. Additionally, higher trans-membrane flux is obtained by operating the vapor permeation system at elevated temperatures.

Despite the advantages of running ethanol/water separation with vapor permeation, finding polymer materials that are stable under these conditions is challenging. MTR has designed their vapor permeation system around perfluoropolymers (*e.g.*, Cytop™ or Hyflon® AD) [389], and they have described some of the important criteria for selecting membranes for ethanol/water separation [388]. Development of other highly stable polymer materials is important to improving membranes in ethanol/water separations.

7.3. Carbon capture

Combustion of fossil fuels (*e.g.*, coal, petroleum, and natural gas) is widely used to produce energy for electricity, industrial processes, and transportation. These processes result in high CO_2 emission to the atmosphere, which has been linked with global warming [392]. In 2007, 37 Gt of CO_2 were released into the atmosphere, and 85% of that CO_2 resulted from global energy use [393]. Furthermore, in the United States, 40% of the CO_2 emitted was attributed to energy production, 30% resulted from industrial processes, and 30% from transportation [393]. Research and government policy are being directed at developing methods of capturing and storing CO_2 to reduce climate change [394,395].

The Department of Energy has recently identified membranes as one of three basic research needs for separation processes in carbon capture [393]. For stationary power production, which appears to be well suited for membrane separations, there are three potential locations for membrane integration in the process stream: post-combustion, pre-combustion, and oxo-combustion. The potential location of membranes in these processes is shown in Fig. 41 [396], and the relevant gas separations are listed in Table 7. For post-combustion capture, membrane units would be installed downstream of the combustion process, and low pressure CO_2 would be separated from N_2 before sequestration. For pre-combustion capture, high pressure CO_2 would be separated from syngas (CO and H_2) before combustion. Oxy-combustion would use membranes to produce high-purity oxygen feeds for combustion reactions, therefore creating a CO_2 and H_2O stream that would be dehydrated and compressed.

Fig. 41 presents the basic gas pairs that would need to be separated for each carbon capture route. The actual separation processes, however, are complex. Post-combustion membranes would be installed downstream of a coal-fired power plant. A typical 550 MW plant produces 2 MMscf of flue gas per minute, and only 12–14% of that gas is CO_2 [393]. Flue gas also contains water, oxygen, nitrogen, and trace amounts of sulfur oxides and nitrogen oxides [393]. Because of the low concentration of CO_2 in post-combustion flue gas, a number of studies have estimated that high membrane CO_2/N_2 selectivities (*i.e.*, ~100) would be needed for membranes to compete with other technologies such as amine absorption, but most of these studies model carbon capture with single-stage membrane systems [397–399]. MTR has recently

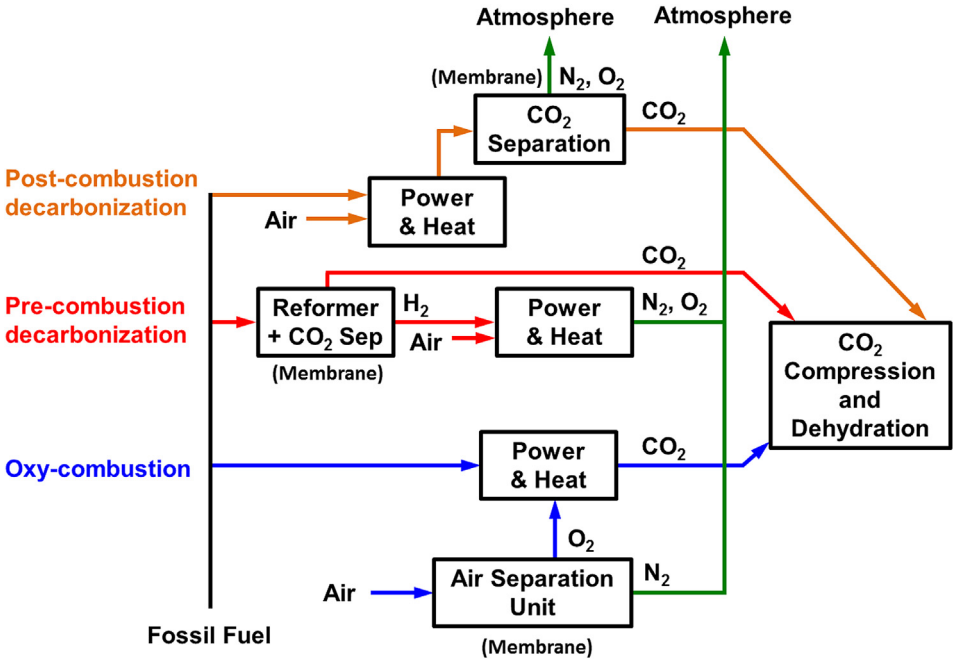

Fig. 41. Potential process locations for membranes in carbon capture applications. Membranes locations are shown in parentheses. Adapted from Ref. [396]; copyright Elsevier.

developed Polaris™ membranes, having a CO_2/N_2 selectivity of 50 and a permeance of 1000 GPU (10^{-6} cm^3(STP)/(cm^2 s (cmHg))), for carbon capture applications [396,400]. With extensive process optimization, a two-stage membrane system, combining slight feed compression, partial permeate vacuum, and a sweep operation, could be competitive with other technologies [396].

Oxy-combustion carbon capture is a very challenging application for polymer membranes. High purity O_2 must be fed to the reactor, and current state-of-the art polymer membranes cannot achieve the required purities in a single stage, as described in the Air Separation section of this review.

Although pre-combustion carbon capture has a much more favorable gas composition of approximately 40% CO_2, 56% hydrogen, and the balance is carbon monoxide, methane, nitrogen, argon and hydrogen sulfide [66], very high temperatures are required to economically achieve these separations. For example, membrane operating temperatures of approximately 700 °C are preferred for reforming reactions, and temperatures between approximately 300 °C and 500 °C are preferred for water gas shift reactors [393]. At these high temperatures and high concentrations of CO_2, it is essentially impossible to find high performing and stable polymer membranes. Still, recent research efforts have focused on CO_2 and H_2 selective membranes for these applications. CO_2 selective membranes operate best at low temperatures [100,101,401], making process integration of these membranes more difficult. Several high temperature, H_2 selective polymer membranes have been investigated for pre-combustion applications. Polybenzimidazole membranes, which have been studied for a variety of applications [402–405], currently have the highest operating temperature of polymer membranes (*e.g.*, 200 °C) [406], and MTR has tested membranes at 150 °C [66]. More research is needed to investigate polymer membrane stability at high temperatures, and better membrane process integration is needed for pre-combustion applications. These higher operating temperatures would be an added benefit to membrane technology, as many of the competing technologies, such as amine absorption, operate at near ambient temperatures or below [96].

Table 7
List of primary gas separations for carbon capture applications with membranes.

Carbon capture application	Primary gas separation
Post-combustion	CO_2/N_2
Pre-combustion	CO_2/H_2
Oxy-combustion	O_2/N_2

8. Conclusions

Materials research during the past 30 years has allowed membrane technology to advance into additional separations and has expanded the viability of current membrane separations. Current commercial membrane materials, including polysulfone, 2,6-dimethylphenylene oxide (PPO), aramids, polyimides, modified polycarbonates, and cellulose acetates, have gas transport properties below current state of the art membrane materials, and some are susceptible to plasticization in certain separations, but many of these polymers have well established synthesis procedures.

Many new families of polymers have been developed to improve permeability and selectivity, and some of these polymers also offer resistance to plasticization. These polymers, including thermally rearranged (TR) polymers, polymers of intrinsic microporosity (PIMs), polymerized room-temperature ionic liquids, perfluoropolymers, and current generation polyimides, are promising materials for membrane gas separations. Within the polymers listed above, TR polymers and PIMs typically show the best permeability and selectivity when placed on an upper-bound plot, and both of these families of polymers have only recently been investigated for gas separations, so additional research may improve their transport properties. Polymerized ionic liquids generally show less favorable permeability/selectivity combinations than other new classes of materials, but still show better performance than current commercial materials. Perfluoropolymers show permeability and selectivity values that are specifically promising for N_2/CH_4 separations, and polyimides have

continued to remain at the forefront of many separations after various modifications of the polymer backbone and functional groups.

Major membrane-based gas separations include hydrogen recovery, air separation, and natural gas purification. However, materials improvements and a changing industrial environment have expanded opportunities for membranes within olefin/paraffin separations, ethanol/water separations, and carbon capture applications. These separations and materials advances will continue to allow the membrane field to evolve and grow.

Acknowledgments

Partial support for this research was provided by the Division of Chemical Sciences, Geosciences, and Biosciences, Office of Basic Energy Sciences of the U.S. Department of Energy (DOE) through Grant DE-FG02-02ER15362. Additionally, funding was provided by the DOE Office of Science Graduate Fellowship Program administered by the Oak Ridge Institute for Science and Education (ORISE). Oak Ridge Associated Universities (ORAU) manages ORISE under DOE contract DE-AC05-06OR23100. The work was also partially supported by the U.S. National Science Foundation under Grant No. DMR #0423914 and by the NSF's Partnership for Innovation: Accelerating Innovation Research (PFI: AIR) Program (Grant # IIP-1237857).

References

[1] Mason EA. Journal of Membrane Science 1991;60:125–45.
[2] Böddeker KW. Journal of Membrane Science 1995;100:65–8.
[3] Nollet JA. Journal of Membrane Science 1995;100:1–3.
[4] Mitchell JK. Journal of Membrane Science 1995;100:11–6.
[5] Koros WJ, Fleming GK. Journal of Membrane Science 1993;83(1):1–80.
[6] Fick A. Journal of Membrane Science 1995;100:33–8.
[7] Graham T. Journal of Membrane Science 1995;100:27–31.
[8] Wijmans JG, Baker RW. Journal of Membrane Science 1995;107(1–2):1–21.
[9] Baker RW. Industrial & Engineering Chemistry Research 2002;41(6):1393–411.
[10] Baker RW, Lokhandwala K. Industrial & Engineering Chemistry Research 2008;47(7):2109–21.
[11] Lonsdale HK. Journal of Membrane Science 1982;10(2–3):81–181.
[12] Stern SA. Journal of Membrane Science 1994;94:1–65.
[13] Ghosal K, Freeman BD. Polymers for Advanced Technologies 1994;5:673–97.
[14] Baker RW. Membrane technology and applications. Chichester: John Wiley & Sons, Ltd; 2004.
[15] Kesting RE, Fritzsche AK. Polymeric gas separation membranes. New York, NY, USA: John Wiley & Sons; 1993.
[16] Yampolskii Y. Macromolecules 2012;45:3298–311.
[17] Du N, Park HB, Dal-Cin MM, Guiver MD. Energy & Environmental Science 2012;5:7306–22.
[18] Matteucci ST, Yampolskii YP, Freeman BD, Pinnau I. Transport of gases and vapors in glassy and rubbery polymers. In: Yampolskii Y, Pinnau I, Freeman BD, editors. Materials science of membranes for gas and vapor separation. Chichester: John Wiley & Sons; 2006. p. 1–47.
[19] Ribeiro CP, Freeman BD, Paul DR. Polymer 2011;52:3970–83.
[20] Allen SM, Fujii M, Stannett V, Hopfenberg HB, Williams JL. Journal of Membrane Science 1977;2(2):153–63.
[21] Hu Y, Shiotsuki M, Sanda F, Freeman BD, Masuda T. Macromolecules 2007;41:8525–32.
[22] Dhoot SN, Freeman BD, Stewart ME. Barrier polymers. In: Kroschwitz J, editor. Encyclopedia of polymer science and technology, vol. 5. New York: John Wiley & Sons; 2003. p. 198–263.
[23] Srinivasan R, Auvil SR, Burban PM. Journal of Membrane Science 1994;86:67–86.
[24] Weinkauf DH, Paul DR. ACS symposium series. Barrier polymers and structures 1990. p. 60–91.
[25] Michaels AS, Parker Jr RB. Journal of Polymer Science 1959;41:53–71.
[26] Michaels AS, Bixler HJ. Journal of Polymer Science 1961;50:393–412.
[27] Michaels AS, Vieth WR, Barrie JA. Journal of Applied Physics 1963;34:1–13.
[28] Lin HQ, Freeman BD. Permeation and diffusion. In: Czichos H, Saito T, Smith L, editors. Springer handbook for materials measurement methods. Berlin: Springer; 2011. p. 426–44.
[29] Cohen MH, Turnbull D. Journal of Physical Chemistry 1959;31(5):1164–9.
[30] Pixton MR, Paul DR. Relationships between structure and transport properties for polymers with aromatic backbones. In: Paul DR, Yampolskii Y, editors. Polymeric gas separation membranes. Boca Raton: CRC Press; 1994. p. 83–154.
[31] Turnbull D, Cohen MH. Journal of Chemical Physics 1961;34(1):120–5.
[32] Fleming GK, Koros WJ. Macromolecules 1986;19:2285–91.
[33] Bondi A. Journal of Physical Chemistry 1964;68(3):441–51.
[34] Bondi A. Physical properties of molecular crystals, liquids, and glasses. Wiley; 1968.
[35] van Krevelen DW. Properties of polymers. Amsterdam: Elsevier; 1972.
[36] Weinkauf DH, Paul DR. Journal of Polymer Science Part B: Polymer Physics 1992;30:837–49.
[37] Lee WM. Polymer Engineering and Science 1980;20(1):65–9.
[38] Park HB, Jung CH, Lee YM, Hill AJ, Pas SJ, Mudie ST, et al. Science 2007;318(5848):254–8.
[39] Hill AJ, Tant MR, McGill RL, Shang RR, Stockl DL, Murray DL, et al. Journal of Coatings Technology 2001;73(913):115–24.
[40] Thornton AW, Nairn KM, Hill AJ. Journal of Membrane Science 2009;338(1–2):29–37.
[41] Loeb S, Sourirajan S. Advances in Chemistry Series 1962;38:117–32.
[42] Sanders ES. BCFD-scale membrane separation systems for CO_2 removal applications in oil and gas production. Gas processors association annual convention. New Orleans, LA, 2004.
[43] Koros WJ, Pinnau I. Membrane formation for gas separation processes. In: Paul DR, Yampolskii YP, editors. Polymeric gas separation membranes. Boca Raton: CRC Press Inc.; 1994. p. 209–73.
[44] Kesting RE, Fritzsche AK, Murphy MK, Handerman AC, Cruse CA, Malon RF. Asymmetric gas separation membranes having graded density skins. US Patent 4,880,441; 1989.
[45] Kesting RE, Fritzsche AK, Murphy MK, Handermann AC, Cruse CA, Malon RF. Process for forming asymmetric gas separation membranes having graded density skins. US Patent 4,871,494; 1989.
[46] Olabisi O, Robeson LM, Shaw MT. Polymer–polymer miscibility. New York: Academic Press; 1969.
[47] Robeson LM. Polymer blends: a comprehensive review. Cincinnati: Hanser Gardner Publications; 2007.
[48] Robeson LM. Polymer membranes. In: Matyjaszewski K, Möller M, editors. Polymers for advanced functional materials. Polymer science: a comprehensive reference, vol. 8. Amsterdam: Elsevier; 2012. p. 325–47.
[49] Kesting RE. Synthetic polymer membranes: a structural perspective. New York: Wiley-Interscience; 1985.
[50] Chen C, Qiu W, Miller SJ, Koros WJ. Journal of Membrane Science 2011;382:212–21.
[51] Kim S, Han SH, Lee YM. Journal of Membrane Science 2012;403–404:169–78.
[52] Ekiner OM, Fleming GK. Process for enhancing the selectivity of mixed gas separations. US Patent 5,168,332; 1997.
[53] Ekiner OM, Fleming GK. Multicomponent or asymmetric gas separation membranes. US Patent 5,468,430; 1998.
[54] Sanders Jr.ES, Clark DO, Jensvold JA, Beck HN, Lipscomb GG, Coan FL. Process for preparing POWADIR membranes from tetrahalobisphenol A polycarbonates. US Patent 4,772,392. 1988.
[55] Henis JMS, Tripodi MK. Journal of Membrane Science 1981;8(3):233–46.
[56] Henis JMS, Tripodi MK. Science 1983;220(4592):11–7.
[57] Coker DT, Freeman BD, Fleming GK. AIChE Journal 1998;44(6):1289–302.
[58] Hao P, Lipscomb GG. The effect of sweep uniformity on gas dehydration module performance. Membrane gas separation 2010. p. 333–53.
[59] Lemanski J, Lipscomb GG. Journal of Membrane Science 1999;153:33–43.
[60] Lemanski J, Lipscomb GG. Journal of Membrane Science 2000;167:241–52.
[61] Lemanski J, Lipscomb GG. AIChE Journal 1995;41(10):2322–6.
[62] Lihong B, Lipscomb GG. Desalination 2002;146(1–3):243–8.
[63] Sonalkar SA, Pingjao H, Lipscomb GG. Industrial & Engineering Chemistry Research 2010;49(23):12074–83.
[64] Rice AW, Murphy MK. Gas dehydration membrane apparatus. US Patent 4,783,201; 1988.
[65] Murphy MK, Rice AW, Freeman JJ. Process for producing high quality gas for instrumentation applications using gas separation membranes. US Patent 4,793,830. 1988
[66] Merkel TC, Zhou M, Baker RW. Journal of Membrane Science 2012;389(1):441–50.
[67] Henis JMS. Commercial and practical aspects of gas separation membranes. In: Paul DR, Yampolskii YP, editors. Polymeric gas separation membranes. Boca Raton: CRC Press Inc.; 1994. p. 441–530.
[68] Ho WSW, Sirkar KK. Membrane handbook. New York: van Hostrand Reinhold; 1992.
[69] Sengupta A, Sirkar KK. Analysis and design of membrane permeators for gas separation. In: Noble RD, Stern SA, editors. Membrane separations technology: principles and applications. Amsterdam: Elsevier; 1995. p. 499–553.
[70] Spillman R. Economics of gas separation membrane processes. In: Noble RD, Stern SA, editors. Membrane separations technology: principles and applications. Amsterdam: Elsevier; 1995. p. 589–669.
[71] US Department of Energy Report. Materials for separation technology: energy and emission reduction opportunities. http://www1.eere.energy.gov/manufacturing/industries_technologies/imf/pdfs/separationsreport.pdf; 2004.
[72] CGA Inc.. Handbook of compressed gases. 4th ed. Norwell, MA: Kluwer Academic Publishers; 1999.
[73] Smith A, Klosek J. Fuel Processing Technology 2001;70(2):115–34.
[74] Gunardson H. Industrial gases in petrochemical processing: chemical industries. New York: Marcel Dekker, Inc.; 1998.

[75] Kerry FG. Industrial gas handbook: gas separation and purification. Boca Raton: CRC Press; 2007.
[76] Văsaru G. Tritium isotope separation. Boca Raton: CRC Press; 1993.
[77] Rao M, Sircar S, Abrardo J, Baade W. Hydrocarbon fractionation by adsorbent membranes. US Patent 5,332,424. 1994
[78] Ruthven DM, Farooq S, Knaebel KS. Pressure swing adsorption. New York: John Wiley & Sons Inc.; 1993.
[79] Lee KB, Beaver MG, Caram HS, Sircar S. Industrial & Engineering Chemistry Research 2008;47(21):8048–62.
[80] Pietraß T. MRS Bulletin 2011;31(10):765–9.
[81] Li Y, Liang F, Bux H, Yang W, Caro J. Journal of Membrane Science 2010;354(1–2):48–54.
[82] Sircar S. Industrial & Engineering Chemistry Research 2002;41(6):1389–92.
[83] Dąbrowski A. Advances in Colloid and Interface Science 2001;93(1–3): 135–224.
[84] Barelli L, Bidini G, Gallorini F, Servili S. Energy 2008;33(4):554–70.
[85] Burchell TD, Judkins RR, Rogers MR, Williams AM. Carbon 1997;35(9): 1279–94.
[86] Kidnay AJ, Parrish WR. Fundamentals of natural gas processing. Boca Raton: CRC Press; 2006.
[87] Prasad R, Notaro F, Thompson DR. Journal of Membrane Science 1994;94: 225–48.
[88] Paul DR, Yampol'skii YP. Polymeric gas separation membranes. Boca Raton, FL: CRC Press, Inc.; 1994. p. 100–26.
[89] Cheng HC, Hill FB. Recovery and purification of light gases by pressure swing adsorption. In: Whyte Jr TE, Yon CM, Wagener EH, editors. Industrial gas separations. ACS symposium series, vol. 223. Washington, D.C: American Chemical Society; 1983.
[90] Santos J, Cruz P, Regala T, Magalhães F, Mendes A. Industrial & Engineering Chemistry Research 2007;46(2):591–9.
[91] Drioli E, Giorno L. Membrane operations: innovative separations and transformations. Weinheim: Wiley-VCH; 2009.
[92] Aaron D, Tsouris C. Separation Science and Technology 2005;40(1–3): 321–48.
[93] Figueroa JD, Fout T, Plasynski S, McIlvried H, Srivastava RD. International Journal of Greenhouse Gas Control 2008;2(1):9–20.
[94] Hampe EM, Rudkevich DM. Tetrahedron 2003;59(48):9619–25.
[95] Calabro DC, Baugh LS, Kortunov P, McCool BA, Siskin M, Peiffer DG, and Li Q. Non-aqueous amine scrubbing for removal of carbon dioxide. US Patent 2012/0061614 A1. 2012
[96] Rochelle GT. Science 2009;325(5948):1652–4.
[97] Bernardo P, Drioli E, Golemme G. Industrial & Engineering Chemistry Research 2009;48:4638–63.
[98] Prasad R, Shaner RL, Doshi KJ. Comparison of membranes with other gas separation technologies. In: Paul DR, Yampolskii YP, editors. Polymeric gas separation membranes. Boca Raton: CRC Press; 1994.
[99] Leigh J, Fellague K, Isella G, and Roach P. Gas generating system and method for inerting aircraft fuel tanks. US 7,081,153 B2. 2006
[100] Robeson LM. Journal of Membrane Science 1991;62(2):165–85.
[101] Robeson LM. Journal of Membrane Science 2008;320(1–2):390–400.
[102] Maeda Y, Paul DR. Journal of Membrane Science 1987;30(1):1–9.
[103] Barbari TA, Koros WJ, Paul DR. Journal of Membrane Science 1989;42(1–2): 69–86.
[104] Stern SA, Mi Y, Yamamoto H. Journal of Polymer Science: Part B: Polymer Physics 1989;27:1887–909.
[105] Kim TH, Koros WJ, Husk GR, O'Brien KC. Journal of Membrane Science 1988;37(1):45–62.
[106] Robeson LM, Burgoyne WF, Langsam M, Savoca AC, Tien CF. Polymer 1994;35(23):4970–8.
[107] Breck DW. Zeolite molecular sieves. New York, NY; 1974.
[108] Robeson LM. Industrial & Engineering Chemistry Research 2010;49(23): 11859–65.
[109] Freeman BD. Macromolecules 1999;32(2):375–80.
[110] Barrer RM. Transactions of the Faraday Society 1942;38:322–30.
[111] Zheng J, Qiu J, Madeira LM, Mendes A. Journal of Physical Chemistry B 2007;111:2828–35.
[112] Meares P. Journal of the American Chemical Society 1954;76:3415–22.
[113] Robeson LM, Freeman BD, Paul DR, Rowe BW. Journal of Membrane Science 2009;341(1–2):178–85.
[114] Robeson LM, Hwu HH, McGrath JE. Journal of Membrane Science 2007;302(1–2):70–7.
[115] Geise GM, Park HB, Sagle AC, Freeman BD, McGrath JE. Journal of Membrane Science 2011;369(1–2):130–8.
[116] Mehta A, Zydney AL. Journal of Membrane Science 2005;249:245–9.
[117] Ribeiro CP, Freeman BD, Kalika DS, Kalakkunnath S. Journal of Membrane Science 2012;390-391:182–93.
[118] Merkel TC, Pinnau I, Prabhakar R, Freeman BD. Gas and vapor transport properties of perfluoropolymers. In: Yampolskii Y, Pinnau I, Freeman BD, editors. Materials science of membranes for gas and vapor separations. John Wiley & Sons Ltd; 2006. p. 251–67.
[119] Alentiev AY, Yampolskii YP. Journal of Membrane Science 2000;165(2): 201–16.
[120] Rowe BW, Robeson LM, Freeman BD, Paul DR. Journal of Membrane Science 2010;360(1–2):58–69.
[121] Park JY, Paul DR. Journal of Membrane Science 1997;125(1):23–39.
[122] Laciak DV, Robeson LM, Smith CD. Group contribution modeling of gas transport inpolymeric membranes. In: Freeman BD, Pinnau I, editors. Polymer membranes for gas and vapor separation. ACS symposium series, vol. 733. Washington D.C: American Chemical Society; 1999.
[123] Robeson LM, Smith CD, Langsam M. Journal of Membrane Science 1997;132(1):33–54.
[124] Rowe BW, Freeman BD, Paul DR. Physical aging of membranes for gas separations. In: Drioli E, Barbieri G, editors. Membrane engineering for the treatment of gases. Gas-separation problems with membranes, vol. 1. Royal Society of Chemistry; 2011.
[125] Struik LCE. Physical aging in amorphous polymers and other materials. Amsterdam, The Netherlands: Elsevier; 1978.
[126] Murphy TM, Offord GT, Paul DR. Fundamentals of membrane gas separation. In: Drioli E, Giorno L, editors. Membrane operations. Innovative separations and transformations. Weinheim, Germany: Wiley-VCH; 2009. p. 63–82.
[127] Rowe BW, Freeman BD, Paul DR. Polymer 2009;50:5565–75.
[128] Rowe BW, Freeman BD, Paul DR. Polymer 2010;51:3784–92.
[129] Murphy TM, Langhe DS, Ponting M, Baer E, Freeman BD, Paul DR. Polymer 2011;52:6117–25.
[130] Rowe BW, Pas SJ, Hill AJ, Suzuki R, Freeman BD, Paul DR. Polymer 2009;50: 6149–56.
[131] Cui L, Qiu W, Paul DR, Koros WJ. Polymer 2011;52:3374–80.
[132] Kim JH, Koros WJ, Paul DR. Polymer 2006;47:3094–103.
[133] Hutchinson JM. Progress in Polymer Science 1995;20(4):703–60.
[134] McCaig MS, Paul DR. Polymer 2000;41:629–37.
[135] Nagai K, Higuchi A, Nakagawa T. Journal of Polymer Science, Part B: Polymer Physics 1995;33(2):289–98.
[136] Langsam M, Robeson LM. Polymer Engineering and Science 1989;29(1):44–54.
[137] Kelman SD, Rowe BW, Bielawski CW, Pas SJ, Hill AJ, Paul DR, et al. Journal of Membrane Science 2008;320:123–34.
[138] Nagai K, Nakagawa T. Journal of Membrane Science 1995;105:261–72.
[139] Nagai K, Freeman BD, Hill AJ. Journal of Polymer Science, Part B: Polymer Physics 2000;38:1222–39.
[140] Dorkenoo KD, Pfromm PH. Macromolecules 2000;33:3747–51.
[141] Horn NR, Paul DR. Polymer 2011;52:1619–27.
[142] Horn NR, Paul DR. Polymer 2011;52:5587–94.
[143] Huang Y, Paul DR. Journal of Membrane Science 2004;244:167–78.
[144] Huang Y, Paul DR. Polymer 2004;45:8377–93.
[145] Huang Y, Paul DR. Macromolecules 2006;39:1554–9.
[146] Huang Y, Paul DR. Industrial & Engineering Chemistry Research 2007;46: 2343–7.
[147] Huang Y, Paul DR. Journal of Polymer Science, Part B: Polymer Physics 2007;45:1390–8.
[148] Rowe BW, Freeman BD, Paul DR. Macromolecules 2007;40(8):2806–13.
[149] McCaig MS, Paul DR. Polymer 1999;40:7209–25.
[150] McCaig MS, Paul DR, Barlow JW. Polymer 2000;41:639–48.
[151] Kim JH, Koros WJ, Paul DR. Journal of Membrane Science 2006;282:21–31.
[152] Kim JH, Koros WJ, Paul DR. Journal of Membrane Science 2006;282:32–43.
[153] Petropoulos JH. Mechanisms and theories for sorption and diffusion of gases in polymers. In: Paul DR, Yampolskii Y, editors. Polymeric gas separation membranes. Boca Raton, Florida, USA: CRC Press; 1994. p. 17–82.
[154] Wessling M, Schoeman S, van der Boomgaard T, Smolders CA. Gas Separation & Purification 1991;5:221–8.
[155] Singh A, Freeman BD, Pinnau I. Journal of Polymer Science, Part B: Polymer Physics 1998;36(2):289–301.
[156] Donohue MD, Minhas BS, Lee SY. Journal of Membrane Science 1989;42: 197–214.
[157] Bos A, Pünt IGM, Wessling M, Strathmann H. Journal of Polymer Science Part B: Polymer Physics 1998;36(9):1547–56.
[158] Bos A, Pünt IGM, Wessling M, Strathmann H. Separation and Purification Technology 1998;14:27–39.
[159] Bos A, Pünt IGM, Wessling M, Strathmann H. Journal of Membrane Science 1999;155:67–78.
[160] Chern RT, Provan CN. Macromolecules 1991;24:2203–7.
[161] Wind JD, Paul DR, Koros WJ. Journal of Membrane Science 2004;228(2): 227–36.
[162] Wind JD, Staudt-Bickel C, Paul DR, Koros WJ. Macromolecules 2003;36(6): 1882–8.
[163] Wind JD, Staudt-Bickel C, Paul DR, Koros WJ. Industrial & Engineering Chemistry Research 2002;41:6139–48.
[164] Wind JD, Sirard SM, Paul DR, Green PF, Johnston KP, Koros WJ. Macromolecules 2003;36:6433–41.
[165] Chiou JS, Paul DR. Journal of Membrane Science 1987;32:195–205.
[166] Kanehashi S, Nakagawa T, Nagai K, Duthie X, Kentish S, Stevens G. Journal of Membrane Science 2007;298:147–55.
[167] Sanders ES. Journal of Membrane Science 1988;37:63–80.
[168] Puleo AC, Paul DR, Kelley SS. Journal of Membrane Science 1989;47(3): 301–32.
[169] Jordan SM, Fleming GK, Koros WJ. Journal of Polymer Science Part B: Polymer Physics 2003;28(12):2305–27.
[170] Fleming GK, Koros WJ. Journal of Polymer Science Part B: Polymer Physics 2003;28(7):1137–52.
[171] Fleming GK, Koros WJ. Macromolecules 1990;23:1353–60.
[172] Lin HQ, Freeman BD, Kalakkunnath S, Kalika DS. Journal of Membrane Science 2007;291:131–9.

[173] Visser T, Masetto N, Wessling M. Journal of Membrane Science 2007;306:16–28.
[174] Tanaka K, Taguchi A, Hao J, Kita H, Okamoto K. Journal of Membrane Science 1996;121:197–207.
[175] White LS, Blinka TA, Kloczewski HA, Wang I. Journal of Membrane Science 1995;103:73–82.
[176] Hydrogen separations in syngas processes. Membrane technology and research. http://www.mtrinc.com/pdf_print/refinery_and_syngas/MTR_Brochure_Hydrogen_Separations.pdf; 2009.
[177] Stookey D, Patton C, Malcolm G. Chemical Engineering Progress 1986;82(11):36–40.
[178] Perry E. Process for the recovery of hydrogen from ammonia purge gases. US Patent 4,172,885; 1979
[179] Air Products. Advanced Prism® membrane systems for cost effective gas separations. http://www.airproducts.com/~/media/Files/PDF/industries/membranes-supply-optionsbrochure-advanced-prism-membrane-systems.ashx.
[180] Scott K. Handbook of industrial membranes. 1st ed. Oxford, UK: Elsevier Science Publishers Ltd.; 1995.
[181] Lu K, Song C, Subramani V. Hydrogen and syngas production and purification technologies. Hoboken, NJ: John Wiley & Sons, Inc.; 2010.
[182] Posey LG. Processes. US Patent 4,367,135; 1983
[183] Ekiner OM, Vassilatos G. Journal of Membrane Science 1990;53:259–73.
[184] Gottschlich DE, Roberts DL. Energy minimization of separation processes using conventional/membrane hybrid systems. Menlo Park: U.S. Department of Energy; 1990.
[185] Spillman RW. Chemical Engineering Progress 1989;85(1):41–62.
[186] Puri PS. Commercial applications of membranes in gas separations. In: Drioli E, Barbieri G, editors. Membrane engineering for the treatment of gases. Gas separation problems with membranes, vol. 1. Cambridge: Royal Society of Chemistry; 2011.
[187] Ekiner OM, Hayes RA, Manos P. Novel multicomponent fluid separation membranes. US Patent 5,085,676; 1992
[188] Fallon O, Milton K. Gas dehydration membrane apparatus. US Patent 4,783,201; 1988
[189] Coan FL, Jensvold JA. Air dehydration membrane. US Patent 2005/0034602 A1; 2005
[190] Theis T, Titus S. Naval Engineers Journal 1996;108(3):243–65.
[191] Saidur R, Rahim NA, Hasanuzzaman M. Renewable and Sustainable Energy Reviews 2010;14:1135–53.
[192] Surawski E, Falke BB, Hurst JP. On-board inert gas generation system with air separation module temperature control. US Patent 12/209,658; 2010.
[193] Jones PE. Modular on-board inert gas generating system. US 6,729,359 B2; 2004.
[194] Schwalm G. Ejector to reduce permeate backpressure of air separation module. US Patent 7,445,659; 2007.
[195] Jensvold J. Air separation membrane module with variable sweep stream. US 7,517,388 B2; 2007.
[196] Jones PE. Increasing the performance of aircraft on-board inert gas generating systems by turbocharging. US 7,172,156 B1; 2007.
[197] Tom R, Gu J, Murphy R, Tang B. Enhanced OBIGGS. US Patent 11/531,246; 2009.
[198] Isella G. Cross ship architecture for dispatch critical fuel tank inerting system. US 8,114,198 B2; 2012.
[199] Bahrami A. Special conditions: Boeing Model 747–100/200B/200F/200C/SR/SP/100B/300/100B SUD/400/400D/400F Airplanes; Flammability reduction means (fuel tank inerting); 2005. http://www.airweb.faa.gov/Regulatory_and_Guidance_Library/rgSC.nsf/0/126825fd59c6dd1b86256fa900619f1c!OpenDocument&ExpandSection=7#_Section7.
[200] On-board inert gas generation system (OBIGGS). HI Inc.. http://www51.honeywell.com/aero/common/documents/myaerospacecatalog-documents/ATR_Brochures-documents/OBIGGS_US.pdf; 2008.
[201] Kohl A, Nielsen R. Gas purification. 5th ed., Houston, TX: Gulf Publishing Company; 1997.
[202] Bottoms RR. Process for separating acidic gases. US Patent 1,834,016; 1931.
[203] Cooley TE, Coady AB. Removal of H_2S and/or CO_2 from a light hydrocarbon stream by use of gas permeable membrane. US Patent 4,130,403; 1978.
[204] Vu DQ, Koros WJ, Miller SJ. Journal of Membrane Science 2003;211(2):311–34.
[205] Zhang Y, Musselman I, Ferraris J, Balkus Jr KJ. Journal of Membrane Science 2008;313:170–81.
[206] Aitken CL, Koros WJ, Paul DR. Macromolecules 1992;25(13):3424–34.
[207] Koros WJ, Fleming GK, Jordan SM, Kim TH, Hoehn HH. Progress in Polymer Science 1988;13(4):339–401.
[208] Muruganandam N, Koros WJ, Paul DR. Journal of Polymer Science Part B: Polymer Physics 1987;25(9):1999–2026.
[209] Huang Y, Wang X, Paul DR. Journal of Membrane Science 2006;277:219–29.
[210] Guo R, McGrath JE. Aromatic polyethers, polyetherketones, polysulfides, and polysulfones. In: Matyjaszewski K, Möller M, editors. Polymer science: a comprehensive reference, vol. 5. Amsterdam: Elsevier BV; 2012. p. 377–430.
[211] McGrail PT. Polymer International 1996;41(2):103–21.
[212] Henis JS, Tripodi MK. Multicomponent membranes for gas separations. US Patent 4,230,463; 1977
[213] Aitken CL, Koros WJ, Paul DR. Macromolecules 1992;25(14):3651–8.
[214] Erb AJ, Paul DR. Journal of Membrane Science 1981;8(1):11–22.
[215] Ghosal K, Chern RT, Freeman BD. Journal of Polymer Science Part B: Polymer Physics 1993;31(7):891–3.
[216] McHattie JS, Koros WJ, Paul DR. Polymer 1991;32(14):2618–25.
[217] Ghosal K, Chern RT. Journal of Membrane Science 1992;72(1):91–7.
[218] Ghosal K, Chern RT, Freeman BD, Daly WH, Negulescu II. Macromolecules 1996;29(12):4360–9.
[219] McHattie JS, Koros WJ, Paul DR. Polymer 1992;33(8):1701–11.
[220] McHattie JS, Koros WJ, Paul DR. Polymer 1991;32(5):840–50.
[221] Haggin J. Chemical and Engineering News 1988;3:7–16.
[222] Schell WJ, Wensley CG, Chen MSK, Venugopal KG, Miller BD, Stuart JA. Gas Separation & Purification 1989;3(4):162–9.
[223] White LS. Evolution of natural gas treatment with membrane systems. In: Yampolskii Y, Freeman BD, editors. Membrane gas separation. Chichester: John Wiley & Sons Ltd; 2010.
[224] Loeb S, Sourirajan S. In saline water conversion II. In: . Advances in chemistry series, vol. 38. Washington, DC: American Chemical Society; 1963. p. 117–32.
[225] Heinze T, Liebert T. Macromolecular Symposia 2004;208:167–237.
[226] Saka S, Matsumura H. Macromolecular Symposia 2004;208:7–48.
[227] Edgar KJ, Buchanan CM, Debenham JS, Rundquist PA, Seiler BD, Shelton MC, et al. Progress in Polymer Science 2001;26:1605–88.
[228] Lee SY, Minhas BS. AIChE Symposium Series 1988;84(264):93–101.
[229] Robeson LM, Farnham AG, McGrath JE. Molecular basis for transitions and relaxations, vol. 4. Gordon and Breach Midland Macromolecular Institute Monographs; 1978. p. 405.
[230] Aycock D. Poly(phenylene ether). In Encyclopedia of polymer science and technology, vol. 13. NY: Interscience Publishers; 1974.
[231] Hay AS, Blanchard HS, Endres GF, Eustance JW. Journal of the American Chemical Society 1959;81(23):6335.
[232] Hay AS. Oxidation of phenols and resulting products US Patent 3,306,875; 1967.
[233] van Dort HM. Process for the formation of high molecular weight polyarylene ethers. CA Patent 798,422; 1968.
[234] Toi K, Morel G, Paul DR. Journal of Applied Polymer Science 1982;27(8):2997–3005.
[235] Aguilar-Vega M, Paul DR. Journal of Polymer Science Part B: Polymer Physics 1993;31(11):1577–89.
[236] Percec S, Li G. Chemical modification of poly(2,6-dimethyl-1,4-phenylene oxide) and properties of the resulting polymers. In ACS symposium series, vol. 364. Washington, DC.: American Chemical Society; 1988.
[237] Hamad F, Khulbe KC, Matsuura T. Desalination 2002;148(1–3):369–75.
[238] Sridhar S, Smitha B, Ramakrishna M, Aminabhavi TM. Journal of Membrane Science 2006;280(1–2):202–9.
[239] Story BJ, Koros WJ. Journal of Applied Polymer Science 1991;42(9):2613–26.
[240] Story BJ, Koros WJ. Journal of Membrane Science 1992;67(2–3):191–210.
[241] Zampini A, Malon RF. Proceedings of the ACS Division of Polymeric Materials: Science & Engineering 1985;52:345.
[242] Chern RT, Sheu FR, Jia L, Stannett VT, Hopfenberg HB. Journal of Membrane Science 1987;35(1):103–15.
[243] Chern RT, Jia L, Shimoda S, Hopfenberg HB. Journal of Membrane Science 1990;48(2–3):333–41.
[244] Henis JMS, Tripodi MK. US Patent 4230426; 1980.
[245] Ekiner OM, Vassilatos G. Journal of Membrane Science 2001;186:71–84.
[246] Gaymans RJ. Polyamides. In: Rogers ME, Long TE, editors. Synthetic methods in step-growth polymers. Hoboken: John Wiley & Sons; 2003.
[247] Yang HH. Aromatic high-strength fibers. High-performance aromatic polyamides. New York: Wiley; 2010.
[248] García JM, García FC, Serna F, de la Peña JL. Progress in Polymer Science 2010;35:623–86.
[249] Preston J. Aromatic polyamides. In: Mark HF BN, Overberger CG, Menges G, editors. Encyclopedia of polymer science and engineering, vol. 11. New York: John Wiley & Sons, Inc.; 1988. p. 381–9.
[250] Cadotte J. Interfacially synthesized reverse osmosis membrane. US Patent 4,277,344; 1981.
[251] Geise GM, Lee HS, Miller DJ, Freeman BD, McGrath JE, Paul DR. Journal of Polymer Science Part B-polymer Physics 2010;48(15):1685–718.
[252] Tien CF, Surnamer AD, Langsam M. Membranes formed from rigid aromatic polyamides. US Patent 5,034,027; 1991.
[253] Espeso JF, Ferrero E, De La Campa JG, Lozano AE, De Abajo J. Journal of Polymer Science Part A: Polymer Chemistry 2001;39(4):475–85.
[254] Carrera-Figueiras C, Aguilar-Vega M. Journal of Polymer Science B: Polymer Physics 2005;43:2625–38.
[255] López-Nava R, Vázquez-Moreno FS, Palí-Casanova R, Aguilar-Vega. M. Polymer Bulletin 2002;49:165–72.
[256] Ding Y, Bikson B. Polymer 2002;43:4709–14.
[257] Ekiner OM, Vassilatos G. Polymeric membranes. US Patent 5,085,774; 1992.
[258] Freitag D. Polycarbonates. In: Kroschwitz J, editor. Encyclopedia of polymer science and engineering, vol. II. John Wiley & Sons; 1988. p. 648–718.
[259] King Jr JA. Synthesis of polycarbonates. In: LeGrand DG, Bendler JT, editors. Handbook of polycarbonate science and technology. Marcel Dekker Inc; 2000. p. 7–27.
[260] Sanders Jr.ES, Overman IIIDC. Process for separating hydrogen from as mixtures using a semi-permeable membrane consisting predominantly of polycarbonates derived from tetrahalobisphenols. 5,000,763; 1991.
[261] Muruganandam N, Paul DR. Journal of Membrane Science 1987;34:1987.

[262] Anand JN, Bales SE, Feay DC, Jeanes TO. Tetrabromo bisphenol based polyestercarbonate membranes and method of using. US. Patent 4,840,646; 1989.
[263] Ohya H, Kudryavtsev VV, Semenova SI. Polyimide membranes - applications, fabrications, and properties. Gordon and Breach; 1996.
[264] Bateman J, Gordon DA. Soluble polyimides derived from phenylindane diamines and dianhydrides. U.S. Patent 3,856,752; 1974.
[265] Falcigno P, Masola M, Williams D, Jasne S. Comparison of properties of polyimides containing DAPI isomers and various dianhydrides. In: Feger C, Khohasteh MM, McGrath JE, editors. Polyimides: materials, chemistry and characterization. Proceedings of the third international conference on polyimides. Ellenville, NY: Elsevier; 1989. p. 497–512.
[266] Farr IV, Kratzner D, Glass TE, Dunson D, Ji Q, McGrath JE. Journal of Polymer Science Part A: Polymer Chemistry 2000;38(15):2840–54.
[267] Bateman JH, Geresy W, Neiditch DS. American Chemical Society, Division of Organic Coatings and Plastics Chemistry 1975;35(2):77–82.
[268] Ekiner OM, Hayes RA, Va W. Phenylindane-containing polyimide gas separation membranes. US Patent 5,015,270; 1991.
[269] Clausi DT, Koros WJ. Journal of Membrane Science 2000;167(1):79–89.
[270] Farr IV, Glass TE, Ji Q, McGrath JE. High Performance Polymers 1997;9(3):345–52.
[271] Lee JS, Madden W, Koros WJ. Journal of Membrane Science 2010;350(1–2):232–41.
[272] Duthie X, Kentish S, Pas SJ, Hill AJ, Powell C, Nagai K, et al. Journal of Polymer Science Part B: Polymer Physics 2008;46(18):1879–90.
[273] Tin PS, Chung TS, Liu Y, Wang R, Liu SL, Pramoda KP. Journal of Membrane Science 2003;225(1–2):77–90.
[274] Zhao H-Y, Cao Y-M, Ding X-L, Zhou M-Q, Liu J-H, Yuan Q. Journal of Membrane Science 2008;320(1–2):179–84.
[275] Sasaki Y, Inoue H, Itatani H, Kashima M. Process for preparing polyimide solution US Pat. 4,290,936; 1981.
[276] Itatani H, Yoshimoto H. The Journal of Organic Chemistry 1973;38:76–9.
[277] Kashima M, Yoshimoto H, Itatani H. Journal of Catalysis 1973;29(1):92–8.
[278] Yamane H. Proceedings of second international conference on polyimides. Ellenville, NY: Society of Plastics Engineers; Oct. 1985. p. 86.
[279] Semenova SI. Introduction: trends in polyimide membrane development. Amsterdam, The Netherlands: Gordon and Breach Science Publisher; 1996.
[280] Sada E, Kumazawa H, Xu P. Journal of Applied Polymer Science 1988;35(6):1497–509.
[281] Okamoto KI, Tanihara N, Watanabe H, Tanaka K, Kita H, Nakamura A, et al. Journal of Polymer Science Part B: Polymer Physics 1992;30(11):1223–31.
[282] Yates S, Zaki R, Arzadon A, Liu C, Choiu J. Thin film gas separation membranes. US Patent AppLication US 2010/026969 A1; 2010.
[283] Zimmerman CM, Singh A, Koros WJ. Journal of Membrane Science 1997;137:145–54.
[284] Chung TS, Jiang LY, Li Y, Kulprathipanja S. Progress in Polymer Science 2007;32:483–507.
[285] Jiang Y, Willmore FT, Sanders D, Smith ZP, Ribeiro CP, Doherty CM, et al. Polymer 2011;52(10):2224–54.
[286] Sanders DF, Smith ZP, Ribeiro CP, Guo R, McGrath JE, Paul DR, et al. Journal of Membrane Science 2012;409–410:232–41.
[287] Smith ZP, Sanders DF, Ribeiro CP, Guo R, Freeman BD, Paul DR, et al. Journal of Membrane Science 2012;415–416:558–67.
[288] Smith ZP, Tiwari RR, Murphy TM, Sanders DF, Gleason KL, Paul DR, et al. Polymer 2013;54(12):3026–37.
[289] Park HB, Han SH, Jung CH, Lee YM, Hill AJ. Journal of Membrane Science 2010;359(1–2):11–24.
[290] Jung CH, Lee JE, Han SH, Park HB, Lee YM. Journal of Membrane Science 2010;350(1–2):301–9.
[291] Choi JI, Jung CH, Han SH, Park HB, Lee YM. Journal of Membrane Science 2010;349(1–2):358–68.
[292] Han SH, Misdan N, Kim S, Doherty CM, Hill AJ, Lee YM. Macromolecules 2010;43(18):7657–67.
[293] Kardash IY, Pravednikov AN. Vysokomolekuliarnye Soedineniia. 1967;B9:873–6.
[294] Tullos GL, Mathias LJ. Polymer 1999;40(12):3463–8.
[295] Tullos GL, Powers JM, Jeskey SJ, Mathias LJ. Macromolecules 1999;32(11):3598–612.
[296] Guo R, Sanders DF, Smith ZP, Freeman BD, Paul DR, McGrath JE. Journal of Materials Chemistry A 2013;1:262–72.
[297] Budd PM, Msayib KJ, Tattershall CE, Ghanem BS, Reynolds KJ, McKeown NB, et al. Journal of Membrane Science 2005;251:263–9.
[298] Ghanem BS, McKeown NB, Budd PM, Al-Harbi NM, Fritsch D, Heinrich K, et al. Macromolecules 2009;42(20):7881–8.
[299] Ma X, Swaidan R, Belmabkhout Y, Zhu Y, Litwiller E, Jouiad M, et al. Macromolecules 2012;45:3841–9.
[300] Fritsch D, Bengston G, Carta M, McKeown NB. Macromolecular Chemistry and Physics 2012;212:1137–46.
[301] Alentiev AY, Shantarovich VP, Merkel TC, Bondar VI, Freeman BD, Yampolskii YP. Macromolecules 2002;35:9513–22.
[302] Merkel TC, Bondar V, Nagai K, Freeman BD, Yampolskii YP. Macromolecules 1999;32:8427–40.
[303] Merkel TC, Pinnau I, Prabhakar R, Freeman BD. Gas and vapor transport properties of perfluoropolymers. In: Yampolskii Y, Pinnau I, Freeman BD, editors. Materials science of membranes for gas and vapor separation. Chichester, UK: Wiley; 2006. p. 251–70.
[304] Lin WH, Chung TS. Journal of Membrane Science 2001;186:183–93.
[305] Stern SA. Journal of Polymer Science, Part B: Polymer Physics 1989;27(9):1887–909.
[306] Wang L, Cao Y, Zhou M, Zhou SJ, Yuan Q. Journal of Membrane Science 2007;305:338–46.
[307] Bara JE, Gin DL, Noble RD. Industrial & Engineering Chemistry Research 2008;47:9919–24.
[308] Bara JE, Hatakeyama ES, Gin DL, Noble RD. Polymers for Advanced Technologies 2008;19:1415–20.
[309] Bara JE, Lessmann S, Gabriel CJ, Hatakeyama ES, Noble RD, Gin DL. Industrial & Engineering Chemistry Research 2007;46:5397–404.
[310] Guo R, Sanders DF, Smith ZP, Freeman BD, McGrath JE. submitted for publication.
[311] Guo R, Sanders DF, Smith ZP, Freeman BD, McGrath JE. Journal of Materials Chemistry A 2013;1:262–72.
[312] Budd PM, Ghanem BS, Makhseed S, McKeown NB, Msayib KJ, Tattershall CE. Chemical Communications 2004;2:230–1.
[313] Budd PM, Elabas ES, Ghanem BS, Makhseed S, McKeown NB, Msayib KJ, et al. Advanced Materials 2004;16(5):456–9.
[314] McKeown NB, Budd PM. Chemical Society Reviews 2006;35(8):675–83.
[315] McKeown NB, Budd PM, Msayib KJ, Ghanem BS, Kingston HJ, Tattershall CE, et al. Chemistry – A European Journal 2005;11(9):2610–20.
[316] Carta M, Malpass-Evans R, Croad M, Rogan Y, Jansen Jc, Bernardo P, et al. Science 2013;339:303–7.
[317] Du N, Park HB, Robertson GP, Dal-Cin MM, Visser T, Scoles L, et al. Nature Materials 2011;10:372–5.
[318] Ghanem BS, McKeown NB, Budd PM, Selbie JD, Fritsch D. Advanced Materials 2008;20(14):2766–71.
[319] Emmler T, Heinrich K, Fritsch D, Budd PM, Chaukura N, Ehlers D, et al. Macromolecules 2010;43(14):6075–84.
[320] Scheirs J. High performance polymer for diverse applications. Chichester: John Wiley & Sons; 1997.
[321] Arcella V, Colaianna P, Maccone P, Sanguineti A, Gordano A, Clarizia G, et al. Journal of Membrane Science 1999;163(2):203–9.
[322] Arcella V, Ghielmi A, Tommasi G. Annals of the New York Academy of Sciences 2003;984(1):226–44.
[323] Squire EN. Amorphous copolymers of perfluoro-2,2-dimethyl-1,3-dioxole. US Patent 4,754,009; 1988.
[324] Squire EN. Amorphous copolymers of perfluoro-2,2-dimethyl-1,3-dioxole US Patent 4,935,477; 1990.
[325] Colaianna P, Brinati G, and Arcekka V. Amorphous perfluoropolymers. US patent 5,883,177; 1999.
[326] Nakamura M, Kaneko I, Oharu K, Kojima G, Matsuo M, Sameijima S, Kamba M. Cyclic Polymerization. U.S. Patent 4,910,276; 1990.
[327] Nakamura M, Sugiyama N, Etoh Y, Endo J. Nippon Kagaku Kaishi 2001;12:659–68.
[328] Sasakura H. Kobunshi Ronbunshu 2003;60:312–7.
[329] Alentiev AY, Yampolskii YP, Shantarovich VP, Nemser SM, Plate NA. Journal of Membrane Science 1997;126(1):123–32.
[330] Bondar VI, Freeman BD, Yampolskii YP. Macromolecules 1999;32(19):6163–71.
[331] Prabhakar RS, Freeman BD, Roman I. Macromolecules 2004;37(20):7688–97.
[332] Tokarev A, Friess K, Machkova J, Sipek M, Yampolskii Y. Journal of Polymer Science Part B: Polymer Physics 2006;44(5):832–44.
[333] Jansen JC, Macchione M, Drioli E. Journal of Membrane Science 2007;287(1):132–7.
[334] Pinnau I, Toy LG. Journal of Membrane Science 1996;109(1):125–33.
[335] Prabhakar RS, Grazia de Angelis M, Sarti GC, Freeman BD, Coughlin MC. Macromolecules 2005;38:7043–55.
[336] Pastermak RA, Burns GL, Heller J. Macromolecules 1971;4(4):470–5.
[337] Xiao Y, Low BT, Hosseini SS, Chung TS, Paul DR. Progress in Polymer Science 2009;34(6):561–80.
[338] Staudt-Bickel C, Koros WJ. Journal of Membrane Science 1999;155:145–54.
[339] Hu L, Xu XL, Coleman MR. Journal of Applied Polymer Science 2007;103(3):1670–80.
[340] Kita H, Inada T, Tanaka K, Okamoto K. Journal of Membrane Science 1994;87(1–2):139–47.
[341] Won J, Kim MH, Kang YS, Park HC, Kim UY, Choi SC, et al. Journal of Applied Polymer Science 2000;75(12):1554–60.
[342] Xiao YC, Chung TS, Guan HM, Guiver MD. Journal of Membrane Science 2007;302(1–2):254–64.
[343] Hillock AMW, Koros WJ. Macromolecules 2007;40(3):583–7.
[344] Kim HS, Kim YH, Ahn SK, Kwon SK. Macromolecules 2003;36(7):2327–32.
[345] Calle M, Lozano AE, de La Campa JG, de Abajo J. Macromolecules;43(5):2268–2275.
[346] Kim YH, Kim HS, Kwon SK. Macromolecules 2005;38(19):7950–6.
[347] Noble RD, Gin DL. Journal of Membrane Science 2011;369:1–4.
[348] Mecerreyes D. Progress in Polymer Science 2011;36(12):1629–48.
[349] Blanchard LA, Hancu D, Beckman EJ, Brennecke JF. Nature 1999;399(6731):28–9.
[350] Scovazzo P, Kieft J, Finan DA, Koval C, DuBois D, Noble R. Journal of Membrane Science 2004;238(1–2):57–63.
[351] Fortunato R, Afonso CAM, Reis MAM, Crespo JG. Journal of Membrane Science 2004;242(1–2):197–209.
[352] Li P, Paul DR, Chung TS. Green Chemistry 2012;14:1052–63.
[353] Scovazzo P. Journal of Membrane Science 2009;343:199–211.

[354] Cadena C, Anthony JL, Shah JK, Morrow TI, Brennecke JF, Maginn EJ. Journal of the American Chemical Society 2004;126(16):5300–8.
[355] Tang JB, Sun WL, Tang HD, Radosz M, Shen YQ. Macromolecules 2005;38(6):2037–9.
[356] Tang JB, Tang HD, Sun WL, Plancher H, Radosz M, Shen YQ. Chemical Communications 2005;26:3325–7.
[357] Tang JB, Tang HD, Sun WL, Radosz M, Shen YQ. Polymer 2005;46(26):12460–7.
[358] Tang JB, Tang HD, Sun WL, Radosz M, Shen YQ. Journal of Polymer Science Part A: Polymer Chemistry 2005;43(22):5477–89.
[359] Bara JE, Gabriel CJ, Hatakeyama ES, Carlisle TK, Lessmann S, Noble RD, et al. Journal of Membrane Science 2008;321(1):3–7.
[360] Bara JE, Gabriel CJ, Lessmann S, Carlisle TK, Finotello A, Gin DL, et al. Industrial & Engineering Chemistry Research 2007;46(16):5380–6.
[361] Bara JE, Noble RD, Gin DL. Industrial & Engineering Chemistry Research 2009;48:4607–10.
[362] Bara JE, Hatakeyama ES, Gabriel CJ, Zeng X, Lessmann S, Gin DL, et al. Journal of Membrane Science 2008;316:186–91.
[363] Carlisle TK, Bara JE, Lafrate AL, Gin DL, Noble RD. Journal of Membrane Science 2010;359:37–43.
[364] Chemical & Engineering News 2010;27:54–62.
[365] Colling C, Huff J, GA, Bartles JV. Processes using solid perm-selective membranes in multiple groups for simultaneous recovery of specified products from a fluid mixture. US Patent 6,830,691 B2; 2004.
[366] Carroll J. Chevron Phillips studying ethylene cracker amid gas glut. http://www.bloomberg.com/news/2012-02-23/chevron-phillips-may-build-ethylene-cracker-amid-shale-gas-glut.html; 2012.
[367] Eldrige RB. Industrial & Engineering Chemistry Research 1993;32(10):2208–12.
[368] Cougard N, Baudot A, Coupard V. Process for separating propane and propylene using a distillation column and a membrane separation column. US Patent 2011/0049051 A1; 2008.
[369] Wang G, Zhang Z, Chen S, and Zhang L. Process for producing olefins. US Patent 2010/0274063 A1; 2010.
[370] Das M, Koros WJ. Journal of Membrane Science 2010;365(1–2):399–408.
[371] Pinnau I, Toy LG. Journal of Membrane Science 2001;184(1):39–48.
[372] Burns RL, Koros WJ. Journal of Membrane Science 2003;211(2):299–309.
[373] Staudt-Bickel C, Koros WJ. Journal of Membrane Science 2000;170(2):205–14.
[374] Koros WJ, Paul DR, Rocha AA. Journal of Polymer Science: Polymer Physics Edition 1976;14(4):687–702.
[375] Paul DR, Yampolskii YP. Polymeric gas separation membranes. Boca Raton: CRC Press; 1994.
[376] Okamoto K, Noborio K, Hao J, Tanaka K, Hidetoshi K. Journal of Membrane Science 1997;134(2):171–9.
[377] Escobar JC, Lora ES, Venturini OJ, Yáñez EE, Castillo EF, Almazan O. Renewable and Sustainable Energy Reviews 2009;13(6–7):1275–87.
[378] Nigam PS, Singh A. Progress in Energy and Combustion Science 2011;37(1):52–68.
[379] Huang H-J, Ramaswamy S, Tschirner UW, Ramarao BV. Separation and Purification Technology 2008;62(1):1–21.
[380] Gmehling J, Menke J, Krafczyk J, Fischer K, Fontaine JC, Kehiaian HV. Azeotropic data for binary mixtures. In: Haynes WM, editor. CRC handbook of chemistry and physics. Internet Version 2012. 92nd ed. Boca Raton, FL: CRC Press/Taylor and Francis; 2012.
[381] ASTM. D4806–11a. Standard specification for denatured fuel ethanol for blending with gasolines for use as automotive spark-ignition engine fuel, 2011.
[382] Vane L. Biofuels, Bioproducts and Biorefining 2008;2(6):553–88.
[383] Kwiatkowski JR, McAloon AJ, Taylor F, Johnston DB. Industrial Crops and Products 2006;23(3):288–96.
[384] Huang Y, Baker RW, Vane LM. Industrial & Engineering Chemistry Research 2010;49(8):3760–8.
[385] Vane LM. Journal of Chemical Technology & Biotechnology 2005;80(6):603–29.
[386] Membrane technology. Sulzer Chemtech. http://www.sulzerchemtech.com/de/portaldata/11/Resources//brochures/pt/Membrane_Technology.pdf; 2012.
[387] Chapman PD, Oliveira T, Livingston AG, Li K. Journal of Membrane Science 2008;318(1–2):5–37.
[388] Huang Y, Ly J, Aldajani T, Baker RW. Liquid-phase and vapor-phase dehydration of organic/water solutions. US 8,000,874 B2; 2008.
[389] Huang Y, Ly J, Nguyen D, Baker RW. Industrial & Engineering Chemistry Research 2010;49(23):12067–73.
[390] Pryde CA. Polyimide hydrolysis measurement by fourier transform — IR spectroscopy. In: Lupinski JH, Moore RS, editors. Polymeric materials for electronics packaging and interconnection, vol. 407. Washington, DC: American Chemical Society; 1989. p. 57–66.
[391] Vane L, Alvarez F, Rosenblum L, Govindaswamy S. Industrial & Engineering Chemistry Research 2012.
[392] Hansen J, Sato M, Ruedy R, Lo K, Lea DW, Medina-Elizade M. Proceedings of the National Academy of Sciences of the United States of America 2006;103(39):14288–93.
[393] Basic research needs for carbon capture: beyond 2020, US Department of Energy Basic Energy Sciences Workshop for Carbon Capture; 2010.
[394] Katzer J, editor. The future of coal: an interdisciplinary MIT study. Massachusetts Institute of Technology; 2007.
[395] Moss RH, Edmonds JA, Hibbard KA, Manning MR, Rose SK, Vuuren DPV, et al. Nature 2010;463(7282):747–56.
[396] Merkel TC, Lin HQ, Wei XT, Baker RR. Journal of Membrane Science 2010;359(1–2):126–39.
[397] Bounaceur R, Lape N, Roizard D, Vallieres C, Favre E. Energy 2006;31:2556–70.
[398] Brunetti A, Scura F, Barbieri G, Drioli E. Journal of Membrane Science 2010;359(1–2):115–25.
[399] Favre E. Journal of Membrane Science 2007;294(1–2):50–9.
[400] Merkel TC. NETL Report: membrane process to capture carbon dioxide from coal-fired power plant flue gas. Project No.: DE-NT0005312. Membrane Technology and Research; 2009.
[401] Lin H, Van Wagner E, Freeman BD, Toy LG, Gupta RP. Science 2006;311(5761):639–42.
[402] Xiao L, Zhang H, Scanlon E, Ramanathan LS, Choe EW, Rogers D, et al. Chemistry of Materials 2005;17:5328–33.
[403] Lee HS, Roy A, Lane O, McGrath JE. Polymer 2008;49(24):5387–96.
[404] Shogbon CB, Brosseau JL, Zhang H, Benicewicz BC, Akpalu Y. Macromolecules 2006;36(26):9409–18.
[405] Mader J, Xiao L, Schmidt T, Benicewicz BC. Advances in polymer science. In Special Vol. Fuel cells 2008;216. p. 63–124.
[406] Krishnan G, Steele D, O'Brien K, Callahan R, Berchtold K, Figueroa J. Energy Procedia 2009;1(1):4079–88.

David F. Sanders received his Ph.D. in Chemical Engineering from The University of Texas at Austin in May 2013 while studying under Dr. Benny D. Freeman and Dr. Donald R. Paul. He received his bachelor's degree in Chemical Engineering from The University of Texas at Austin in 2008. David's graduate work focused on the gas transport properties of thermally rearranged polymers. After graduation, he will begin work with ExxonMobil Chemical.

Zachary P. Smith is a graduate student at the University of Texas at Austin. He received his bachelor's degree in chemical engineering from the Pennsylvania State University Schreyer Honors College in 2008 and he earned a master of science degree in chemical engineering from the University of Texas at Austin in 2011. Zach has been awarded a Department of Energy Office of Science Graduate Fellowship. His doctoral research, conducted under the guidance of Professors Benny D. Freeman and Donald R. Paul, focuses on the fundamentals of gas sorption and transport in polymers for membrane applications.

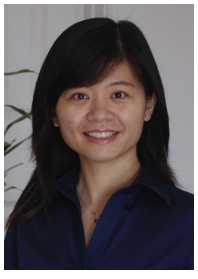

Ruilan Guo is currently an Assistant Professor of Chemical and Biomolecular Engineering at The University of Notre Dame (Notre Dame, IN). She earned a B.E. in Polymer Science and Engineering and a M.E. in Materials Science and Engineering at Beijing University of Chemical Technology (Beijing, China), and completed her Ph.D. in Polymer Engineering from Georgia Institute of Technology (Atlanta, GA). Before joining Notre Dame in 2012, Dr. Ruilan Guo was a postdoctoral fellow at Virginia Tech (Blacksburg, VA) working with Professor James E. McGrath. Her research is focused on the synthesis and characterization of new functional polymer materials with applications in the areas impacting both energy and the environment. Research projects in the Guo lab span several fields, including gas/liquid membrane separations, fuel cell membranes, and water purification. Dr. Guo has received the Department of Energy (DOE) Early Career Research Award in 2013.

James E. McGrath received a BS in Chemistry from Siena College in New York and his MS and PhD in Polymer Science from the University of Akron, where he worked on emulsion and anionic polymerization of synthetic rubbers, ozone cracking and triblock copolymer thermoplastic elastomers. After 19 years in industry [Rayonier (cellulose), Goodyear (synthetic rubbers) and Union Carbide (engineering thermoplastics, polyolefins)], he joined the Chemistry Department at Virginia Tech in 1975. He is now Ethyl Chair and a University Distinguished Professor. He was director of the first group of NSF Science and Technology Centers from 1989 to 2000 on Structural Adhesives and Composites and focused on high temperature polymers including polyimides, polysulfones and toughened epoxy polymeric matrix resins for carbon fiber composites. He has many contributions to the anionic and ring opening polymerization of dienes, epoxides and organosiloxanes. His current focus is on polymeric materials for carbon fibers and membranes for fuel cells, reverse (or forward) osmosis water purification and gas separation systems. He has 50 patents, over 500 publications and has received numerous awards, including election to the National Academy of Engineers (1994), The International SPE award, the Plastics Hall of Fame, the ACS Awards in Applied Polymer Science (2002) and Polymer Chemistry (2008), Fellow of the American Chemical Society (2009) and the Charles Overberger Award (2013). He has graduated more than 100 PhD chemists and engineers and remains one of the leaders in polymer science and engineering, with a current group (2013) of 13 students and postdoctoral fellows.

Lloyd M. Robeson received his BS degree in Chemical Engineering from Purdue University in 1964 and his PhD in Chemical Engineering from the University of Maryland in 1967. He was employed at Union Carbide Corporation from 1967 to 1986 and at Air Products and Chemicals, Inc. from 1986 to 2007 at which time he retired. His career in industry was primarily involved with polymer science and engineering. During his industrial career he worked in areas of polymer blends, polymer composites, permeability, engineering polymers, extrusion polymerization, flame retardant polymers, thermoplastic polyurethanes, polyolefins and ethylene copolymers, environmental stress failure, biomedical applications, carbon fiber reinforced thermoplastics, water soluble polymers, polymer processing, reactive extrusion compatibilization, dynamic mechanical properties, block and graft copolymers, emulsion polymers, adhesives, water soluble polymers, polymers for electronic applications, conducting polymers and membrane separation processes. He is a member of the National Academy of Engineering (class of 2001) and is in the College of Engineering Innovation Hall of Fame at the University of Maryland along with Distinguished Alumnus Honors from both Purdue University and the University of Maryland. His awards include the Industrial Polymer Award: Polymer Division of ACS (2002), the Applied Polymer Science Award of ACS (2003) and the SPE International Award (2012). His publications number ~100 including two books on the subject of polymer blends. He is the (co)author of 100 US patents which has translated into a number of commercial products. Presently, he is an Adjunct Professor at Lehigh University.

D.R. Paul holds the Ernest Cockrell, Sr. Chair in Engineering at the University of Texas at Austin. He received degrees in Chemical Engineering from North Carolina State University (B.S.) and the University of Wisconsin (M.S. and Ph.D.) and then worked at the Chemstrand Research Center. He joined the Department of Chemical Engineering at the University of Texas at Austin in 1967 where he served as department chairman during 1977–1985 and the Director of the Texas Materials Institute during 1998–2011. His research has involved various aspects of polymer blends, membranes for separation, drug delivery, packaging, processing, and nanocomposites. He has edited numerous books on blends and membranes and is listed by ISI as a Highly Cited Researcher. He has received awards for teaching, research, and leadership from the University of Texas, ACS, AIChE, SPE, and the Council for Chemical Research. He has been designated a distinguished graduate of North Carolina State University and of the University of Wisconsin. He is a member of the National Academy of Engineering and the Mexican Academy of Sciences. He has served as Editor of Industrial and Engineering Chemistry Research, published by the American Chemical Society, since 1986.

Benny Freeman holds the Richard B. Curran Centennial Chair in Engineering at The University of Texas at Austin in the Department of Chemical Engineering. He completed his graduate training in Chemical Engineering at the University of California, Berkeley, earning a Ph.D. in 1988. In 1988 and 1989, he was a postdoctoral fellow at the Ecole Supérieure de Physique et de Chimie Industrielles de la Ville de Paris (ESPCI), Laboratoire Physico-Chimie Structurale et Macromoléculaire in Paris, France. Dr. Freeman's research is in polymer science and engineering and, more specifically, in mass transport of small molecules in solid polymers. His research group focuses on structure/property correlation development for desalination and vapor separation membrane materials, new materials for hydrogen separation and natural gas purification, nanocomposite membranes, reactive barrier packaging materials, and new materials for improving fouling resistance and permeation performance in liquid separation membranes. His research is described in more than 300 publications and 16 patents/patent applications. He has co-edited 5 books on these topics. He has won numerous awards, including the Society of Plastics Engineers International Award (2013), Roy W. Tess Award in Coatings from the PMSE Division of ACS (2012), the ACS Award in Applied Polymer Science (2009), the AIChE Institute Award for Excellence in Industrial Gases Technology (2008), and the Strategic Environmental Research and Development Program Project of the Year (2001). He is a Fellow of the AAAS, AIChE, ACS, and the PMSE Division of ACS. He has served as chair of the PMSE Division of the ACS, chair of the Gordon Research Conference on Membranes: Materials and Processes, President of the North American Membrane Society, and Chair of the Separations Division of AIChE.